LITHUANIAN UNIVERSITY OF HEALTH SCIENCES

Agneta Virbickienė

PROGNOSTIC VALUE OF CARDIAC MAGNETIC RESONANCE PARAMETERS AND BLOOD BIOMARKERS IN THE ASSESSMENT OF MYOCARDIAL INJURY, LEFT VENTRICULAR FUNCTIONAL RECOVERY, AND REMODELING IN PATIENTS AFTER ACUTE MYOCARDIAL INFARCTION

Doctoral Dissertation
Medical and Health Sciences,
Medicine (M 001)

Kaunas, 2026

Dissertation has been prepared at the Laboratory of Molecular Cardiology of the Institute of Cardiology of the Lithuanian University of Health Sciences during the period of 2020–2026.

Scientific Supervisor

Prof. Dr. Olivija Dobilienė (Lithuanian University of Health Sciences, Medical and Health Sciences, Medicine – M 001).

Consultant

Prof. Dr. Vacis Tatarūnas (Lithuanian University of Health Sciences, Natural Sciences, Biology – N 010).

Dissertation is defended at the Medical Research Council of the Lithuanian University of Health Sciences:

Chairperson

Prof. Dr. Andrius Macas (Lithuanian University of Health Sciences, Medical and Health Sciences, Medicine – M 001).

Members:

Dr. Karolina Mėlinytė-Ankudavičė (Lithuanian University of Health Sciences, Medical and Health Sciences, Medicine – M 001);

Prof. Dr. Povilas Jakuška (Lithuanian University of Health Sciences, Medical and Health Sciences, Medicine – M 001);

Prof. Dr. Sigita Glaveckaitė (Vilnius University, Medical and Health Sciences, Medicine – M 001);

Prof. Dr. Andrejs Ērglis (University of Latvia, Medical and Health Sciences, Medicine – M 001).

Dissertation will be defended at the open session of the Medical Research Council of the Lithuanian University of Health Sciences on the 1st of October, 2026, at 11 a.m. in Auditorium 356 of the Department of Cardiology, Hospital of the Lithuanian University of Health Sciences Kauno Klinikos.
Address: Eivenių 2, LT-50161 Kaunas, Lithuania.

LIETUVOS SVEIKATOS MOKSLŲ UNIVERSITETAS

Agneta Virbickienė

ŠIRDIES MAGNETINIO REZONANSO RODIKLIŲ IR KRAUJO BIOŽYMENŲ PROGNOZINĖ VERTĖ VERTINANT MIOKARDO PAŽAIDĄ, KAIRIOJO SKILVELIO FUNKCINĮ ATSISTATYMĄ IR REMODELIAVIMĄSI PACIENTAMS PO ŪMINIO MIOKARDO INFARKTO

Daktaro disertacija
Medicinos ir sveikatos mokslai,
medicina (M 001)

Kaunas, 2026

Disertacija rengta 2020–2026 metais Lietuvos sveikatos mokslų universiteto Kardiologijos instituto Molekulinės kardiologijos laboratorijoje.

Mokslinė vadovė

Prof. dr. Olivija Dobilienė (Lietuvos sveikatos mokslų universitetas, medicinos ir sveikatos mokslai, medicina – M 001).

Konsultantas

Prof. dr. Vacis Tatarūnas (Lietuvos sveikatos mokslų universitetas, gamtos mokslai, biologija – N 010).

Disertacija ginama Lietuvos sveikatos mokslų universiteto Medicinos mokslo krypties taryboje:

Pirmininkas

prof. dr. Andrius Macas (Lietuvos sveikatos mokslų universitetas, medicinos ir sveikatos mokslai, medicina – M 001).

Nariai:

dr. Karolina Mėlinytė-Ankudavičė (Lietuvos sveikatos mokslų universitetas, medicinos ir sveikatos mokslai, medicina – M 001);

prof. dr. Povilas Jakuška (Lietuvos sveikatos mokslų universitetas, medicinos ir sveikatos mokslai, medicina – M 001);

prof. dr. Sigita Glaveckaitė (Vilniaus universitetas, medicinos ir sveikatos mokslai, medicina – M 001);

prof. dr. Andrejs Ērglis (Latvijos universitetas, medicinos ir sveikatos mokslai, medicina – M 001).

Disertacija bus ginama viešajame Medicinos mokslo krypties tarybos posėdyje 2026 m. spalio 1 d. 11.00 val. Lietuvos sveikatos mokslų universiteto ligoninės Kauno klinikų Kardiologijos klinikos 356 auditorijoje.
Disertacijos gynimo vietos adresas: Eivenių g. 2, LT-50161 Kaunas, Lietuva.

CONTENTS

LIST OF ABBREVIATIONS

15(S)-HETE – 15(S)-hydroxyeicosatetraenoic acid
20-HETE – 20-hydroxyeicosatetraenoic acid
ACE – angiotensin-converting enzyme
AHA – American Heart Association
ALT – alanine aminotransferase
ALVR – adverse left ventricular remodeling
ARB – angiotensin receptor blocker
AST – aspartate aminotransferase
AUC – area under the curve
BMI – body mass index
BNP – B-type natriuretic peptide
BSA – body surface area
bSSFP – balanced steady-state free precession
CAD – coronary artery disease
CI – confidence interval
CMR – cardiovascular magnetic resonance
CRP – C-reactive protein
CS – circumferential strain
ECG – electrocardiography
ECV – extracellular volume
eGFR – estimated glomerular filtration rate
ESC – European Society of Cardiology
GCS – global circumferential strain
GLS – global longitudinal strain
HbA1c – glycated hemoglobin
HDL – high-density lipoprotein
hs-CRP – high-sensitivity C-reactive protein
IHD – ischemic heart disease
IMH – intramyocardial hemorrhage
IQR – interquartile range
IS – infarct size
LAD – left anterior descending artery
LCX – left circumflex artery
LDL – low-density lipoprotein
LGE – late gadolinium enhancement

LS – longitudinal strain
LV – left ventricle / left ventricular
LVEDV – left ventricular end-diastolic volume
LVEDVi – left ventricular end-diastolic volume index
LVEF – left ventricular ejection fraction
LVESV – left ventricular end-systolic volume
LVESVi – left ventricular end-systolic volume index
LVSV – left ventricular stroke volume
MACE – major adverse cardiovascular events
MI – myocardial infarction
MOLLI – modified Look-Locker inversion recovery
MVO – microvascular obstruction
NADPH – nicotinamide adenine dinucleotide phosphate
NETs – neutrophil extracellular traps
NETosis – neutrophil extracellular trap formation
NLR – neutrophil-to-lymphocyte ratio
NT-proBNP – N-terminal pro-B-type natriuretic peptide
OR – odds ratio
PCI – percutaneous coronary intervention
RCA – right coronary artery
ROC – receiver operating characteristic
SCMR – Society for Cardiovascular Magnetic Resonance
SD – standard deviation
STEMI – ST-segment elevation myocardial infarction
TIMI – Thrombolysis In Myocardial Infarction

INTRODUCTION

Cardiovascular disease remains the leading cause of morbidity and mortality worldwide. IHD is one of its most common forms, and acute myocardial infarction (MI) is among its most severe clinical manifestations [1, 2]. According to the 2021 European Society of Cardiology (ESC) guidelines on cardiovascular disease prevention, Lithuania is still classified as a very high cardiovascular risk country [3].

ST-segment elevation myocardial infarction (STEMI) usually results from acute occlusion or subocclusion of a coronary artery, and primary percutaneous coronary intervention (PCI) is the main method of reperfusion therapy. Timely PCI reduces mortality, reinfarction, and stroke [4]. Even after successful reperfusion, a substantial proportion of patients sustain ischemia–reperfusion injury. Experimental data indicate that ischemia itself produces only minor microcirculatory changes, whereas pronounced microvascular injury typically starts when reperfusion begins [5]. Two related mechanisms contribute to this injury: luminal obstruction of the microvasculature and external compression. Luminal obstruction may arise from distal thromboembolization, blood-cell aggregation, local thrombosis, and vasospasm, whereas external compression is usually related to interstitial and cellular edema, intramyocardial hemorrhage, and elevated left ventricular (LV) filling pressure [5]. One of the most important manifestations of this injury is microvascular obstruction (MVO), in which tissue-level perfusion in the small myocardial vessels remains impaired despite restored epicardial flow. MVO is associated with larger infarct size (IS), poorer LV functional recovery, adverse LV remodeling, and worse prognosis [6, 7].

LV remodeling after acute MI involves changes in LV size, geometry, mass, and function. Adverse remodeling is associated with persistent LV dysfunction, heart failure, and poorer long-term outcomes [8–10]. Its extent is determined not only by IS but also by increased myocardial wall stress arising from altered preload and afterload, activation of the renin–angiotensin–aldosterone and sympathetic nervous systems, inflammatory processes, extracellular matrix turnover, and progressive fibrosis [8]. Myocardial healing varies across regions: the most pronounced structural and functional changes occur in the infarcted zone, but measurable changes are also found in the adjacent and remote myocardium. These regional differences in healing may partly explain why LV functional recovery and the course of remodeling differ even between patients with comparable IS [10].

Cardiovascular magnetic resonance (CMR) is the reference standard for non-invasive quantification of LV volumes, mass, and ejection fraction, with

high interobserver reproducibility that makes it particularly suited to tracking structural and functional change after MI [11, 12]. A single examination characterizes not only LV function but also IS and MVO on late gadolinium enhancement (LGE) imaging [13]. Parametric mapping, including native and post-contrast T1 mapping, T2 mapping, and extracellular volume (ECV) quantification, characterizes the underlying tissue by capturing edema, extracellular expansion, and fibrosis, while myocardial deformation (strain) analysis provides a quantitative measure of regional mechanics through longitudinal and circumferential strain [14]. Together, these parameters distinguish the infarcted, adjacent, and remote zones and characterize regional healing [15]. Integrating tissue mapping and strain within one study allows structural, functional, and tissue-level changes to be followed from the acute phase through recovery and related to myocardial healing and LV remodeling [10].

Despite the capabilities of advanced imaging, early assessment of the risk of impaired LV functional recovery and adverse remodeling remains challenging. Conventional clinical, angiographic, and laboratory variables account for only part of the individual variation in myocardial injury, healing, and recovery. Additional information may be provided by blood markers associated with inflammatory and thrombotic processes and by products of eicosanoid metabolism. In this study, platelet count [16], NETosis expression, defined as the formation of neutrophil extracellular traps (NETs), and the eicosanoids 20-hydroxyeicosatetraenoic acid (20-HETE) and 15(S)-hydroxyeicosatetraenoic acid (15(S)-HETE) were assessed.

20-HETE is formed from arachidonic acid by cytochrome P450 4A and 4F enzymes. It regulates vascular tone and promotes microvascular vasoconstriction [17, 18], endothelial activation, and platelet adhesion to the vessel wall [19]. This metabolite also activates nicotinamide adenine dinucleotide phosphate (NADPH) oxidase, increasing reactive oxygen species generation and oxidative stress, and may thereby contribute to endothelial dysfunction and microvascular injury [20].

15(S)-HETE is formed from arachidonic acid through the activity of 12/15-lipoxygenase. Increased concentrations of 15(S)-HETE have been detected in human ischemic myocardium, and experimental studies have shown that this metabolite promotes thrombus formation [21]. In addition, 15(S)-HETE promotes the differentiation of fibroblasts into myofibroblasts and may enhance myocardial fibrosis [22]. Deletion of the 12/15-lipoxygenase gene in an experimental model of myocardial infarction reduced fibrosis and adverse LV remodeling [23]. These findings suggest that 15(S)-HETE may be involved in myocardial healing and LV remodeling after infarction.

During NETosis, activated neutrophils release decondensed chromatin, histones, and granule proteins, forming NETs [24]. NETs accumulate within culprit coronary thrombi and may promote platelet recruitment, fibrin deposition, endothelial injury, and microvascular plugging [25–28].

The associations of these circulating biomarkers with CMR-defined acute myocardial injury, subsequent myocardial healing, and LV remodeling after a first STEMI remain insufficiently characterized [29, 30]. Combined assessment of CMR parameters and circulating biomarkers may provide additional information on LV functional recovery and remodeling after STEMI.

1. THE AIM AND OBJECTIVES OF THE STUDY

The aim of the study

To evaluate myocardial ischemia–reperfusion injury and healing, left ventricular function, and remodeling after a first ST-segment elevation myocardial infarction using multiparametric CMR and circulating biomarkers and to identify predictors of acute myocardial injury, impaired functional recovery, and adverse remodeling.

The objectives of the study

1. To evaluate acute myocardial infarct size and microvascular obstruction using CMR and to determine their associations with clinical, angiographic, laboratory, and specialized circulating biomarker variables.
2. To evaluate 6-month changes in left ventricular systolic function and infarcted tissue after myocardial infarction and to determine the associations of residual infarct size with baseline CMR parameters and blood markers.
3. To compare CMR-derived myocardial characteristics and strain parameters in infarcted, adjacent, and remote myocardial regions during the acute phase and at 6-month follow-up after MI.
4. To identify baseline clinical, angiographic, laboratory, biomarker, and CMR predictors of impaired left ventricular systolic function recovery at 6 months and to assess their predictive value.
5. To identify baseline clinical, angiographic, laboratory, biomarker, and CMR predictors of adverse left ventricular remodeling at 6 months and to assess their predictive value.

Scientific novelty of the study

In this study, patients with a first STEMI underwent CMR at baseline and at 6-month follow-up. In addition to conventional measures, including LV volumes, left ventricular ejection fraction (LVEF), IS, and MVO, the analysis included regional tissue characterization and myocardial deformation, with native T1, post-contrast T1, T2, ECV, and longitudinal and circumferential strain assessed in the infarcted, adjacent, and remote zones.

To our knowledge, this is among the first studies to relate circulating biomarkers to paired baseline and follow-up CMR after a first STEMI and the first study of this kind in Lithuania. Three biomarkers, 20-HETE, 15(S)-

HETE, and NETosis expression, were analyzed together in a single cohort alongside CMR tissue-characterization and strain parameters.

The predictors differed according to the outcome assessed. Acute myocardial injury and MVO were associated mainly with angiographic findings, markers of myocardial necrosis, and NETosis expression; impaired functional recovery was associated with baseline LVEF, IS, and infarcted-region circumferential strain; and adverse remodeling was associated with lower platelet count, lower 20-HETE concentration, and infarcted-region post-contrast T1. These findings support combined CMR and biomarker assessment for individual risk stratification after reperfusion.

2. LITERATURE REVIEW

2.1. ST-segment elevation myocardial infarction

Cardiovascular disease remains the leading cause of mortality worldwide, accounting for approximately one-third of all global deaths [1]. Ischemic heart disease (IHD) is the largest contributor to cardiovascular mortality and disability-adjusted life years lost, with acute MI representing one of its most severe clinical manifestations [1, 2]. Although age-standardized IHD mortality has declined in many high-income countries over recent decades, the absolute global burden continues to rise, largely because of population aging and the persistent prevalence of cardiovascular risk factors [1, 31].

Cardiovascular mortality across Europe is not uniform. Western European countries have seen substantial declines in age-standardized cardiovascular mortality over recent decades, while Central and Eastern Europe continue to carry a disproportionately high burden [32]. Lithuania is still classified as a very high-risk country in the 2021 ESC cardiovascular prevention guidelines [3]. Data from the population-based Kaunas Ischemic Heart Disease Register reflect this profile: between 2000 and 2023, morbidity from acute MI and mortality from IHD have declined, but the burden remains substantial [33].

STEMI is the most severe clinical manifestation of complete or near-complete coronary artery occlusion and carries significant early morbidity and mortality. Primary PCI is the preferred reperfusion strategy when it can be delivered within the guideline-recommended timeframe, as it reduces mortality, reinfarction, and stroke compared with fibrinolysis [4]. Total ischemia time is a key factor in outcomes, since prolonged ischemia leads to progressive transmural necrosis, as described by the wavefront phenomenon, with the subendocardium affected first and the subepicardium last [34, 35]. This time-dependent injury progression means that delayed reperfusion results in larger IS, reduced LV recovery, and adverse remodeling.

However, restoration of epicardial coronary flow does not necessarily restore myocardial tissue-level reperfusion or prevent ongoing injury. Reperfusion itself may contribute to additional cellular damage through ischemia–reperfusion injury, involving oxidative stress, calcium overload, mitochondrial dysfunction, endothelial activation, and inflammatory cell recruitment [35, 36]. One important manifestation is MVO, which reflects impaired myocardial tissue reperfusion despite angiographically restored epicardial artery flow and is associated with larger IS, impaired functional recovery, and adverse left ventricular remodeling (ALVR) [6, 7]. This residual injury explains why early characterization of post-STEMI myocardial injury

remains important for identifying patients at risk of unfavorable structural and functional outcomes [8].

2.2. Left ventricular remodeling

LV remodeling after MI involves time-dependent changes in ventricular size, geometry, mass, and function in response to ischemic injury. These changes begin within hours of infarction and continue through the subacute and chronic phases. Remodeling may include infarct expansion, wall thinning, chamber dilatation, increased wall stress, and reduced systolic function. ALVR is clinically significant, as it is associated with persistent dysfunction, heart failure, and poorer long-term outcomes after MI [8–10]. In contrast, some patients experience reverse remodeling, with reduced ventricular volumes and improved systolic function on follow-up imaging, which is associated with better clinical outcomes [9].

The criteria used to define ALVR have evolved with advances in cardiac imaging. In earlier echocardiographic studies, remodeling was commonly defined as a relative increase of ≥ 20% in left ventricular end-diastolic volume (LVEDV) between baseline and follow-up imaging [37]. Using this threshold, ALVR was reported in approximately one-third of patients treated with primary PCI, although interobserver variability in echocardiographic volumes contributed to heterogeneous incidence estimates across studies [37, 38]. With wider use of CMR, more reproducible volume-based definitions became feasible, and several CMR-based criteria have been proposed [10, 38]. Bulluck et al. proposed defining ALVR as a relative increase of ≥ 12% in both LVEDV and LV end-systolic volume left ventricular end-systolic volume (LVESV) between acute and follow-up CMR [39]. These thresholds were derived from an interobserver reproducibility analysis and represent the minimal detectable change beyond measurement variability. Although receiver operating characteristic (ROC) analyses for predicting follow-up LVEF below 50% identified lower cut-points, the authors recommended the more conservative, reproducibility-based thresholds [39]. This criterion has since been included in CMR-based studies of post-STEMI remodeling [38].

The extent and pattern of remodeling are influenced by the severity of acute myocardial injury. Larger IS increases mechanical stress on the remaining myocardium and reduces the amount of viable contractile tissue. MVO and other manifestations of severe reperfusion injury may further compromise myocardial recovery and have been associated with ALVR. However, remodeling is not determined by IS alone; it reflects the combined influence of infarcted-region injury, peri-infarct tissue changes, inflammation,

extracellular matrix turnover, neurohormonal activation, and adaptive responses in remote non-infarcted myocardium [6, 8].

Post-infarction repair is a coordinated biological response involving inflammatory, proliferative, and maturation phases. In the early inflammatory phase, necrotic cardiomyocytes and damaged extracellular matrix components trigger innate immune activation and recruitment of inflammatory cells, leading to protease release and clearance of necrotic tissue [40]. This response is necessary for tissue clearance, but excessive or prolonged inflammation may contribute to infarct expansion and extracellular matrix degradation [40]. During the proliferative phase, cardiac fibroblasts drive the synthesis of new extracellular matrix, with collagen deposition and scar formation stabilizing the infarcted-region [40, 41]. Over time, myocardial edema resolves and the infarcted tissue matures into a stable fibrotic scar [41].

This repair process varies across the myocardium [8]. The infarcted-region typically shows the most pronounced structural and functional impairment, but peri-infarct and remote myocardium can also undergo measurable changes. Peri-infarct tissue may develop edema, inflammation, extracellular expansion, or impaired deformation, even without clear infarct enhancement. Remote myocardium may respond to increased wall stress and altered loading conditions through hypertrophy, interstitial fibrosis, and changes in myocardial mechanics [10]. This regional variability helps explain why patients with similar acute MI can have different patterns of LV recovery and remodeling.

Because these structural, functional, and tissue-level changes can be captured in a single examination, CMR is particularly suited to serial assessment of the post-infarction left ventricle, as described in the following section.

2.3. Cardiovascular magnetic resonance after STEMI

CMR provides comprehensive characterization of the post-infarction myocardium, combining accurate measurement of LV structure and systolic function with tissue characterization of infarction, microvascular injury, edema, and extracellular expansion (Figure 2.3.1). These capabilities have made CMR central to research on post-STEMI remodeling and recovery, and increasingly important for prognostic assessment [10].

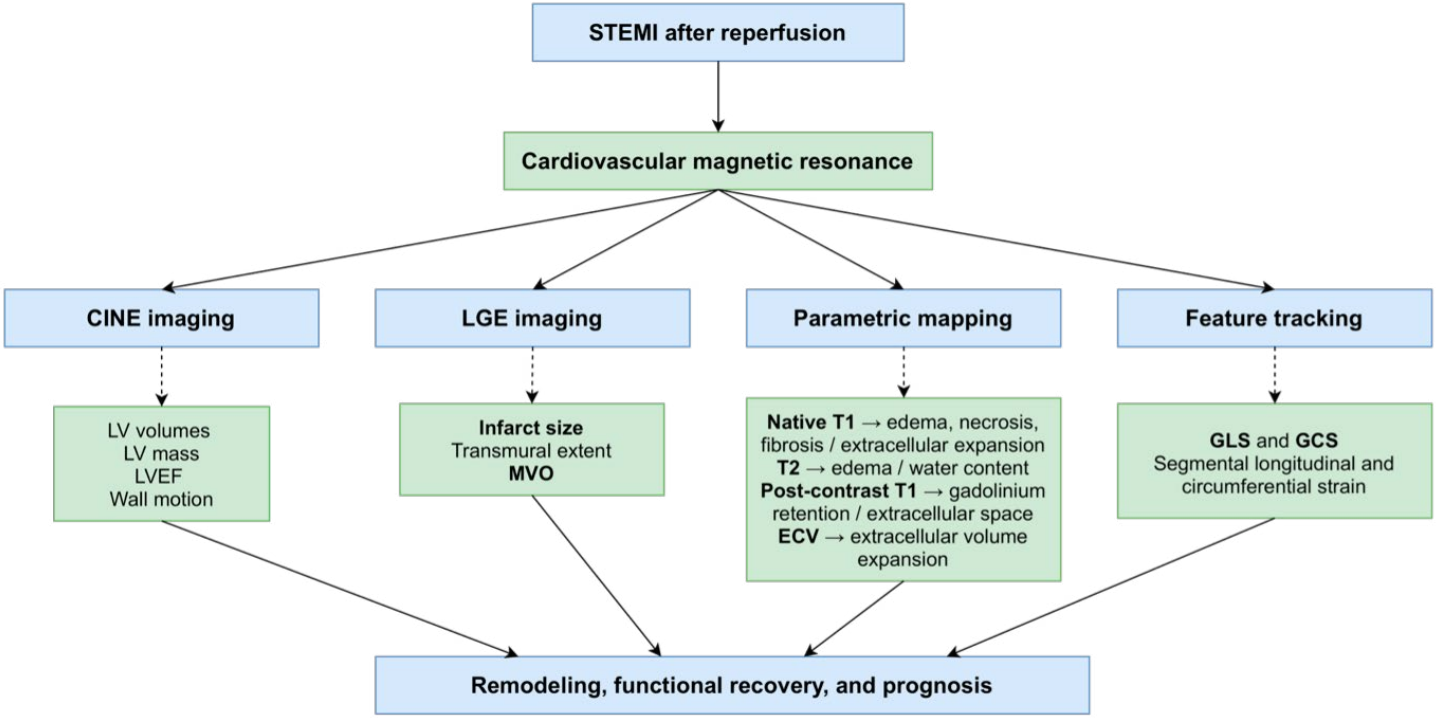

Fig. 2.3.1. *Components of cardiovascular magnetic resonance assessment after STEMI*

LV – left ventricular; LVEF – left ventricular ejection fraction; LGE – late gadolinium enhancement; MVO – microvascular obstruction; ECV – extracellular volume; GLS – global longitudinal strain; GCS – global circumferential strain. Adapted from Bulluck et al. [39] and Gissler et al. [10].

2.3.1. CMR as the reference standard

CMR is the reference standard for in vivo assessment of cardiac volumes, mass, and systolic function. Steady-state free precession cine imaging acquired in contiguous short-axis stacks allows direct three-dimensional measurement of LV chamber volumes without geometric assumptions, which is a key methodological advantage over two-dimensional echocardiography [11]. This approach provides high intra- and interobserver reproducibility for LVEDV, LVESV, LV mass, and LVEF, and can detect smaller longitudinal changes than echocardiography for the same sample size [11, 12]. These properties are particularly relevant for serial post-STEMI studies, in which modest changes in LV volumes and function over weeks to months may have important clinical and prognostic implications [39].

Beyond volumetric assessment, CMR combines functional measurements with tissue characterization in the same examination. LGE imaging visualizes irreversible myocardial injury with high spatial resolution and provides a quantitative measure of IS, which has been validated against histology in experimental models and is associated with clinical outcomes after MI [42, 43]. Early and late gadolinium enhancement imaging also allow assessment of MVO. Myocardial edema and the ischemic area at risk have historically been assessed with T2-weighted imaging, but contemporary protocols increasingly rely on parametric T1 and T2 mapping, which offer higher reproducibility and have shown comparable or superior performance for these measurements [44]. Native T1, T2, post-contrast T1, and ECV mapping characterize edema, interstitial expansion, and tissue composition in both infarcted and remote myocardium [14]. This integration of structural, functional, and tissue-level information in a single non-invasive examination is the principal reason CMR is widely used as a reference modality in post-STEMI research and prognostic assessment [13].

2.3.2. LV volumes, mass, and systolic function

LVEF is the most established imaging marker of systolic function and prognosis after STEMI. Reduced LVEF measured soon after primary PCI is linked to mortality and heart failure hospitalization, and remains central to post-MI risk stratification, including decisions about primary-prevention implantable cardioverter-defibrillator therapy [13, 43]. However, LVEF alone does not fully capture post-infarction injury, as patients with similar LVEF may differ significantly in IS, MVO, and remote myocardial status [10, 44].

LV volumes provide complementary prognostic information. LVESV in particular has been associated with mortality after myocardial infarction

and reflects the combined influence of IS, loading conditions, and contractile reserve in the non-infarcted myocardium [45]. LVEDV reflects chamber dilatation and is the volumetric parameter most used to define ALVR, as discussed in Section 2.2. LV mass is less established as an acute prognostic marker after STEMI than volumes or LVEF, but may contribute to characterization of hypertrophic or remote myocardial responses during follow-up [10].

Serial CMR assessment from the acute to the chronic phase provides information beyond a single time point. Changes in LV volumes and LVEF between baseline (typically within the first week after PCI) and follow-up at three to six months help identify patients with adverse remodeling, reverse remodeling, or stable function, each with distinct prognostic implications [38, 39]. The high reproducibility of CMR volumetric measurements (Section 2.3.1) makes these serial comparisons possible. Volumes and ejection fraction, however, do not show where the injury lies or whether tissue-level repair is occurring – questions that LGE and parametric mapping are designed to answer.

2.3.3. Late gadolinium enhancement

LGE is an established reference CMR technique for non-invasive visualization of irreversible myocardial injury. Gadolinium-based contrast agents primarily distribute in the extracellular space, with increased volume of distribution in areas of cell membrane disruption and extracellular matrix expansion, such as acutely necrotic or chronically scarred myocardium [42, 44]. Following intravenous contrast administration, an inversion time is chosen to null the signal from normal myocardium. As a result, infarcted myocardium appears bright on LGE images, while viable myocardium appears dark (Figure 2.3.2). LGE has been validated against histology in experimental MI models and allows high-resolution delineation of the spatial extent of irreversible myocardial injury [42].

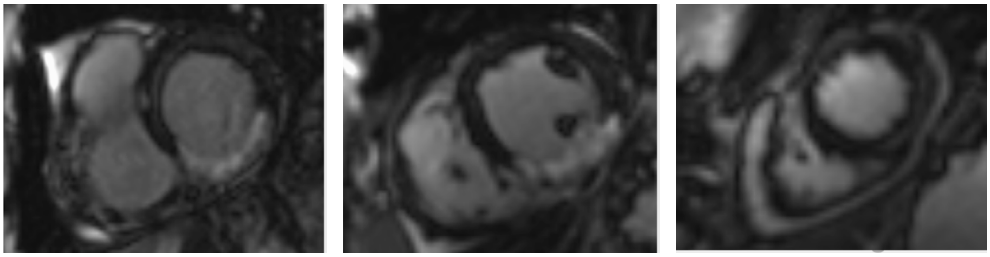

A **B** **C**

Fig. 2.3.2. *Baseline LGE imaging in a patient after STEMI involving the right coronary artery territory*

Short-axis slices are shown from base to apex. **(A)** Basal slice demonstrating hyperenhancement of the inferior septum, inferior wall, and inferolateral wall. **(B)** Mid-ventricular slice with hyperenhancement of the inferior septum and inferior wall. **(C)** Apical slice without hyperenhancement. Hyperenhanced (bright) areas represent LGE.

In the setting of acute STEMI, LGE provides a quantitative assessment of IS, reported as either absolute infarct mass or as a percentage of LV myocardial mass. Quantification methods include manual planimetry and semi-automated threshold-based techniques. The full-width-at-half-maximum (FWHM) method and signal-intensity thresholding, typically using 5 standard deviations above remote myocardium, are commonly used. FWHM is generally preferred because of its higher reproducibility [13]. IS determined within the first month after primary PCI has been strongly associated with subsequent all-cause mortality and hospitalization for heart failure, as evidenced by a pooled patient-level analysis of ten randomized trials involving over 2,600 patients [43]. This relationship was independent of traditional clinical predictors and provided additional prognostic information beyond LVEF.

The transmural extent of LGE, measured as the proportion of myocardial wall thickness with hyperenhancement, predicts segmental functional recovery. Segments with minimal or no transmural enhancement on early post-MI CMR are more likely to recover contractile function, while those with near-transmural infarction rarely improve. This demonstrates a continuous inverse relationship between transmural extent and the likelihood of functional recovery [46]. Transmural extent is therefore valuable for viability assessment and risk stratification in the early post-STEMI period.

LGE imaging also identifies MVO, which provides prognostic information beyond IS and is discussed in the following subsection [13, 44].

2.3.4. Microvascular obstruction

MVO is defined as impaired myocardial tissue-level reperfusion despite restored epicardial coronary flow and is closely associated with the no-reflow pheno-menon. On CMR, MVO appears as a hypointense core within the hyper-enhanced infarct zone on LGE images acquired 10 to 15 minutes after gadolinium administration, indicating delayed contrast wash-in and wash-out in obstructed microvasculature (Figure 2.3.3).

MVO can also be detected during first-pass perfusion imaging as a subendocardial perfusion defect within the infarct territory. MVO is reported as present or absent, and its extent can be quantified in grams or as a percentage of LV myocardial mass. For IS quantification, the hypoenhanced MVO core is conventionally included in the total infarct area to avoid underestimating IS [11, 44]. The original CMR description by Wu and colleagues showed that CMR-defined MVO was present in a substantial proportion of patients after myocardial infarction and identified those at increased risk of adverse cardiovascular events [47].

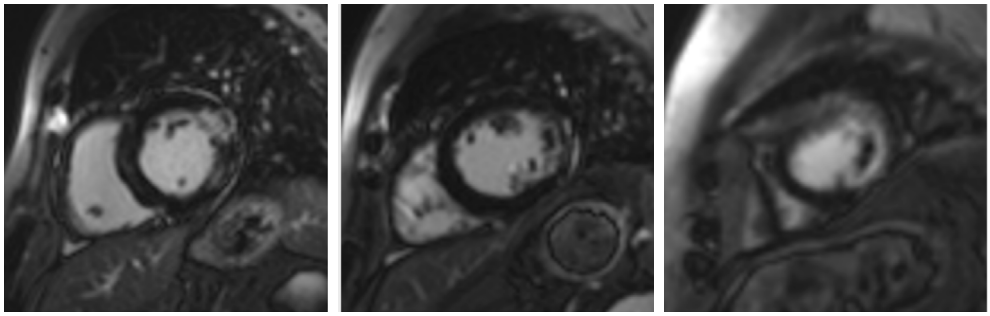

A **B** **C**

Fig. 2.3.3. *MVO on LGE CMR after acute STEMI*

Short-axis slices (A–C) are shown from base to apex. Hypointense regions within the hyperenhanced infarct zone are visible in the lateral wall across the basal, mid-ventricular, and apical slices, consistent with lateral-wall MVO.

2.3.4.1. Pathophysiology

Several mechanisms contribute to the development of MVO, and in clinical STEMI they usually overlap. Distal embolization may occur after plaque rupture and during primary PCI, when atherothrombotic material, including cholesterol crystals, platelet aggregates, and fibrin fragments, is displaced into the distal coronary circulation. This material can mechanically obstruct the downstream microvasculature. Higher angiographic thrombus burden has

been associated with more severe microvascular injury and worse clinical outcomes [7].

Prolonged ischemia also causes direct structural injury to the microcirculation. Capillary endothelial cells and pericytes are damaged, endothelial swelling narrows the vascular lumen, and capillary integrity becomes disrupted. At the same time, edema of surrounding cardiomyocytes may externally compress the capillary network, further limiting tissue perfusion [6].

Microvascular injury may be further amplified after reperfusion. Restoration of flow is accompanied by oxidative stress, intracellular calcium overload, mitochondrial dysfunction, complement activation, and recruitment of inflammatory cells. Neutrophils and platelets may aggregate within capillaries and form intravascular plugs. Neutrophil-derived reactive oxygen species, proteases, and neutrophil extracellular trap formation (NETosis) may further impair tissue-level perfusion despite restoration of epicardial coronary patency [5, 48].

The severity of MVO is also influenced by individual microvascular susceptibility. Patients with diabetes, arterial hypertension, hypercholesterolemia, or advanced age often have pre-existing endothelial dysfunction and reduced vasodilator reserve. During the acute MI, increased release of endothelin-1 and thromboxane A_2, sympathetic activation, and reduced nitric oxide bioavailability may promote sustained constriction of microvessels that were not directly occluded [5, 7].

IMH represents a severe form of micro-vascular injury, caused by leakage of erythrocytes through damaged capillary walls into the myocardial interstitium. MVO and IMH are closely related but not identical: MVO may occur without hemorrhage, whereas IMH is usually found within areas of MVO [49]. On CMR, IMH is most commonly assessed with T2* mapping, which is sensitive to the paramagnetic effects of hemoglobin breakdown products, and recent multicenter data suggest it may carry additional prognostic information beyond MVO [50].

2.3.4.2. Prognostic significance

The prognostic value of MVO has since been confirmed in larger cohorts. Eitel and colleagues, in a multicenter CMR substudy of 738 STEMI patients from the AIDA-STEMI trial, identified MVO of at least 1.4% of LV mass as an independent predictor of major adverse cardiovascular events (MACE) at 12 months, together with IS and LVEF [51]. Van Kranenburg and colleagues, in an analysis of 1,025 STEMI patients, reported that MVO was independently associated with adverse outcomes beyond IS and LVEF [52].

The largest evidence comes from de Waha and colleagues, who pooled individual patient data from 1,688 STEMI patients across seven randomized primary PCI trials with CMR performed within seven days of reperfusion. MVO was independently associated with all-cause mortality and hospitalization for heart failure, with a relationship between MVO extent and event risk after adjustment for IS and LVEF [53]. MVO is therefore considered a marker of severe reperfusion injury and a useful component of CMR-based risk stratification after STEMI.

2.3.4.3. Resolution and persistence at follow-up

MVO typically resolves over the weeks to months following reperfusion. In a minority of patients, however, MVO is detected in the chronic phase. Persistence is more common in patients with larger acute MVO and with intramyocardial hemorrhage, where capillary rupture and residual iron deposition leave the infarct microvasculature permanently damaged [39]. Troger and colleagues recently reported that persistent MVO at 4 and 12 months after STEMI was independently associated with MACE, beyond acute infarct extent and LV function [54].

2.3.5. Parametric mapping

Parametric mapping is a CMR technique that generates pixel-wise quantitative maps of myocardial relaxation times and derived parameters, allowing quantification of native T1, T2, post-contrast T1, and ECV. Relaxation times are expressed in milliseconds, and ECV as a percentage. In contrast to weighted imaging, which provides qualitative signal-intensity differences, parametric mapping yields numerical values that can be compared across myocardial regions, patients, and time points, provided that acqui-sition and analysis methods are standardized [14]. Parametric mapping characterizes tissue changes after STEMI that LGE cannot detect, including diffuse interstitial changes and alterations in the peri-infarct and remote myocardium [44]. The CMR protocol in the present study included native T1, T2, post-contrast T1, and ECV mapping (Figure 2.3.4).

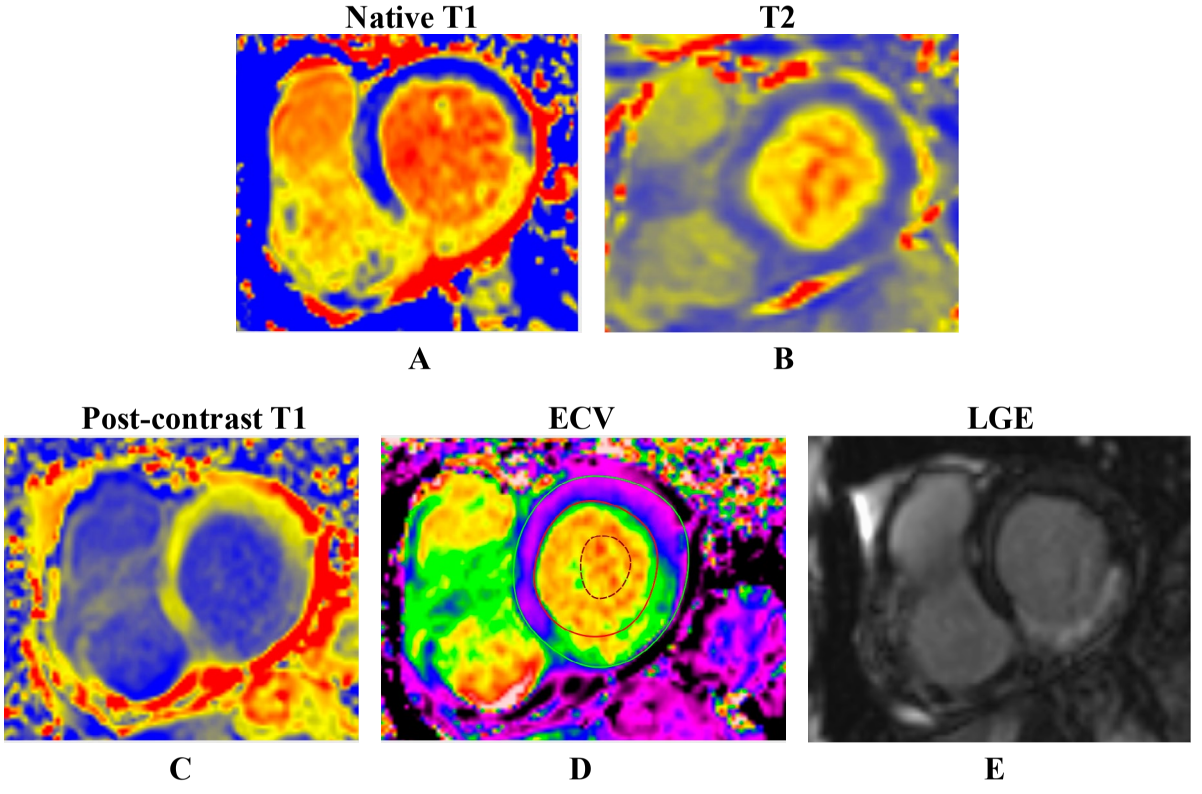

Fig. 2.3.4. *Multiparametric CMR tissue characterization after STEMI in the right coronary artery territory*

Representative short-axis images include native T1 mapping (A), T2 mapping (B), post-contrast T1 mapping (C), extracellular volume (ECV) mapping with myocardial regions of interest (D), and late gadolinium enhancement imaging (E).

2.3.5.1. Native T1 mapping

Native T1 represents the longitudinal relaxation time of the myocardium measured before contrast administration. It is influenced by tissue water content and by changes in myocardial composition, including edema, necrosis, fibrosis, fat, iron, and amyloid deposition [14]. In the context of acute STEMI, values of native T1 are substantially increased within infarcted tissue, reflecting both intracellular and extracellular edema, sarcolemma disruption, and necrosis [44]. More modest elevations may also be observed in the adjacent zone and, in some studies, in remote myocardium. Carrick and colleagues reported that elevated native T1 in remote, non-infarcted myocardium correlated with subsequent LV remodeling and adverse clinical outcomes, raising the possibility that native T1 may reflect a wider myocardial involvement extending beyond the primary infarct [56]. Reinstadler and colleagues similarly showed that remote-zone native T1 measured within the first week after STEMI provided incremental prognostic information in addition to IS and LV function [57].

2.3.5.2. T2 mapping

T2 reflects the transverse relaxation time of myocardium and is sensitive to tissue water content. In acute STEMI, T2 is elevated in infarcted myocardium and in the edematous ischemic territory, reflecting intracellular and extracellular edema [44]. As edema resolves, T2 values decline over the following weeks, making T2 mapping useful for differentiating acute from chronic infarction [14]. Compared with T2-weighted imaging, T2 mapping provides quantitative values in milliseconds that can be analyzed at the segmental level [14]. In the present study, T2 mapping was used to obtain segmental, regional, and mean T2 values for the quantitative assessment of acute myocardial edema. T2-weighted imaging was acquired but was not used for quantitative analysis.

2.3.5.3. Post-contrast T1 and ECV mapping

Post-contrast T1 reflects the longitudinal relaxation time of myocardium after gadolinium administration, when contrast distributes within the extracellular space and shortens local T1. In acute STEMI, post-contrast T1 is markedly shortened within infarcted myocardium because contrast accumulates in the expanded extracellular compartment created by edema, sarcolemma disruption, and necrosis, whereas remote myocardium retains higher post-contrast T1 values [14]. Absolute post-contrast T1 values are influenced by contrast dose, time between injection and acquisition, renal

function, and hematocrit, and are therefore not directly comparable between studies using different acquisition protocols [14]. ECV, calculated from native and post-contrast T1 values together with the patient's hematocrit, partially corrects for these factors and provides a more standardized estimate of the myocardial extracellular compartment [14, 44]. ECV is expressed as a percentage and is sensitive to expansion of the contrast-accessible space, including interstitial edema and diffuse or focal fibrosis. In acute STEMI, ECV is markedly elevated in infarcted myocardium because of edema, sarcolemma rupture, and necrosis. In chronic scar, ECV remains elevated because collagen-rich fibrosis expands the interstitial space [44]. Modest ECV elevations have also been detected in the adjacent and remote zones. Previous studies have demonstrated that ECV elevations in non-infarcted myocardium are associated with subsequent ALVR [58]. Although ECV has been more widely analyzed in post-STEMI cohorts, post-contrast T1 retains independent information about gadolinium kinetics in injured myocardium. In the present study, native T1, post-contrast T1, and ECV were analyzed separately in the infarcted, adjacent, and remote regions to assess each parameter's contribution to predicting ALVR.

2.3.5.4. Regional analysis

Global mean values of native T1, T2, post-contrast T1, and ECV summarize myocardial tissue characteristics but may mask heterogeneity of injury after STEMI. Mapping values can vary substantially between infarcted, adjacent, and remote myocardium, reflecting differences in edema, necrosis, contrast retention, and extracellular expansion. Therefore, post-STEMI CMR studies increasingly assess mapping parameters at the segmental or regional level, often using the American Heart Association 16- or 17-segment model. Infarcted segments are identified on LGE, while non-infarcted regions are defined by their spatial relationship to the infarct zone [11, 14]. The tissue surrounding the infarct is biologically heterogeneous and may include viable, injured, and edematous myocardium. Adjacent regions typically show intermediate mapping values between infarcted and remote myocardium. Remote myocardium may also show changes, and elevated remote-zone native T1 and ECV early after STEMI have been associated with adverse LV remodeling [56–58]. In this study, native T1, T2, post-contrast T1, and ECV were analyzed separately in infarcted, adjacent, and remote regions to assess the regional contribution of myocardial tissue changes to adverse LV remodeling.

2.3.5.5. Follow-up dynamics

Parametric mapping values change significantly between the acute and chronic phases following STEMI. Serial CMR enables detailed characterization of these temporal dynamics [14, 44]. In infarcted myocardium, native T1 and T2 values typically decrease over the initial weeks to months as edema resolves, while ECV may remain elevated due to persistent extracellular expansion and replacement fibrosis [44]. Alterations in adjacent and remote myocardium are more heterogeneous, and incomplete normalization of mapping abnormalities may indicate ongoing tissue remodeling. In a longitudinal CMR study, Mayr and colleagues demonstrated that MVO was present in 61% of STEMI patients within the first week but resolved at subsequent follow-up, whereas infarct-core iron deposition persisted in 29% of patients at nine years [55]. In the current study, paired baseline and six-month CMR examinations were performed to evaluate changes in mapping parameters and their relationship with adverse LV remodeling.

2.4. Myocardial deformation and regional phenotype

2.4.1. Feature-tracking strain

Strain is a mechanical measure describing the relative change in length of a tissue segment between two states. If the segment changes from an initial length L_0 to a length L, strain is defined as:

$$\varepsilon = (L - L_0) / L_0$$

It is expressed as a percentage, with negative values reflecting myocardial shortening. In the left ventricle, deformation is assessed in the longitudinal and circumferential directions: longitudinal strain reflects shortening from base to apex, and circumferential strain reflects shortening around the circumference. Longitudinal strain is derived from long-axis cine views, and circumferential strain from short-axis views [59]. Segmental values may be averaged to obtain global longitudinal strain (GLS) and global circumferential strain (GCS).

CMR feature tracking is a post-processing method that quantifies strain from routinely acquired cine images, without additional scanning [60]. After the endocardial border is outlined manually, the software tracks tissue features throughout the cardiac cycle. GLS and GCS detect contractile impairment more sensitively than LVEF, particularly when regional dysfunction is present [61].

2.4.2. Infarcted, adjacent, and remote myocardium

After STEMI, the LV can be divided into infarcted, adjacent, and remote regions. These regions differ in tissue injury and mechanical function. Segmental strain varies with infarct transmurality and distinguishes LGE-negative, non-transmural, and transmural segments [60].

The infarcted-region shows the greatest mechanical impairment, reflecting acute necrosis, edema, microvascular injury, and later scar formation [60]. Adjacent myocardium represents the border zone between infarcted and remote tissue; its function may be affected by border-zone injury, increased wall stress, and mechanical interaction with neighboring dysfunctional segments [60]. Remote myocardium shows the most preserved deformation but cannot be considered entirely normal.

Changes in remote myocardium after STEMI may include elevated native T1 [57, 62] and increased ECV, even in regions without LGE-defined infarction. Increased ECV in non-infarcted myocardium has been linked to worsening regional contractile function [63]. Remote myocardial abnormalities have been associated with adverse remodeling and worse outcomes [64]. Separate assessment of infarcted, adjacent, and remote regions therefore provides more detailed information than global LV parameters alone.

2.4.3. Regional changes during follow-up

During post-infarction healing, regional myocardial characteristics change as edema resolves and the infarct matures into scar. IS typically decreases over time, although tissue abnormalities within the infarct core may persist for years [55]. Regional strain improves unevenly, reflecting recovery of stunned but viable myocardium and persistent dysfunction in irreversibly injured segments [60]. Characterizing these regional changes over time complements global measures of LV function and forms the basis for the longitudinal regional analysis in the present study.

2.5. Circulating biomarkers

Circulating biomarkers complement CMR by reflecting systemic responses to ischemia and reperfusion, including cardiomyocyte necrosis, ventricular wall stress, inflammation, renal and metabolic dysfunction, platelet-related activity, and lipid-mediator pathways [4, 65].

Routine laboratory markers are widely available and clinically useful, but most are not specific to a single mechanism. Their interpretation may depend on sampling time, renal function, comorbidities, medication use, and the acute stress response.

In this dissertation, routine laboratory markers and specialized circulating biomarkers were analyzed together with CMR-derived measures. This integrated approach was used to evaluate whether systemic biomarker signals were associated with acute IS, MVO, impaired functional recovery, and adverse LV remodeling. The following sections first summarize routine laboratory markers and then focus on the specialized biomarkers relevant to this study: NETosis expression, 20-HETE, and 15(S)-HETE.

2.5.1. Routine laboratory markers

Cardiac troponin is the central marker of myocardial injury and is essential for the diagnosis of myocardial infarction [4, 65]. In reperfused STEMI, higher troponin release reflects larger irreversible myocardial damage, and troponin I measured during the first days after STEMI has been associated with CMR-defined IS and MVO [66, 67].

In reperfused STEMI, N-terminal pro-B-type natriuretic peptide (NT-proBNP) measured 40 hours after admission correlated strongly with CMR-defined IS ($r = 0.74$) and MVO ($r = 0.70$), supporting its role as a complementary marker to troponin that reflects the hemodynamic consequences of myocardial injury [68].

Reduced estimated glomerular filtration rate (eGFR) identifies patients with greater systemic vulnerability and has been linked to slow-flow/no-reflow after primary PCI [69]. Admission hyperglycemia reflects acute metabolic stress and has been associated with MVO after STEMI [70]. Aspartate and alanine aminotransferases may also rise after large infarction, reflecting cardiomyocyte release, hepatic congestion from impaired cardiac output, or coexisting hepatic or skeletal muscle injury. Hepatic transaminases correlate with IS in STEMI cohorts but are not cardiac-specific [71].

Inflammatory and hematological markers, including C-reactive protein (CRP), leukocyte count, and the neutrophil-to-lymphocyte ratio (NLR), reflect the systemic response to myocardial necrosis and reperfusion. Higher CRP and post-PCI NLR have been associated with larger CMR-defined IS, MVO, LV remodeling, or adverse outcomes after acute MI [72, 73]. Platelet count provides an indirect measure of thromboinflammatory activity, but it does not assess platelet function. Nonetheless, lower admission platelet count has been associated with adverse outcomes in acute coronary syndromes [16]. Platelet reactivity may be more directly related to microvascular injury. In STEMI patients treated with dual antiplatelet therapy, suboptimal platelet inhibition was associated with greater CMR-defined MVO and IS [74]. Therefore, platelet count should be interpreted as an accessible but nonspecific marker, while platelet function reflects more specific information.

2.5.2. Thromboinflammation

Thromboinflammation refers to the close two-way interaction between thrombosis and inflammation, where each process amplifies the other [27]. In STEMI, this begins immediately after an atherosclerotic plaque ruptures. The exposed plaque core is highly thrombogenic, leading to platelet adhesion, activation, and aggregation, as well as activation of the coagulation cascade with thrombin generation and fibrin deposition. Within minutes, an occlusive thrombus forms in the epicardial coronary artery, causing downstream myocardial ischemia. Ischemic cardiomyocytes and the damaged extracellular matrix release damage-associated molecular patterns, which activate the endothelium, complement system, and circulating neutrophils and monocytes. Consequently, the inflammatory response starts during ischemia, before the artery is reopened [75].

Thromboinflammation also influences infarct healing. In the initial days after reperfusion, neutrophils and monocytes enter the necrotic zone. Their protease release and phagocytosis remove cellular debris and prepare the lesion for repair. This early inflammatory phase is essential, and excessive suppression can impair scar formation. However, if the response is excessive or unresolved, ongoing protease activity and oxidative stress degrade the extracellular matrix beyond the infarct core, thin the ventricular wall, and promote infarct expansion. Persistent thromboinflammation links the acute injury to ALVR [27, 76].

Standard blood tests provide only a partial picture of thromboinflammation. Leukocyte count, NLR, and CRP indicate systemic inflammation, while platelet count measures platelet availability, not function. These tests do not describe neutrophil-driven processes that obstruct coronary microcirculation. NETosis is a more specific marker, reflecting the release of decondensed chromatin and granule proteins by activated neutrophils [24]. These traps accumulate within the coronary thrombus in STEMI [25]. Elevated NETosis expression at admission has been linked to MACE after STEMI [77].

2.5.3. NETosis and microvascular injury

NET release in STEMI is triggered locally by multiple stimuli, including ischemic cell death, endothelial activation, oxidative stress, complement activation, and contact with activated platelets [27, 78]. Although NET formation is part of innate immune defense, in this setting it can amplify local thromboinflammation and contribute to microvascular injury [26].

NETs may contribute to microvascular injury through several mechanisms. Their DNA–histone scaffold binds platelets, erythrocytes, fibrinogen, von Willebrand factor, and coagulation factors, supporting thrombus growth and

stabilizing microthrombi. NET-associated histones and proteases can also injure endothelial cells, increase vascular permeability, and amplify local inflammation. In the reperfused infarct territory, these effects may promote capillary plugging and impaired tissue-level perfusion despite restoration of epicardial coronary flow [26].

The link between NETs and reperfusion injury has been documented in several STEMI studies. Mangold and colleagues first showed that NETs accumulate within the culprit coronary thrombus, where higher NET burden correlated with impaired ST-segment resolution after primary PCI [25]. A later CMR-based study from the same group extended this observation: at the culprit site, higher extracellular DNA and lower endogenous DNase activity tracked with greater MVO and lower LVEF [26]. Circulating NET-related markers measured shortly after STEMI have been linked to MACE during follow-up [77, 79]. Together, these data show that NETosis is a marker of thromboinflammatory microvascular injury rather than of cardiomyocyte necrosis per se.

NETosis is closely connected with platelet activation. Activated platelets stimulate neutrophils to release NETs, and once formed, NETs serve as an adhesive surface for further platelet recruitment and fibrin deposition. The result is a self-reinforcing loop linking neutrophils, platelets, coagulation, and endothelial injury [27, 28]. These observations suggest that NETosis and platelet measures reflect partly overlapping aspects of thromboinflammatory microvascular injury.

2.5.4. 20-hydroxyeicosatetraenoic acid

20-HETE is a cytochrome P450-derived metabolite of arachidonic acid. It is produced mainly by CYP4A and CYP4F enzymes and acts as a vasoactive lipid mediator. It participates in the regulation of vascular tone, endothelial function, oxidative stress, inflammation, and renal–vascular homeostasis [17, 18].

In myocardial ischemia–reperfusion injury, 20-HETE may aggravate tissue damage through two linked mechanisms. First, as a potent vasoconstrictor, 20-HETE narrows small coronary arteries and impairs microvascular perfusion during the period of reperfusion. Second, 20-HETE activates NADPH oxidase in vascular smooth muscle and endothelial cells, increasing the production of reactive oxygen species, which damage cell membranes, mitochondria, and the endothelial barrier. Together, these effects worsen the damage caused by ischemia alone. Inhibition of 20-HETE synthesis has been shown to reduce IS and oxidative stress in experimental ischemia–reperfusion models [17, 20].

20-HETE also contributes to thrombosis. In experimental studies, 20-HETE induces endothelial cells to release von Willebrand factor and express adhesion molecules, thereby attracting platelets to the vessel wall and promoting thrombus formation in the microcirculation [19]. Clinically, in a prospective cohort of 2,239 patients with stable coronary artery disease, higher baseline 20-HETE was associated with subsequent acute myocardial infarction during 2-year follow-up [80]. Together, these data suggest that 20-HETE is a vasoactive lipid with potential relevance to atherosclerotic risk and acute microvascular injury.

Direct human evidence linking circulating 20-HETE with CMR-defined myocardial injury after STEMI is limited. Previous metabolomic studies have shown dynamic changes in eicosanoid concentrations after PCI, including 20-HETE. However, these studies mainly described circulating profiles and their correlations with biochemical injury markers such as troponin T and creatine kinase, not serial CMR-defined infarct healing or remodeling [29, 30]. To our knowledge, no clinical study has examined the relationship between circulating 20-HETE and the broader spectrum of CMR endpoints, including IS, MVO, infarct shrinkage, functional recovery, and ALVR in STEMI patients. The clinical role of 20-HETE in post-STEMI remodeling remains insufficiently defined.

2.5.5. 15(S)-hydroxyeicosatetraenoic acid

15(S)-HETE is a lipid mediator formed from arachidonic acid by 12/15-lipoxygenase; in the literature it is often referred to as 15-HETE.

Experimental data and studies in human myocardial tissue suggest a potential role of 15-HETE in post-infarction injury and repair. In human ischemic heart tissue, 15-HETE has been detected at higher concentrations than in non-ischemic tissue and was shown to enhance clot formation [21]. More recently, 15-HETE was reported to be increased in experimental myocardial infarction and in patients with myocardial infarction, and to promote fibroblast-to-myofibroblast conversion through a 15-HETE-mediated pathway, which aggravates myocardial fibrosis [22]. This enzyme system is also involved in post-infarction repair. In experimental myocardial infarction, deletion of 12/15-lipoxygenase improved resolution of inflammation and reduced fibrosis and adverse remodeling [23].

Despite these results, direct clinical data linking circulating 15(S)-HETE with CMR-defined myocardial injury, infarct healing, or LV remodeling after STEMI remain limited. Its role in post-infarction remodeling therefore remains insufficiently defined.

2.6. Predictors of outcomes after STEMI

2.6.1. Predictors of impaired functional recovery

Recovery of LV systolic function after STEMI depends largely on the severity of the initial injury. Lower baseline LVEF, larger LVESV, and larger IS have each been associated with worse functional outcome and higher mortality [43, 45]. Early imaging of infarct characteristics after reperfusion predicts late systolic dysfunction, adding to traditional clinical risk factors [81]. Microvascular injury adds information beyond IS: segments with MVO are less likely to recover. IMH and persistent MVO identify patients with poorer recovery [50, 52, 56].

Beyond global indices, myocardial deformation reflects regional contractile reserve, and circumferential strain has been particularly informative for functional recovery. Infarct-region circumferential strain provides an assessment of contractile improvement beyond IS [82] and predicts segmental recovery independently of infarct transmurality [83]. Longitudinal strain depends mainly on subendocardial fibers, which are the first to be affected by ischemia. Because even limited subendocardial injury impairs it, longitudinal strain signals damage early but does not show how deep that damage extends. Circumferential strain depends on the mid-wall fibers, which fail only as the infarct extends through the wall, so it more specifically reflects the depth of irreversible injury [61]. Early CMR markers of infarct severity, microvascular injury, and regional deformation are therefore the principal imaging predictors of LV functional recovery, although the most informative marker varies with how recovery is defined.

2.6.2. Predictors of adverse remodeling

Building on the definitions in Section 2.2, the markers that predict adverse remodeling are largely those that quantify injury severity. IMH and persistent MVO mark the highest-risk phenotypes [49, 50]. Tissue characterization adds further predictive information: infarcted-region ECV predicts later volume enlargement, and contrast-enhanced mapping has outperformed non-contrast mapping for forecasting six-month remodeling [62], while higher native T1 and ECV in the remote, non-infarcted myocardium predicts adverse remodeling independently of IS [39, 56, 57]. Myocardial deformation carries additional prognostic information, although the relevant parameter differs from that for functional recovery. While circumferential strain most closely reflects recovery (Section 2.6.1), global longitudinal strain has emerged as the main deformational predictor of volume-defined remodeling. In a large feature-tracking cohort (n = 232), impaired global longitudinal strain was

independently associated with adverse remodeling after adjustment for IS and ejection fraction [84].

2.6.3. Combined imaging and biomarkers

Circulating biomarkers have been analyzed across several pathways. Natriuretic peptides and markers of fibrosis and matrix turnover, including galectin-3 and soluble ST2, have been associated with post-infarction remodeling [85–87]. Among thromboinflammatory markers, CRP relates to IS, MVO, and remodeling [72], platelet reactivity was independently associated with adverse remodeling in the REMODELING trial [88], and NET markers reflect IS and ventricular function [79]. Few studies, however, have integrated CMR with circulating biomarkers within the same cohort; most work has examined the two domains in isolation, either relating blood markers to an imaging finding such as MVO [71] or using imaging alone to predict long-term outcomes [64] rather than testing their combined, incremental value. Whether early biomarkers add prognostic information beyond established imaging predictors of recovery and remodeling therefore remains poorly defined.

3. METHODS

3.1. Study design and setting

3.1.1. Overview of the research

This prospective, observational, single-center study was carried out at the Cardiology Department of the Hospital of the Lithuanian University of Health Sciences, Kauno klinikos (Kaunas, Lithuania). Between September 2020 and January 2022, consecutive patients with a first STEMI undergoing reperfusion were recruited. Diagnosis was made according to the Fourth Universal Definition of Myocardial Infarction [65]: an acute coronary occlusion on angiography in a patient with ischemic symptoms, ST-segment elevation on the surface ECG, and troponin I above the 0.04 μg/L reference threshold. All patients underwent reperfusion within 24 hours of symptom onset. Of the 112 initially enrolled patients, 104 underwent primary PCI, whereas 8 received thrombolysis followed by PCI. All patients received guideline-directed medical therapy in accordance with the 2017 European Society of Cardiology guidelines for the management of acute myocardial infarction in patients presenting with ST-segment elevation [89]. Baseline CMR imaging was performed at a median of 3 days [interquartile range (IQR), 2–5] after reperfusion therapy, and follow-up CMR was scheduled at 6 months (±11 days). Two main analytic cohorts were defined according to imaging availability: the baseline CMR cohort (n = 105), used for acute-phase analyses, and the paired-CMR cohort (n = 93), used for longitudinal analyses. The number of patients included in individual subanalyses varied according to data availability and image evaluability.

3.2. Study population and patient flow

The study population consisted of consecutive patients with first STEMI treated with reperfusion therapy and screened for baseline CMR during the index hospitalization. Of the 112 initially enrolled patients, 7 were excluded before baseline CMR: 4 because of claustrophobia, 2 declined participation, and 1 died before the baseline examination. Thus, 105 patients underwent baseline CMR and constituted the baseline CMR cohort. Follow-up CMR was scheduled 6 months after the index event. Repeat CMR was unavailable in 12 patients: 2 were unreachable, 9 declined follow-up imaging, and 1 underwent implantable cardioverter-defibrillator implantation, which precluded further CMR. The remaining 93 patients had paired baseline and 6-month follow-up CMR data and constituted the paired-CMR cohort.

The baseline CMR cohort was used to characterize the acute myocardial injury phenotype, including IS, MVO, global left ventricular structure and function, segmental myocardial characteristics, and associations with clinical, procedural, laboratory, and biomarker variables. The paired-CMR cohort was used for longitudinal analyses of left ventricular structural and functional changes, IS regression, myocardial deformation recovery, impaired functional recovery, and adverse left ventricular remodeling.

The availability of individual CMR sequences and laboratory measurements varied slightly. At baseline, cine images were not acquired or were non-evaluable in 1 patient; late gadolinium enhancement images in 2 patients; T1 mapping in 5 patients; post-contrast T1 mapping and ECV data in 6 patients; and T2 mapping in 9 patients. At follow-up, T1 mapping was not acquired or was non-evaluable in 2 patients, post-contrast T1 mapping and ECV data in 7 patients, and T2 mapping in 1 patient.

Routine laboratory data were available for most patients in the baseline cohort, including routine laboratory parameters for 105 patients and B-type natriuretic peptide (BNP) for 102 patients. Specialized biomarker analyses were available for 20-HETE in 105 patients, 15(S)-HETE in 104 patients, and NETosis expression in 105 patients. The exact analytic sample size is reported separately for each analysis in the corresponding Results tables and figures. The overall study flow is shown in Figure 3.2.1.

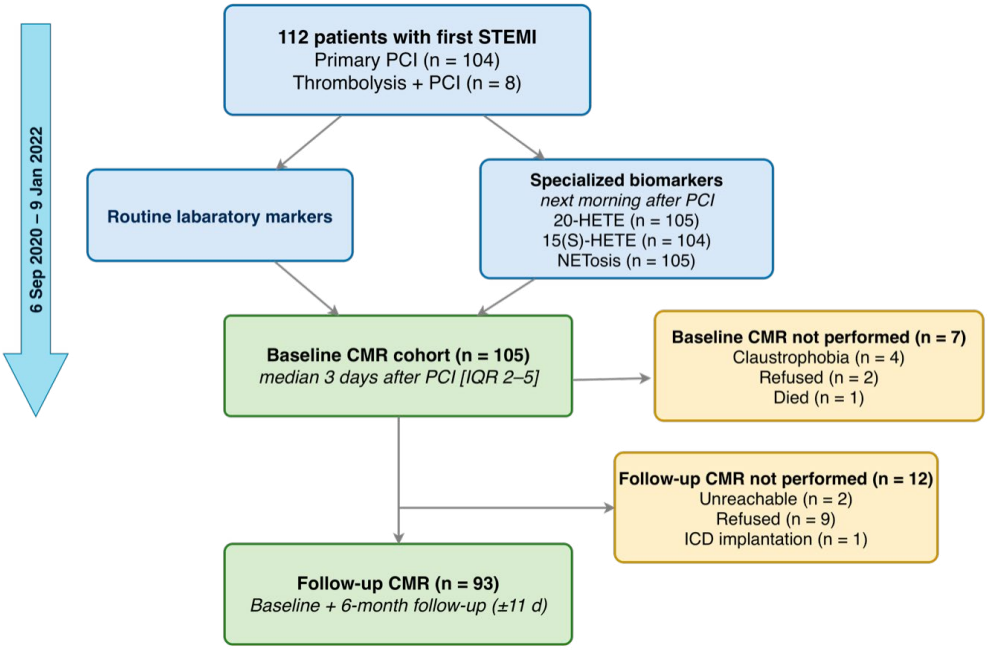

Fig. 3.2.1. *Study flow diagram*

Of 112 patients with a first STEMI, 7 were excluded before baseline CMR, and 105 underwent baseline imaging. Follow-up CMR at 6 months was available in 93 patients. The number of patients in specific analyses varied slightly according to data availability and evaluability.

3.3. Eligibility criteria

Patients were eligible for inclusion if they were older than 18 years and presented with a first STEMI treated with reperfusion therapy within 24 hours of symptom onset.

Patients were excluded if they had IHD, including previous MI, previous PCI, or coronary artery bypass grafting; moderate or severe valvular heart disease, including prior valve surgery; previous myocarditis; active malignancy; an eGFR below 30 mL/min/1.73 m²; or pregnancy. Additional exclusion criteria were standard contraindications to CMR, including incompatible ferromagnetic implants or devices, intracranial aneurysm clips, and severe claustrophobia. Patients with atrial fibrillation at the time of CMR acquisition were also excluded because of its potential impact on image quality and strain analysis.

The study was conducted in accordance with the Declaration of Helsinki and was approved by the Kaunas Regional Biomedical Research Ethics

Committee (Approval No. BE-2-6, approved 5 February 2020). All patients provided written informed consent before enrollment.

3.4. Clinical, angiographic, and procedural data

Clinical data were extracted from electronic medical records and included age, sex, comorbidities, cardiovascular risk factors, pre-hospital medications, and anthropometric measurements (weight and height). Body surface area (BSA) was calculated using the Du Bois formula:

$BSA = 0.007184 \times \text{weight (kg)}^{0.425} \times \text{height (cm)}^{0.725}$.

Body mass index (BMI) was calculated as weight in kilograms divided by height in meters squared.

Angiographic and procedural variables included the culprit artery, pre- and post-procedural Thrombolysis in Myocardial Infarction (TIMI) flow grade, multivessel coronary artery disease, non-culprit PCI during the index hospitalization, thrombus aspiration, and glycoprotein IIb/IIIa inhibitor use. Reperfusion timing was characterized by two intervals: the symptom-to-balloon time, measured from symptom onset to first device deployment during PCI, and the door-to-balloon time, measured from hospital arrival to first device deployment.

In-hospital complications and clinical severity indicators of STEMI were recorded and included Killip class, atrial fibrillation or flutter, ventricular tachycardia or fibrillation, and second- or third-degree atrioventricular block. For descriptive and comparative analyses, Killip class was also categorized as Killip class ≥ 2.

3.5. Blood sampling and biomarker assessment

Fasting venous blood samples were collected on the morning after PCI. Routine laboratory parameters were measured in the central laboratory of the Hospital of the Lithuanian University of Health Sciences, Kauno klinikos, using standard institutional methods, whereas specialized biomarker analyses were performed at the Laboratory of Molecular Cardiology, Institute of Cardiology, Lithuanian University of Health Sciences.

3.5.1. Routine laboratory parameters

The complete blood count included hemoglobin, red blood cell count, white blood cell count, platelet count, and the differential leukocyte count (neutrophils and lymphocytes). The NLR was calculated as the absolute neutrophil count divided by the absolute lymphocyte count and used as an index of systemic inflammation. Biochemical parameters included cardiac troponin I, BNP,

creatinine, eGFR, urea, glucose, HbA1c, and serum electrolytes (sodium and potassium). The lipid profile comprised total cholesterol, high-density lipoprotein (HDL) cholesterol, low-density lipoprotein (LDL) cholesterol, and triglycerides. Liver enzymes included alanine aminotransferase (ALT) and aspartate aminotransferase (AST). Systemic inflammation was additionally assessed using CRP.

3.5.2. 20-HETE and 15(S)-HETE assessment

Plasma samples were used to measure 20-HETE and 15(S)-HETE. Eicosanoids were isolated from plasma by organic extraction. Samples were supplemented with butylated hydroxytoluene (10 mg/mL), acidified with acetic acid to approximately pH 4, and extracted with ethyl acetate (1:1, v/v). The samples were vortex-mixed for 2 minutes and centrifuged at 2000 rpm for 10 minutes at room temperature. The organic phase was evaporated to dryness under a stream of nitrogen at 40 °C using a Multivap Nitrogen Evaporator (Organomation, USA), and the residue was reconstituted in ethanol and diluted with the sample dilution buffer before analysis. Concentrations of 20-HETE and 15(S)-HETE were determined using commercially available competitive enzyme-linked immunosorbent assay kits (Abcam, UK; Cat# ab175817 and ab133035, respectively). Optical density was measured using an Infinite M Plex microplate reader (Tecan, Switzerland) at 450 nm for 20-HETE and at 405 nm with a reference wavelength of 590 nm for 15(S)-HETE.

3.5.3. NETosis assessment

NETosis expression was assessed by measuring the activity of neutrophil elastase, a NETosis marker, in serum using a colorimetric assay kit (Abcam, UK; Cat# ab235979) according to the manufacturer's instructions. The reported sensitivity of this assay was 0.56 mU. Serum was diluted 1:10 with NET assay buffer and combined with neutrophil elastase substrate. Neutrophil elastase selectively cleaves the substrate to yield a 4-nitroaniline product that absorbs light at 405 nm. The 96-well plate containing the substrate was incubated for 1.5 hours at 37 °C, and the absorbance of the samples was read at 405 nm using the Infinite M Plex microplate reader.

3.6. Cardiac magnetic resonance imaging

3.6.1. CMR acquisition protocol

All CMR examinations were performed on the same 3.0 T clinical scanner (Magnetom Skyra, Siemens Healthineers, Erlangen, Germany) using an 18-channel phased-array body coil and a spine coil. The same standardized

imaging protocol was applied at baseline and at 6-month follow-up to allow direct comparison between time points. All image acquisitions were electrocardiographically gated and performed during end-expiratory breath-holds. The imaging protocol was performed in accordance with Society for Cardiovascular Magnetic Resonance (SCMR) recommendations for CMR assessment after myocardial infarction [11].

3.6.2. Cine imaging

Cine images were acquired with a balanced steady-state free precession (bSSFP) sequence, retrospectively gated and obtained during end-expiratory breath-holds (echo time 1.39 ms, repetition time 2.5 ms, field of view 320–360 mm, matrix 192 × 146, flip angle 47°, slice thickness 8 mm, inter-slice gap 2 mm). A contiguous short-axis stack covered the left ventricle from base to apex, and two-, three-, and four-chamber long-axis views were also acquired. These images were used for volumetric, functional, and feature-tracking strain analysis.

3.6.3. T1 and T2 mapping

Native T1 mapping used an electrocardiography-gated single-shot modified Look-Locker inversion recovery (MOLLI) sequence with a 5(3)3 scheme (eight images over eleven heartbeats, bSSFP readout; echo time 1.07 ms, repetition time 2.58 ms, field of view 320–360 mm, matrix 192 × 144, flip angle 35°, slice thickness 8 mm, minimum inversion time 100 ms with 80 ms increments, generalized autocalibrating partially parallel acquisition factor 2, imaging window 136 ms per heartbeat). The same sequence was repeated approximately 15 minutes after contrast for post-contrast T1 mapping. T2 mapping used a T2-prepared bSSFP sequence with preparation times of 0, 30, and 55 ms.

Reference ranges for the mapping parameters were established at our center in 25 healthy volunteers (mean age 35 ± 8 years; 52% male) imaged on the same scanner with identical sequences and post-processing: native T1 1250 ± 45 ms, post-contrast T1 385 ± 42 ms, ECV 26.2 ± 2.8%, and T2 43.5 ± 2.5 ms.

3.6.4. Late gadolinium enhancement imaging

Late gadolinium enhancement was performed 10–15 minutes after intravenous gadobutrol (0.2 mmol/kg; Gadovist, Bayer Healthcare, Berlin, Germany), using a short-axis stack covering the entire left ventricle. A phase-sensitive inversion-recovery gradient-echo sequence was used, with the inversion time set to null normal myocardium.

3.7. CMR image analysis

All images were analyzed offline by a single reader with more than five years of CMR experience (Agneta Virbickienė), blinded to clinical and outcome data, using commercially available software (Medis Suite, version 3.2; Medis Medical Imaging Systems, Leiden, The Netherlands).

3.7.1. Left ventricular volumes, mass, and systolic function

Endocardial and epicardial borders were traced on the short-axis cine stack at end-diastole and end-systole. Papillary muscles and trabeculations were treated as part of the cavity (blood-pool method). From these contours, LVEDV, LVESV, LVEF, stroke volume, and myocardial mass were derived; volumes and mass were indexed to BSA. Volumetric quantification was carried out in QMass, following SCMR standards for left ventricular function and mass quantification [11].

3.7.2. Infarct size and microvascular obstruction

IS was measured on the LGE short-axis stack after manual tracing of endocardial and epicardial borders on every slice. Hyperenhanced myocardium was defined using the signal-threshold-versus-reference-myocardium approach, with a cut-off greater than 5 standard deviations above the mean signal of the remote myocardium [90, 91]. MVO was identified as a hypointense core within a hyperenhanced region and was incorporated into the total infarct measurement. Both IS and MVO were expressed in grams and as a percentage of total LV mass.

3.7.3. Segmental myocardial classification

Myocardial segments were assigned according to LGE using the American Heart Association (AHA) 16-segment model, with the anterior right ventricular insertion point as the reference landmark [92]. Segments containing any enhancement were classified as infarcted, those immediately bordering an infarcted segment as adjacent, and all remaining non-enhanced segments as remote. The same classification was used consistently for the strain and parametric mapping analyses. A representative example of segment classification across the three short-axis slices is shown in Figure 3.7.1.

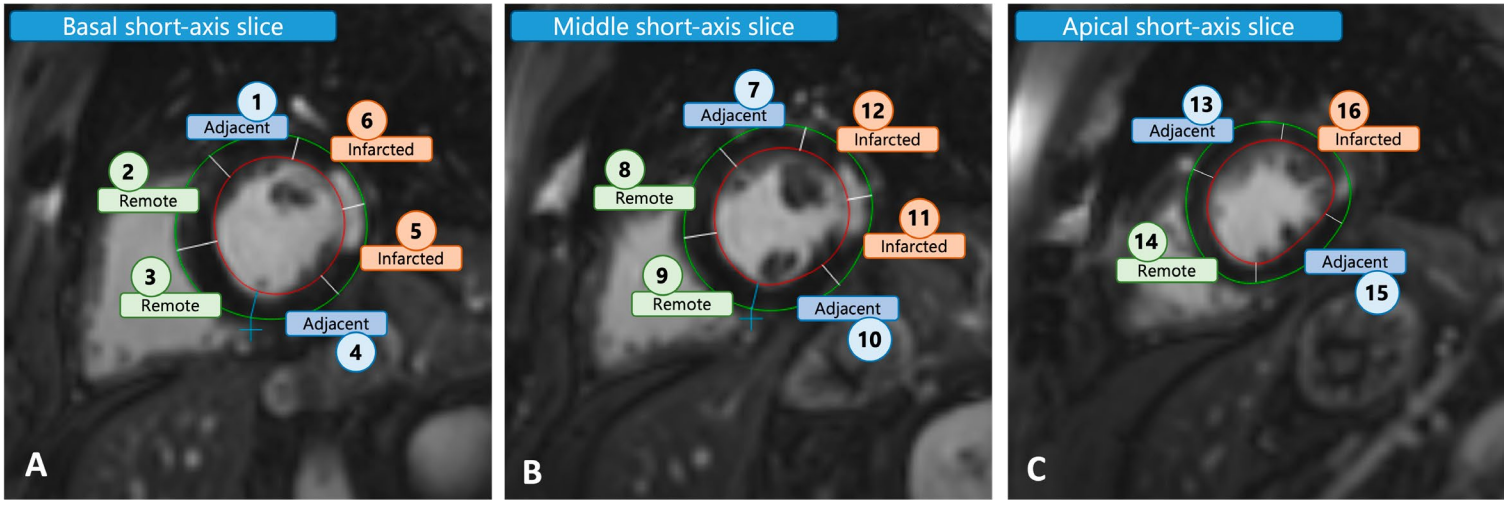

Fig. 3.7.1. *Representative CMR images of myocardial segment classification based on late gadolinium enhancement (LGE) according to the American Heart Association (AHA) 16-segment model*

Basal (A), mid-ventricular (B), and apical (C) short-axis slices illustrate infarcted, adjacent, and remote segments used for segmental strain and parametric mapping analyses. CMR – cardiovascular magnetic resonance.

3.7.4. Feature-tracking strain analysis

Myocardial deformation was assessed by feature tracking in QStrain. GLS was derived from the two-, three-, and four-chamber long-axis views, and GCS from the basal, mid-ventricular, and apical short-axis slices. Endocardial and epicardial contours were drawn at end-diastole and propagated automatically across the cardiac cycle, with manual correction where tracking was inadequate. GLS and GCS were calculated as the mean of segmental values. Segmental strain values were additionally averaged within the infarcted, adjacent, and remote regions defined in Section 3.7.3.

3.7.5. Parametric mapping analysis

Parametric mapping was analyzed on the basal, mid-ventricular, and apical short-axis slices. Endocardial and epicardial contours were drawn with a 10% offset from the blood-pool and epicardial boundaries to limit partial-volume contamination. Native T1, post-contrast T1, and T2 were measured, and the ECV fraction was calculated from myocardial and blood-pool T1 values before and after contrast, corrected for the hematocrit obtained within 24 hours of the CMR examination [14]. For each patient, native T1, post-contrast T1, T2, and ECV were obtained for all 16 segments and averaged within the infarcted, adjacent, and remote regions across the three slices. Global values were derived as the segment-weighted average.

3.8. Study outcomes

Four outcomes were evaluated.

3.8.1. Large acute infarct size

Large acute IS was defined as a baseline IS in the upper tertile of the study cohort ($\geq 41.91\%$ of LV mass).

3.8.2. Microvascular obstruction

MVO was assessed on baseline CMR using LGE images and classified as present or absent.

3.8.3. Impaired left ventricular functional recovery

Impaired LV functional recovery was defined as a follow-up LVEF below 50% on 6-month CMR, a threshold used to denote reduced LV systolic function in CMR-based STEMI studies [39]. Patients were dichotomized into

impaired recovery (follow-up LVEF < 50%) and preserved function (follow-up LVEF ≥ 50%).

3.8.4. Adverse left ventricular remodeling

ALVR was defined as an increase of at least 12% in both LVEDV and LVESV at 6-month follow-up relative to baseline. This CMR-specific threshold, proposed by Bulluck et al. [39], was selected because a concurrent rise in both volumes reflects a more consistent pattern of adverse ventricular enlargement than a change in either volume alone, and because these reproducibility-based cut-offs represent the minimal detectable change beyond CMR measurement variability.

3.9. Statistical analysis

3.9.1. General approach and data presentation

Data distribution was tested with the Shapiro–Wilk test. Normally distributed continuous variables are given as mean (standard deviation), and non-normally distributed variables as median [interquartile range]. Categorical variables are given as numbers and percentages. The number of patients included differed between analyses, depending on data availability, and is given in each table and figure. All tests were two-sided, and $p < 0.05$ was considered significant.

3.9.2. Group comparisons

Differences in continuous variables between two groups were assessed using the Mann–Whitney U test for non-normally distributed data and the Student's t-test for normally distributed data. Categorical variables were compared using the chi-square test or Fisher's exact test, as appropriate.

3.9.3. Within-patient longitudinal comparisons

Changes in CMR parameters between baseline and 6-month follow-up were evaluated using the Wilcoxon signed-rank test for paired data. For comparisons across the infarcted, adjacent, and remote myocardial regions, the Friedman test was used to assess overall differences, followed by pairwise Wilcoxon signed-rank tests with Bonferroni correction for multiple comparisons.

3.9.4. Correlation analyses

Associations between continuous laboratory, biomarker, and cardiac magnetic resonance variables were evaluated using the Spearman rank correlation coefficient (r_s). The strength of correlation was interpreted according to Schober et al. as negligible ($|r_s|$ 0.00–0.09), weak (0.10–0.39), moderate (0.40–0.69), strong (0.70–0.89), or very strong (0.90–1.00) [93].

3.9.5. Logistic regression analyses

Univariable and multivariable binary logistic regression were used to identify factors associated with four outcomes: large acute IS (defined as an IS in the upper tertile of the study cohort, corresponding to ≥ 41.91% of LV mass), MVO presence, impaired left ventricular functional recovery, and adverse left ventricular remodeling. Demographic, clinical, angiographic, procedural, laboratory, and biomarker variables were first tested in univariable models. Variables for the multivariable models were selected based on clinical relevance, intercorrelation among candidate predictors, and the limited number of outcome events, to reduce overfitting. Results are given as odds ratios with 95% confidence intervals.

3.9.6. Receiver operating characteristic analysis

The discriminatory performance of selected laboratory and biomarker variables was assessed using ROC analysis for MVO presence, impaired LV functional recovery, and adverse LV remodeling, with the area under the curve (AUC) reported with its 95% confidence interval. Optimal cut-off values were determined using the Youden index.

3.9.7. Software

Statistical analyses were performed using IBM SPSS Statistics, version 31.0 (IBM Corp., Armonk, NY, USA).

4. RESULTS

4.1. Study population characteristics

4.1.1. Clinical and procedural characteristics

The baseline study cohort included 105 patients with a first STEMI. Primary PCI was performed in 97 patients (92.4%), while 8 patients (7.6%) received thrombolysis followed by PCI. The mean age was 60.3 (10.0) years, and 81 patients (77.1%) were men. Mean BMI reached 28.1 (4.5) kg/m².

Cardiovascular risk factors were common in this cohort. Dyslipidemia was documented in 95 patients (90.5%) and arterial hypertension in 84 (80.0%). More than half of the patients (54, 51.4%) were current smokers at the time of admission. A family history of coronary artery disease was reported by 36 patients (34.3%), and diabetes mellitus was present in 14 (13.3%).

Mean symptom-to-balloon time was 424.8 (286.6) minutes, and door-to-balloon time was 65.0 (63.9) minutes. Anterior STEMI was diagnosed in 43 patients (41.0%). Pre-PCI TIMI flow 0–1 was documented in 71.4% of patients, and post-PCI TIMI flow 3 was achieved in 93.3%. Multivessel coronary artery disease was present in 52 patients (49.5%). Killip class ≥ 2 was observed in 27 patients (25.7%), and sustained ventricular arrhythmias occurred in 9 (8.6%). Baseline clinical and procedural characteristics are summarized in Table 4.1.1. A summary of the study cohort and available investigations is provided in Figure 4.1.1.

Table 4.1.1. *Baseline clinical and procedural characteristics of the study cohort*

Characteristic	Overall (n = 105)
Demographics and cardiovascular risk factors	
Age, years	60.3 (10.0)
Male sex, n (%)	81 (77.1)
BMI, kg/m²	28.1 (4.5)
Family history of CAD, n (%)	36 (34.3)
Diabetes mellitus, n (%)	14 (13.3)
Arterial hypertension, n (%)	84 (80.0)
Dyslipidemia, n (%)	95 (90.5)
Current smoking, n (%)	54 (51.4)
Pre-hospital medications	
Beta-blockers, n (%)	34 (32.4)
ACE inhibitor/ARB, n (%)	47 (44.8)
Calcium channel blockers, n (%)	11 (10.5)

Table 4.1.1 cont.

Characteristic	Overall (n = 105)
Thiazide/thiazide-like diuretics, n (%)	14 (13.3)
Statins, n (%)	8 (7.6)
Antiplatelet therapy, n (%)	3 (2.9)
Clinical and procedural characteristics	
Symptom-to-balloon time, min	424.8 (286.6)
Door-to-balloon time, min	65.0 (63.9)
Thrombolysis before PCI, n (%)	8 (7.6)
Anterior MI, n (%)	43 (41.0)
Culprit artery: LAD, n (%)	43 (41.0)
Culprit artery: RCA, n (%)	47 (44.8)
Culprit artery: LCX, n (%)	15 (14.3)
Pre-PCI TIMI flow 0–1, n (%)	75 (71.4)
Post-PCI TIMI flow 3, n (%)	98 (93.3)
Thrombus aspiration, n (%)	13 (12.4)
Multivessel disease, n (%)	52 (49.5)
Non-culprit PCI during hospitalization, n (%)	27 (25.7)
GP IIb/IIIa inhibitor use, n (%)	4 (3.8)
Clinical complications during STEMI	
Killip class ≥ 2, n (%)	27 (25.7)
Atrial fibrillation/flutter, n (%)	7 (6.7)
Ventricular tachycardia/fibrillation, n (%)	9 (8.6)
Second-degree or third-degree AV block, n (%)	5 (4.8)

ACE – angiotensin-converting enzyme; ARB – angiotensin receptor blocker; AV – atrioventricular; BMI – body mass index; CAD – coronary artery disease; GP – glycoprotein; LAD – left anterior descending artery; LCX – left circumflex artery; MI – myocardial infarction; PCI – percutaneous coronary intervention; RCA – right coronary artery; STEMI – ST-segment elevation myocardial infarction; TIMI – Thrombolysis in Myocardial Infarction. Values are mean (SD) or n (%), as appropriate.

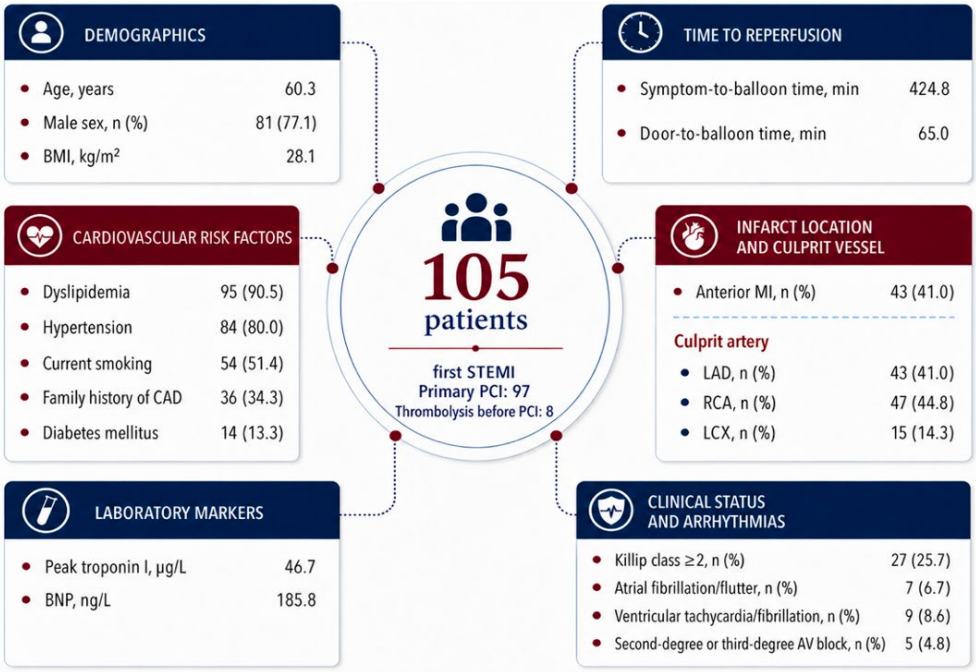

Fig. 4.1.1. *Overview of the study cohort*

AV – atrioventricular; BMI – body mass index; BNP – B-type natriuretic peptide; CAD – coronary artery disease; LAD – left anterior descending artery; LCX – left circumflex artery; MI – myocardial infarction; PCI – percutaneous coronary intervention; RCA – right coronary artery; STEMI – ST-segment elevation myocardial infarction.

4.1.2. Baseline laboratory parameters and specialized biomarkers

Mean peak troponin I concentration was 46.7 (52.6) µg/L and mean BNP was 185.8 (127.2) ng/L. Renal function was preserved (mean eGFR 91.1 (17.7) mL/min/1.73 m²). The lipid profile reflected the high prevalence of dyslipidemia in the cohort, with mean LDL cholesterol of 3.9 (1.0) mmol/L. Specialized biomarkers showed wide interindividual variability: mean 20-HETE was 122.6 (252.5) ng/mL, 15(S)-HETE 1.1 (1.4) ng/mL, and NETosis expression 62.5 (41.2) mU/mL. Baseline laboratory parameters and specialized biomarkers are presented in Table 4.1.2.

Table 4.1.2. *Baseline laboratory and specialized biomarker characteristics of the study cohort*

Characteristic	Overall (n = 105)
Routine laboratory parameters	
Peak troponin I, μg/L	46.7 (52.6)
BNP, ng/L	185.8 (127.2)
eGFR, mL/min/1.73 m²	91.1 (17.7)
Hemoglobin, g/L	140.9 (15.4)
Platelet count, ×10⁹/L	226.3 (59.2)
Total cholesterol, mmol/L	5.8 (1.4)
HDL cholesterol, mmol/L	1.3 (0.3)
LDL cholesterol, mmol/L	3.9 (1.0)
Triglycerides, mmol/L	1.9 (2.1)
HbA1c, %	6.1 (1.3)
Specialized biomarkers	
20-HETE, ng/mL	122.6 (252.5)
15(S)-HETE, ng/mL	1.1 (1.4)
NETosis expression, mU/mL	62.5 (41.2)

BNP – B-type natriuretic peptide; eGFR – estimated glomerular filtration rate; HbA1c – glycated hemoglobin; HDL – high-density lipoprotein; HETE – hydroxyeicosatetraenoic acid; LDL – low-density lipoprotein; NETosis – neutrophil extracellular trap formation. Values are mean (SD).

4.2. Acute CMR-defined myocardial injury phenotype

Acute myocardial injury after STEMI was characterized by baseline CMR. The two principal markers analyzed were IS and MVO size, both expressed as a percentage of LV mass. These parameters were evaluated in relation to baseline clinical, procedural, laboratory, and specialized biomarker characteristics.

4.2.1. Acute infarct size

4.2.1.1. Associations of acute infarct size with clinical, procedural, laboratory, and biomarker variables

Mean IS on baseline CMR was 34.2 (19.4)% of LV mass. IS was analyzed in relation to clinical presentation, angiographic and procedural characteristics, routine laboratory parameters, and specialized biomarkers.

There was a strong positive IS correlation with troponin I ($r_s = 0.738$, $p < 0.001$) and AST ($r_s = 0.704$, $p < 0.001$), and a moderate correlation with ALT ($r_s = 0.602$, $p < 0.001$). Weaker positive correlations were observed with

BNP, glycemia, and urea, and a weak inverse correlation with eGFR (all $p < 0.01$). Statistically significant but weak correlations were also observed with high-sensitivity C-reactive protein (hs-CRP), NLR, potassium, and platelet count (all $|r_s| \leq 0.21$). IS was not significantly correlated with CRP, 20-HETE, 15(S)-HETE, or NETosis expression. Spearman correlation coefficients and p-values are shown in Figure 4.2.1.

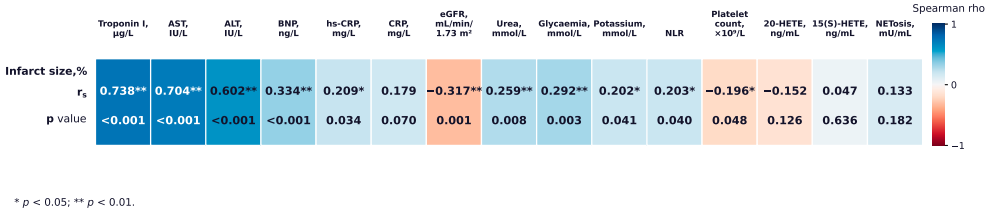

* $p < 0.05$; ** $p < 0.01$.

Fig. 4.2.1. *Correlations of IS with selected blood markers*

ALT – alanine aminotransferase; AST – aspartate aminotransferase; BNP – B-type natriuretic peptide; CRP – C-reactive protein; eGFR – estimated glomerular filtration rate; HETE – hydroxyeicosatetraenoic acid; hs-CRP – high-sensitivity C-reactive protein; NETosis – neutrophil extracellular trap formation; NLR – neutrophil-to-lymphocyte ratio. Cell color indicates the direction and strength of the Spearman correlation. Values within cells are Spearman correlation coefficients (r_s) and p-values.

Among clinical and procedural variables, IS was greater in patients with anterior than non-anterior STEMI (42.0 (18.7) vs. 28.6 (18.0)%; $p < 0.001$) and varied significantly by infarct-related artery: left anterior descending (LAD) artery infarction was associated with the largest infarcts (42.7 (19.1)%), followed by left circumflex (LCX) artery (35.3 (21.2)%) and right coronary artery (RCA) infarction (25.7 (15.4)%; overall $p < 0.001$). In post-hoc analysis, only the difference between LAD and RCA remained statistically significant. Patients with pre-PCI TIMI flow 0–1 had larger infarcts than those with TIMI flow 2–3 (38.5 (18.9) vs. 23.6 (16.5)%; $p < 0.001$), and IS was larger in patients with ventricular tachycardia or fibrillation during the acute phase than in those without (54.3 (15.7) vs. 32.3 (18.6)%; $p < 0.001$). Killip class was not significantly associated with IS. Detailed comparisons are presented in Tables 4.2.1 and 4.2.2.

In additional analyses, patients were stratified into IS tertiles: small ($\leq 23.83\%$), medium (23.84–41.90%), and large ($\geq 41.91\%$). Higher tertiles were characterized by higher troponin I, AST, ALT, BNP, glycemia, and urea, and by lower eGFR (all $p \leq 0.013$). Symptom-to-balloon time, demographic characteristics, lipid profile, hematological parameters, and HbA1c did not differ between tertiles. The specialized biomarkers – 20-HETE, 15(S)-HETE,

and NETosis expression – did not differ across tertiles. Detailed comparisons are presented in Table 4.2.2.

In summary, larger acute IS was associated with anterior infarct location, impaired pre-PCI coronary flow, ventricular arrhythmias, and conventional biochemical markers of myocardial injury. The investigated specialized biomarkers were not associated with IS.

Table 4.2.1. *Infarct size according to baseline clinical, procedural, and angiographic characteristics*

Variable (n)	Infarct size, % of LV mass, mean (SD)	p-value
Demographics and cardiovascular risk factors		
Male sex		
No (23)	32.1 (19.1)	0.564
Yes (80)	34.8 (19.5)	
Diabetes mellitus		
No (90)	34.2 (19.8)	0.956
Yes (13)	34.5 (17.1)	
Dyslipidemia		
No (10)	39.1 (19.0)	0.406
Yes (93)	33.7 (19.4)	
Arterial hypertension		
No (21)	35.1 (21.3)	0.815
Yes (82)	34.0 (19.0)	
Current smoking		
No (49)	32.9 (18.9)	0.527
Yes (54)	35.3 (19.9)	
Family history of CAD		
No (67)	33.3 (19.5)	0.517
Yes (36)	35.9 (19.4)	
Clinical characteristics and complications		
Anterior MI		
No (60)	28.6 (18.0)	**< 0.001**
Yes (43)	42.0 (18.7)	
Killip class ≥ 2		
No (76)	32.8 (18.9)	0.208
Yes (27)	38.2 (20.5)	
Atrial fibrillation/flutter		
No (98)	34.4 (18.9)	0.671
Yes (5)	30.6 (29.2)	

Table 4.2.1 cont.

Variable (n)	Infarct size, % of LV mass, mean (SD)	p-value
Ventricular tachycardia/fibrillation		
No (94)	32.3 (18.6)	**< 0.001**
Yes (9)	54.3 (15.7)	
Second-degree or third-degree AV block		
No (99)	34.4 (19.6)	0.512
Yes (4)	27.9 (10.7)	
Procedural characteristics		
Multivessel disease		
No (53)	35.6 (20.6)	0.455
Yes (50)	32.7 (18.1)	
Infarct-related artery		
RCA (45)	25.7 (15.4)	**< 0.001**
LAD (43)	42.7 (19.1)	
LCX (15)	35.3 (21.2)	
Pre-PCI TIMI flow		
0–1 (73)	38.5 (18.9)	**< 0.001**
2–3 (30)	23.6 (16.5)	
Manual thrombus aspiration		
No (90)	33.7 (19.8)	0.467
Yes (13)	37.9 (16.2)	
Administration of GP IIb/IIIa inhibitor		
No (99)	34.2 (19.6)	0.964
Yes (4)	34.6 (15.8)	

AV – atrioventricular; CAD – coronary artery disease; GP – glycoprotein; LAD – left anterior descending artery; LCX – left circumflex artery; LV – left ventricular; MI – myocardial infarction; PCI – percutaneous coronary intervention; RCA – right coronary artery; SD – standard deviation; TIMI – Thrombolysis in Myocardial Infarction. Values are mean (SD). P-values were calculated using the independent samples t-test or one-way ANOVA, as appropriate.

Table 4.2.2. *Baseline characteristics according to tertiles of infarct size*

Variable	Small IS ≤ 23.83% (n = 34)	Medium IS, 23.84–41.90% (n = 35)	Large IS ≥ 41.91% (n = 34)	p-value
Demographics and timing variables				
Age, years	58.5 (9.9)	60.5 (7.4)	61.4 (12.2)	0.467
BMI, kg/m²	27.8 [24.7–31.7]	26.8 [24.5–30.7]	28.2 [25.1–30.0]	0.857
Symptom-to-balloon time, min	310.0 [166.3–623.3]	390.0 [260.0–620.0]	267.5 [195.0–442.5]	0.107
Door-to-balloon time, min	46.5 [30.8–60.0]	56.0 [34.0–89.0]	49.0 [38.5–66.3]	0.684
Laboratory parameters				
Troponin I, µg/L	11.8 [4.3–19.5]	32.5 [21.5–39.7]	62.7 [38.6–116.0]	**< 0.001**
BNP, ng/L	118.8 [67.5–169.9]	169.3 [104.9–233.5]	218.3 [125.3–311.3]	**0.004**
Potassium, mmol/L	3.9 [3.8–4.2]	4.0 [3.9–4.3]	4.1 [3.9–4.5]	0.118
Magnesium, mmol/L	0.9 [0.8–0.9]	0.9 [0.8–1.0]	0.9 [0.8–1.0]	0.092
Sodium, mmol/L	137.0 [136.0–139.0]	137.0 [136.0–138.0]	136.0 [135.0–138.3]	0.449
Creatinine, µmol/L	66.0 [57.8–74.8]	70.0 [59.0–86.0]	73.0 [59.8–92.0]	0.168
eGFR, mL/min/1.73 m²	99.5 [91.8–105.0]	96.4 [82.0–101.0]	90.2 [77.3–96.0]	**0.010**
Urea, mmol/L	4.8 [3.9–5.8]	5.5 [4.7–7.4]	5.6 [4.5–7.6]	**0.013**
Glycemia, mmol/L	5.8 [5.5–7.1]	6.1 [5.7–6.9]	6.6 [6.1–7.5]	**0.007**
Total cholesterol, mmol/L	5.8 [5.4–6.6]	5.5 [4.6–6.3]	5.6 [4.9–6.9]	0.229
HDL cholesterol, mmol/L	1.2 [1.0–1.4]	1.2 [1.1–1.5]	1.3 [1.1–1.4]	0.740
LDL cholesterol, mmol/L	4.0 (1.1)	3.6 (1.0)	3.9 (1.0)	0.279
Triglycerides, mmol/L	1.5 [1.1–2.1]	1.2 [0.9–1.8]	1.5 [1.1–2.3]	0.130
ALT, IU/L	34.0 [24.8–43.8]	51.0 [40.0–66.0]	77.0 [49.5–105.0]	**< 0.001**
AST, IU/L	79.5 [45.8–125.3]	167.0 [130.0–256.0]	323.5 [188.5–456.8]	**< 0.001**
CRP, mg/L	5.8 [5.0–17.6]	10.1 [5.0–16.3]	9.6 [5.0–20.4]	0.473
hs-CRP, mg/L	5.8 [2.8–13.2]	9.1 [3.6–16.1]	9.0 [4.5–19.9]	0.322
Hemoglobin, g/L	137.7 (12.7)	143.2 (15.1)	143.7 (15.4)	0.167

Table 4.2.2 cont.

Variable	Small IS ≤ 23.83% (n = 34)	Medium IS, 23.84–41.90% (n = 35)	Large IS ≥ 41.91% (n = 34)	p-value
Hematocrit, %	40.5 (3.9)	41.0 (4.5)	40.9 (4.3)	0.871
Red blood cells, $\times 10^{12}$/L	4.4 (0.5)	4.5 (0.6)	4.6 (0.5)	0.553
Platelet count, $\times 10^{9}$/L	224.5 [204.8–241.8]	210.0 [184.0–243.0]	207.0 [170.0–244.3]	0.190
White blood cells, $\times 10^{9}$/L	8.8 [7.2–11.2]	9.9 [8.6–11.7]	9.5 [8.1–12.3]	0.120
Neutrophils, $\times 10^{9}$/L	6.2 [4.8–7.9]	6.6 [5.3–9.1]	7.0 [5.5–8.8]	0.126
Lymphocytes, $\times 10^{9}$/L	2.0 (0.7)	1.9 (0.6)	1.8 (0.6)	0.403
Neutrophil-to-lymphocyte ratio	3.2 [2.1–4.9]	3.9 [2.6–5.2]	4.3 [3.3–5.6]	0.105
HbA1c, %	5.8 [5.5–6.0]	5.9 [5.5–6.2]	5.9 [5.6–6.2]	0.475
Specialized biomarkers				
20-HETE, ng/mL	39.8 [2.8–215.9]	28.5 [4.3–65.4]	17.4 [2.5–95.7]	0.412
15(S)-HETE, ng/mL	0.4 [0.2–1.1]	0.8 [0.2–2.2]	0.5 [0.2–2.5]	0.538
NETosis expression, mU/mL	55.0 [43.6–68.2]	49.6 [45.1–68.5]	56.3 [45.1–76.8]	0.657

ALT – alanine aminotransferase; AST – aspartate aminotransferase; BMI – body mass index; BNP – B-type natriuretic peptide; CRP – C-reactive protein; eGFR – estimated glomerular filtration rate; HbA1c – glycated hemoglobin; HDL – high-density lipoprotein; HETE – hydroxyeicosatetraenoic acid; hs-CRP – high-sensitivity C-reactive protein; IQR – interquartile range; IS – infarct size; LDL – low-density lipoprotein; LV – left ventricular; NETosis – neutrophil extracellular trap formation; SD – standard deviation. Values are mean (SD) or median [IQR], as appropriate. P-values were calculated using one-way ANOVA or Kruskal–Wallis test, as appropriate.

4.2.1.2. Logistic regression analysis of factors associated with large acute infarct size

Univariable and multivariable logistic regression analyses were used to identify factors associated with large acute IS, defined as IS ≥ 41.91% of LV mass. Demographic, clinical, angiographic, procedural, laboratory, and biomarker variables were tested in univariable analysis.

In univariable analysis, large acute IS was associated with anterior myocardial infarction, pre-PCI TIMI flow 0–1, higher troponin I, higher AST, higher ALT, and lower eGFR. Symptom-to-balloon time showed an inverse association with large IS (OR 0.998 per minute, 95% CI 0.996–1.000; p = 0.034). However, symptom-to-balloon time did not differ significantly across infarct-size tertiles in the Kruskal–Wallis test (p = 0.107), and the median values showed no consistent linear gradient. Therefore, this finding was interpreted cautiously and was not retained in the multivariable model. Troponin I and AST were strongly correlated (r = 0.669, p < 0.001) and were therefore not entered simultaneously into the multivariable model. Troponin I was retained because of its higher cardiac specificity. ALT was not entered as a separate predictor, as troponin I provides a more cardiac-specific measure of myocardial injury.

In the final multivariable model, which included anterior myocardial infarction, pre-PCI TIMI flow 0–1, troponin I, and eGFR, pre-PCI TIMI flow 0–1 (OR 8.08, 95% CI 1.45–45.15; p = 0.017) and higher troponin I (OR 1.28 per 10 μg/L increase, 95% CI 1.10–1.45; p < 0.001) remained independently associated with large acute IS. Anterior myocardial infarction (OR 1.75, 95% CI 0.63–4.80; p = 0.282) and lower eGFR (OR 0.85 per 10 mL/min/1.73 m² increase, 95% CI 0.64–1.14; p = 0.300) were not significant after adjustment. Univariable and multivariable results are presented in Table 4.2.3, and adjusted odds ratios from the final model are illustrated in Figure 4.2.2.

Table 4.2.3. *Univariable and multivariable logistic regression analysis of factors associated with large acute infarct size*

Variable	Univariable OR (95% CI)	p-value	Multivariable OR (95% CI)	p-value
Age, years	1.020 (0.978–1.065)	0.355	—	—
Male sex	0.903 (0.340–2.399)	0.837	—	—
BMI, kg/m²	0.987 (0.899–1.083)	0.781	—	—
Diabetes mellitus	1.315 (0.395–4.372)	0.655	—	—
Arterial hypertension	0.754 (0.279–2.043)	0.579	—	—
Current smoking	1.031 (0.453–2.347)	0.942	—	—
Family history of CAD	0.560 (0.227–1.381)	0.208	—	—

Table 4.2.3 cont.

Variable	Univariable OR (95% CI)	p-value	Multivariable OR (95% CI)	p-value
Symptom-to-balloon time, min	0.998 (0.996–1.000)	**0.034**	—	—
Anterior MI	2.375 (1.026–5.495)	**0.043**	1.745 (0.633–4.801)	0.282
Infarct-related artery	1.678 (0.934–3.015)	0.083	—	—
Pre-PCI TIMI flow 0–1	6.643 (1.847–23.890)	**0.004**	8.081 (1.445–45.147)	**0.017**
Thrombolysis before PCI	0.656 (0.125–3.437)	0.618	—	—
Manual thrombus aspiration during PCI	1.315 (0.395–4.372)	0.655	—	—
GP IIb/IIIa inhibitor use during PCI	2.094 (0.282–15.544)	0.470	—	—
Troponin I, µg/L	1.028 (1.014–1.042)	**< 0.001**	1.025 (1.010–1.038)	**< 0.001**
AST, IU/L	1.010 (1.005–1.014)	**< 0.001**	—	—
ALT, IU/L	1.019 (1.007–1.031)	**0.002**	—	—
eGFR, mL/min/1.73 m²	0.974 (0.950–1.000)	**0.046**	0.984 (0.956–1.013)	0.300
Glycemia, mmol/L	1.174 (0.996–1.384)	0.056	—	—
BNP, ng/L	1.003 (1.000–1.006)	0.062	—	—
CRP, mg/L	1.011 (0.995–1.028)	0.188	—	—
Hemoglobin, g/L	1.016 (0.987–1.045)	0.288	—	—
White blood cell count, ×10⁹/L	1.063 (0.922–1.225)	0.403	—	—
Neutrophil count, ×10⁹/L	1.096 (0.943–1.272)	0.231	—	—
Neutrophil-to-lymphocyte ratio	1.110 (0.957–1.287)	0.168	—	—
Platelet count, ×10⁹/L	0.995 (0.987–1.003)	0.189	—	—
20-HETE, ng/mL	0.999 (0.997–1.001)	0.381	—	—
15(S)-HETE, ng/mL	1.112 (0.827–1.496)	0.481	—	—
NETosis expression, mU/mL	1.007 (0.996–1.017)	0.199	—	—

ALT – alanine aminotransferase; AST – aspartate aminotransferase; BMI – body mass index; BNP – B-type natriuretic peptide; CAD – coronary artery disease; CI – confidence interval; CRP – C-reactive protein; eGFR – estimated glomerular filtration rate; GP – glycoprotein; HETE – hydroxyeicosatetraenoic acid; MI – myocardial infarction; NETosis – neutrophil extracellular trap formation; OR – odds ratio; PCI – percutaneous coronary intervention; TIMI – Thrombolysis in Myocardial Infarction. Values are odds ratios with 95% confidence intervals. Odds ratios for continuous variables are expressed per 1-unit increase. The multivariable model included anterior MI, pre-PCI TIMI flow 0–1, troponin I, and eGFR.

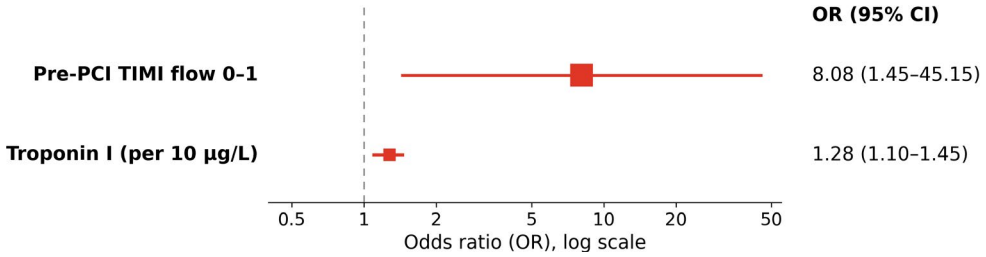

Fig. 4.2.2. *Independent predictors of large infarct size (≥ 41.91% of LV mass) in multivariable logistic regression*

Squares represent odds ratios; horizontal lines indicate 95% confidence intervals. CI – confidence interval; LV – left ventricular; OR – odds ratio; PCI – percutaneous coronary intervention; TIMI – Thrombolysis in Myocardial Infarction.

4.2.2. Acute microvascular obstruction

4.2.2.1. Frequency and extent of MVO

MVO was assessed on baseline late gadolinium enhancement CMR in 103 of 105 patients; in two patients LGE images were not evaluable for MVO and were excluded from this analysis. MVO was present in 73 of 103 patients (70.9%). Among MVO-positive patients, median MVO size was 4.1% [2.4–8.3] of left ventricular mass.

4.2.2.2. MVO size according to clinical, procedural, and angiographic characteristics

In our study, the analyses of MVO size were restricted to the 73 patients in whom MVO was detected on baseline CMR. Among these patients, MVO size was similar across all assessed demographic, clinical, procedural, and angiographic characteristics. A trend of greater relative MVO size was observed in patients with arterial hypertension compared with normotensive patients (5.10% [2.68–8.66] vs. 3.30% [1.44–4.11]; p = 0.055), as well as in patients without dyslipidemia compared with those with dyslipidemia (8.03% [4.87–9.95] vs. 3.84% [2.39–7.74]; p = 0.062), but neither difference reached statistical significance. The exact comparisons are presented in Table 4.2.4.

Table 4.2.4. *MVO size according to baseline clinical, procedural, and angiographic characteristics*

Variable (n)	MVO size, % of LV mass, median [IQR]	p-value
Demographics and cardiovascular risk factors		
Male sex		
No (13)	4.06 [3.46–7.13]	0.908
Yes (60)	4.55 [2.24–8.66]	
Diabetes mellitus		
No (63)	4.06 [2.24–8.32]	0.205
Yes (10)	5.90 [3.46–7.58]	
Dyslipidemia		
No (6)	8.03 [4.87–9.95]	0.062
Yes (67)	3.84 [2.39–7.74]	
Arterial hypertension		
No (14)	3.30 [1.44–4.11]	0.055
Yes (59)	5.10 [2.68–8.66]	
Current smoking		
No (32)	4.79 [2.78–7.81]	0.317
Yes (41)	4.01 [1.99–8.16]	
Family history of CAD		
No (46)	4.99 [2.70–8.91]	0.349
Yes (27)	3.84 [2.04–6.64]	
Clinical characteristics and complications		
Anterior MI		
No (39)	3.66 [2.56–7.36]	0.426
Yes (34)	4.74 [2.39–8.83]	
Killip class ≥ II		
No (53)	3.84 [2.49–7.13]	0.459
Yes (20)	4.85 [2.68–8.95]	
Atrial fibrillation/flutter		
No (70)	4.29 [2.49–8.16]	0.551
Yes (3)	2.66 [2.07–5.58]	
Ventricular tachycardia/fibrillation		
No (65)	4.48 [2.64–8.16]	0.609
Yes (8)	3.36 [2.08–7.61]	
Second- or third-degree AV block		
No (69)	4.06 [2.39–8.16]	0.261
Yes (4)	7.36 [5.32–8.30]	
Procedural characteristics		
Multivessel disease		
No (34)	4.27 [2.39–9.01]	0.634
Yes (39)	4.11 [2.56–8.03]	

Table 4.2.4 cont.

Variable (n)	MVO size, % of LV mass, median [IQR]	p-value
Infarct-related artery		
RCA (29)	3.50 [1.99–7.13]	0.556
LAD (33)	4.62 [2.39–8.83]	
LCX (11)	5.27 [3.23–6.69]	
Pre-PCI TIMI flow		
0–1 (59)	4.48 [2.65–8.66]	0.212
2–3 (14)	3.64 [1.41–5.10]	
Manual thrombus aspiration		
No (65)	4.06 [2.38–7.89]	0.124
Yes (8)	6.90 [3.40–13.22]	
GP IIb/IIIa inhibitor administration		
No (70)	4.29 [2.39–8.49]	0.906
Yes (3)	3.66 [3.15–5.62]	

AV – atrioventricular; CAD – coronary artery disease; GP – glycoprotein; IQR – interquartile range; LAD – left anterior descending artery; LCX – left circumflex artery; LV – left ventricular; MI – myocardial infarction; MVO – microvascular obstruction; PCI – percutaneous coronary intervention; RCA – right coronary artery; TIMI – Thrombolysis in Myocardial Infarction. Values are median [IQR]. P-values were calculated using the Mann–Whitney U test for two-group comparisons and the Kruskal–Wallis test for comparisons across infarct-related artery groups.

4.2.2.3. Correlations of MVO size with continuous laboratory and biomarker variables

We further evaluated the associations between MVO size and continuous laboratory and biomarker variables in MVO-positive patients (n = 73, 70.9%). Troponin I showed the strongest association with MVO size, with a moderate positive correlation ($r_s = 0.559$, $p < 0.001$). A moderate positive correlation was also found with AST ($r_s = 0.436$, $p < 0.001$), and a weak positive correlation with ALT ($r_s = 0.389$, $p < 0.001$). A weak positive correlation was observed with admission glycemia ($r_s = 0.248$, $p = 0.035$). No significant correlations were observed between MVO size and renal function parameters (creatinine, eGFR, urea), electrolytes (sodium, potassium, magnesium), lipid profile (total cholesterol, HDL, LDL, triglycerides), HbA1c, CRP, hs-CRP, BNP, or hematological parameters. Spearman correlation coefficients and p-values are presented in Figure 4.2.3.

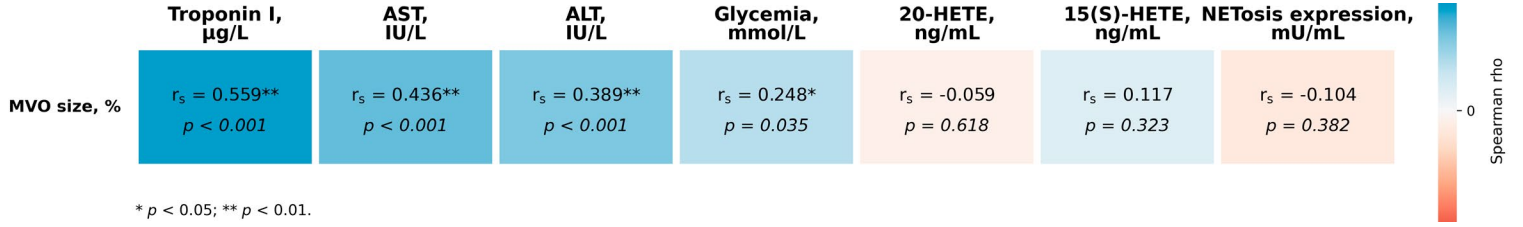

* $p < 0.05$; ** $p < 0.01$.

Fig. 4.2.3. *Correlations of MVO size with selected laboratory and biomarker variables in MVO-positive patients (n = 73)*

Cell color indicates the direction and strength of the Spearman correlation. Values within cells are Spearman correlation coefficients (r_s) and p-values. ALT – alanine aminotransferase; AST – aspartate aminotransferase; BNP – B-type natriuretic peptide; CRP – C-reactive protein; eGFR – estimated glomerular filtration rate; HbA1c – glycated hemoglobin; HDL – high-density lipoprotein; HETE – hydroxyeicosatetraenoic acid; hs-CRP – high-sensitivity C-reactive protein; LDL – low-density lipoprotein; MVO – microvascular obstruction; NETosis – neutrophil extracellular trap formation; NLR – neutrophil-to-lymphocyte ratio.

4.2.2.4. Baseline characteristics according to MVO presence

We compared baseline clinical, laboratory, and biomarker characteristics between patients with and without MVO on baseline CMR (73 with MVO, 30 without).

Patients with MVO had higher troponin I values than those without (36.4 [21.4–77.3] vs. 12.5 [4.3–33.6] µg/L; $p < 0.001$). Higher values were also observed for the aminotransferases AST (186.0 [123.5–311.5] vs. 111.5 [46.8–198.8] IU/L; $p = 0.003$) and ALT (51.0 [38.0–85.5] vs. 38.5 [30.0–56.5] IU/L; $p = 0.013$). Among renal function parameters, serum creatinine was higher in patients with MVO (71.0 [59.0–90.5] vs. 68.0 [55.8–74.5] µmol/L; $p = 0.038$), eGFR was lower (93.0 [79.0–100.5] vs. 100.4 [93.8–103.5] mL/min/1.73 m²; $p = 0.006$), and urea was higher (5.5 [4.5–7.5] vs. 4.7 [3.9–5.8] mmol/L; $p = 0.006$). Patients with MVO also had higher CRP values (10.6 [5.0–19.2] vs. 5.0 [5.0–13.5] mg/L; $p = 0.037$) and lower platelet counts (210.0 [181.0–240.0] vs. 228.0 [203.3–303.5] $\times 10^9$/L; $p = 0.035$). Among the specialized biomarkers, NETosis expression was higher in patients with MVO (56.4 [42.1–71.3] vs. 48.7 [36.7–60.7] mU/mL; $p = 0.011$), whereas 20-HETE and 15(S)-HETE did not differ between groups. Other demographic, clinical, and laboratory characteristics did not differ significantly between groups. Detailed comparisons are presented in Table 4.2.5.

Table 4.2.5. *Baseline clinical, laboratory, and biomarker characteristics according to MVO presence*

Variable	MVO absent (n = 30)	MVO present (n = 73)	p-value
Demographics and timing variables			
Age, years	57.5 (10.8)	61.2 (9.5)	0.088
BMI, kg/m²	26.9 [24.5–29.4]	28.1 [25.0–30.8]	0.338
Symptom-to-balloon time, min	427.5 [203.8–583.8]	355.0 [202.5–540.0]	0.772
Door-to-balloon time, min	47.5 [31.8–63.8]	51.0 [36.0–68.0]	0.537
Laboratory parameters			
Troponin I, µg/L	12.5 [4.3–33.6]	36.4 [21.4–77.3]	**< 0.001**
BNP, ng/L	144.6 [92.5–221.9]	161.5 [94.6–252.8]	0.567
Potassium, mmol/L	4.0 [3.8–4.2]	4.1 [3.9–4.3]	0.083
Magnesium, mmol/L	0.9 [0.8–0.9]	0.9 [0.8–1.0]	0.655
Sodium, mmol/L	136.0 [135.8–138.0]	137.0 [135.0–139.0]	0.447
Creatinine, µmol/L	68.0 [55.8–74.5]	71.0 [59.0–90.5]	**0.038**
eGFR, mL/min/1.73 m²	100.4 [93.8–103.5]	93.0 [79.0–100.5]	**0.006**
Urea, mmol/L	4.7 [3.9–5.8]	5.5 [4.5–7.5]	**0.006**
Glycemia, mmol/L	6.0 [5.6–6.6]	6.3 [5.7–7.2]	0.110
Total cholesterol, mmol/L	5.9 [5.3–6.6]	5.5 [4.7–6.5]	0.179

Table 4.2.5 cont.

Variable	MVO absent (n = 30)	MVO present (n = 73)	p-value
HDL cholesterol, mmol/L	1.3 [1.1–1.4]	1.2 [1.1–1.4]	0.232
LDL cholesterol, mmol/L	4.0 (1.2)	3.8 (0.9)	0.296
Triglycerides, mmol/L	1.3 [1.1–2.0]	1.5 [1.0–2.0]	0.791
ALT, IU/L	38.5 [30.0–56.5]	51.0 [38.0–85.5]	**0.013**
AST, IU/L	111.5 [46.8–198.8]	186.0 [123.5–311.5]	**0.003**
CRP, mg/L	5.0 [5.0–13.5]	10.6 [5.0–19.2]	**0.037**
hs-CRP, mg/L	4.5 [3.3–12.1]	9.6 [4.0–18.3]	0.061
Hemoglobin, g/L	139.0 (14.4)	142.6 (14.6)	0.266
Hematocrit, %	40.1 (4.1)	41.1 (4.2)	0.256
Red blood cells, $\times 10^{12}$/L	4.4 (0.5)	4.6 (0.5)	0.115
Platelet count, $\times 10^{9}$/L	228.0 [203.3–303.5]	210.0 [181.0–240.0]	**0.035**
White blood cells, $\times 10^{9}$/L	9.0 [7.3–10.6]	9.5 [8.0–11.7]	0.221
Neutrophils, $\times 10^{9}$/L	6.2 [5.2–7.9]	7.1 [5.1–8.6]	0.177
Lymphocytes, $\times 10^{9}$/L	1.9 [1.4–2.4]	1.8 [1.5–2.1]	0.441
Neutrophil-to-lymphocyte ratio	3.3 [2.1–4.8]	4.1 [3.0–5.4]	0.091
HbA1c, %	5.8 [5.6–6.0]	5.9 [5.5–6.3]	0.466
Specialized biomarkers			
20-HETE, ng/mL	22.7 [0.0–212.2]	22.8 [0.0–72.5]	0.490
15(S)-HETE, ng/mL	0.7 [0.3–2.3]	0.5 [0.2–1.4]	0.277
NETosis expression, mU/mL	48.7 [36.7–60.7]	56.4 [42.1–71.3]	**0.011**

ALT – alanine aminotransferase; AST – aspartate aminotransferase; BMI – body mass index; BNP – B-type natriuretic peptide; CRP – C-reactive protein; eGFR – estimated glomerular filtration rate; HbA1c – glycated hemoglobin; HDL – high-density lipoprotein; HETE – hydroxyeicosatetraenoic acid; hs-CRP – high-sensitivity C-reactive protein; IQR – interquartile range; LDL – low-density lipoprotein; MVO – microvascular obstruction; NETosis – neutrophil extracellular trap formation; SD – standard deviation. Values are mean (SD) or median [IQR], as appropriate.

4.2.2.5. Logistic regression analysis of factors associated with MVO presence

Univariable and multivariable logistic regression analyses were used to identify factors independently associated with MVO presence on baseline CMR, defined as visible MVO on late gadolinium enhancement imaging. Demographic, clinical, angiographic, procedural, laboratory, and biomarker variables were tested in univariable analysis.

In univariable analysis, MVO presence was significantly associated with pre-PCI TIMI flow 0–1, higher troponin I, higher AST, higher ALT, lower

eGFR, lower platelet count, and higher NETosis expression. Troponin I, AST, and ALT were strongly intercorrelated (Spearman's $r_s \geq 0.60$ between all pairs, all $p < 0.001$) and were therefore not entered simultaneously into the multivariable model. Troponin I was retained because of its higher cardiac specificity. The primary multivariable model included pre-PCI TIMI flow 0–1, troponin I, eGFR, and NETosis expression. Because NETosis expression and platelet count may reflect overlapping pathophysiology, platelet count was not included in the primary model; a sensitivity analysis additionally including platelet count was performed to assess robustness.

In the primary multivariable model, pre-PCI TIMI flow 0–1 (OR 3.974, 95% CI 1.284–12.300; p = 0.017), higher troponin I (OR 1.029 per 1 μg/L increase, 95% CI 1.006–1.053; p = 0.015), lower eGFR (OR 0.963 per 1 mL/min/1.73 m² increase, 95% CI 0.929–0.998; p = 0.038), and higher NETosis expression (OR 1.025 per 1 mU/mL increase, 95% CI 1.004–1.047; p = 0.020) remained independently associated with MVO presence.

In the sensitivity model that additionally included platelet count, pre-PCI TIMI flow 0–1 (OR 4.611, 95% CI 1.405–15.128; p = 0.012) and higher troponin I (OR 1.028 per 1 μg/L increase, 95% CI 1.005–1.052; p = 0.017) remained independently associated with MVO presence. Lower eGFR (p = 0.060), higher NETosis expression (p = 0.055), and lower platelet count (p = 0.068) showed borderline associations that did not reach statistical significance. Univariable and primary multivariable results are presented in Table 4.2.6 and Figure 4.2.4; the sensitivity analysis is presented in Table 4.2.7.

Table 4.2.6. *Univariable and multivariable logistic regression analysis of factors associated with microvascular obstruction presence*

Variable	Univariable OR (95% CI)	p-value	Multivariable OR (95% CI)	p-value
Age, years	1.038 (0.994–1.084)	0.092	—	—
Male sex	2.308 (0.877–6.071)	0.090	—	—
BMI, kg/m²	1.050 (0.950–1.161)	0.342	—	—
Diabetes mellitus	1.429 (0.364–5.603)	0.609	—	—
Arterial hypertension	1.283 (0.459–3.583)	0.635	—	—
Current smoking	1.675 (0.711–3.949)	0.238	—	—
Family history of CAD	1.370 (0.549–3.416)	0.500	—	—
Symptom-to-balloon time, min	1.000 (0.998–1.002)	0.951	—	—
Anterior MI	2.034 (0.822–5.035)	0.125	—	—
Infarct-related artery	1.374 (0.736–2.565)	0.318	—	—

Table 4.2.6 cont.

Variable	Univariable OR (95% CI)	p-value	Multivariable OR (95% CI)	p-value
Pre-PCI TIMI flow 0–1	4.816 (1.912–12.135)	**< 0.001**	3.974 (1.284–12.300)	**0.017**
Thrombolysis before PCI	3.076 (0.362–26.150)	0.304	—	—
Manual thrombus aspiration during PCI	0.615 (0.184–2.061)	0.431	—	—
GP IIb/IIIa inhibitor use during PCI	1.243 (0.124–12.449)	0.853	—	—
Troponin I, µg/L	1.037 (1.013–1.063)	**0.003**	1.029 (1.006–1.053)	**0.015**
AST, IU/L	1.004 (1.000–1.007)	**0.031**	—	—
ALT, IU/L	1.017 (1.001–1.034)	**0.032**	—	—
eGFR, mL/min/1.73 m²	0.966 (0.938–0.995)	**0.023**	0.963 (0.929–0.998)	**0.038**
Glycemia, mmol/L	1.127 (0.914–1.389)	0.263	—	—
BNP, ng/L	1.001 (0.997–1.004)	0.766	—	—
CRP, mg/L	1.042 (0.995–1.090)	0.078	—	—
Hemoglobin, g/L	1.017 (0.987–1.048)	0.264	—	—
White blood cell count, ×10⁹/L	1.148 (0.963–1.367)	0.123	—	—
Neutrophil count, ×10⁹/L	1.162 (0.964–1.400)	0.115	—	—
Neutrophil-to-lymphocyte ratio	1.167 (0.951–1.434)	0.140	—	—
Platelet count, ×10⁹/L	0.992 (0.984–0.999)	**0.036**	—	—
20-HETE, ng/mL	0.999 (0.998–1.001)	0.516	—	—
15(S)-HETE, ng/mL	0.871 (0.644–1.179)	0.371	—	—
NETosis expression, mU/mL	1.019 (1.000–1.038)	**0.045**	1.025 (1.004–1.047)	**0.020**

ALT – alanine aminotransferase; AST – aspartate aminotransferase; BMI – body mass index; BNP – B-type natriuretic peptide; CAD – coronary artery disease; CI – confidence interval; CRP – C-reactive protein; eGFR – estimated glomerular filtration rate; GP – glycoprotein; HETE – hydroxyeicosatetraenoic acid; MI – myocardial infarction; MVO – microvascular obstruction; NETosis – neutrophil extracellular trap formation; OR – odds ratio; PCI – percutaneous coronary intervention; TIMI – Thrombolysis in Myocardial Infarction. Values are odds ratios with 95% confidence intervals. Odds ratios for continuous variables are expressed per 1-unit increase. The primary multivariable model included pre-PCI TIMI flow 0–1, troponin I, eGFR, and NETosis expression.

Table 4.2.7. *Sensitivity multivariable model for MVO presence including platelet count*

Variable	OR (95% CI)	p-value
Pre-PCI TIMI flow 0–1	4.611 (1.405–15.128)	**0.012**
Troponin I, µg/L	1.028 (1.005–1.052)	**0.017**
eGFR, mL/min/1.73 m²	0.966 (0.932–1.001)	0.060
NETosis expression, mU/mL	1.021 (1.000–1.043)	0.055
Platelet count, ×10⁹/L	0.990 (0.979–1.001)	0.068

CI – confidence interval; eGFR – estimated glomerular filtration rate; MVO – microvascular obstruction; NETosis – neutrophil extracellular trap formation; OR – odds ratio; PCI – percutaneous coronary intervention; TIMI – Thrombolysis in Myocardial Infarction. This sensitivity model included the primary multivariable predictors with platelet count additionally entered. Values are odds ratios with 95% confidence intervals. Odds ratios for continuous variables are expressed per 1-unit increase.

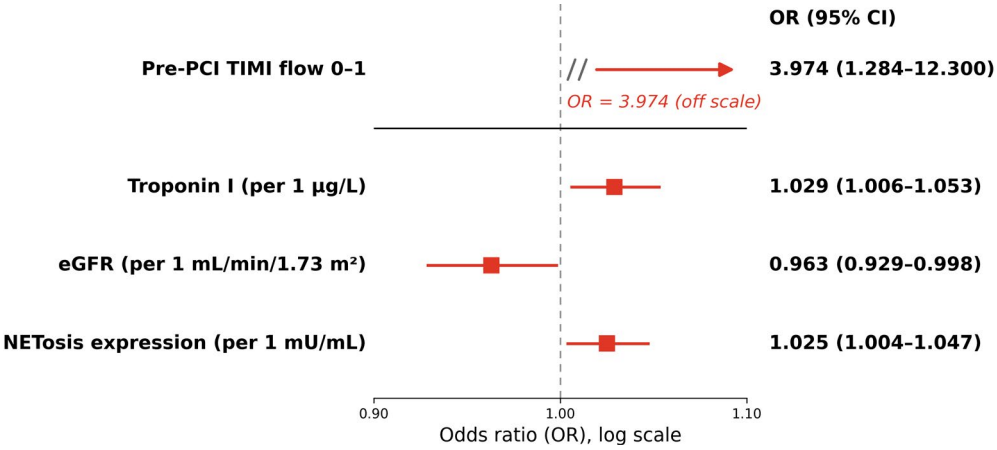

Fig. 4.2.4. *Independent predictors of microvascular obstruction presence in the primary multivariable logistic regression model (n = 103)*

Squares represent odds ratios; horizontal lines indicate 95% confidence intervals. The odds ratio for pre-PCI TIMI flow 0–1 is shown off scale. CI – confidence interval; eGFR – estimated glomerular filtration rate; MVO – microvascular obstruction; NETosis – neutrophil extracellular trap formation; OR – odds ratio; PCI – percutaneous coronary intervention; TIMI – Thrombolysis in Myocardial Infarction.

4.2.2.6. Diagnostic performance of selected laboratory and biomarker variables for MVO presence

ROC analysis was used to assess the diagnostic performance of troponin I, eGFR, NETosis expression, and platelet count for MVO presence. Troponin

I showed the strongest discrimination, with an AUC of 0.78 (95% CI 0.67–0.88; $p < 0.001$) at an optimal cut-off of ≥ 18.56 µg/L (sensitivity 81%, specificity 70%). Lower eGFR also discriminated MVO presence (AUC 0.67, 95% CI 0.56–0.78; $p = 0.003$) at a cut-off of ≤ 97 mL/min/1.73 m² (sensitivity 69%, specificity 70%). Higher NETosis expression showed modest discrimination (AUC 0.66, 95% CI 0.54–0.77; $p = 0.007$) at a cut-off of ≥ 62 mU/mL (sensitivity 47%, specificity 90%). Lower platelet count showed weaker discrimination (AUC 0.63, 95% CI 0.52–0.75; $p = 0.024$) at a cut-off of ≤ 214 ×10⁹/L (sensitivity 59%, specificity 70%). Detailed results are presented in Table 4.2.8, and ROC curves are illustrated in Figure 4.2.5.

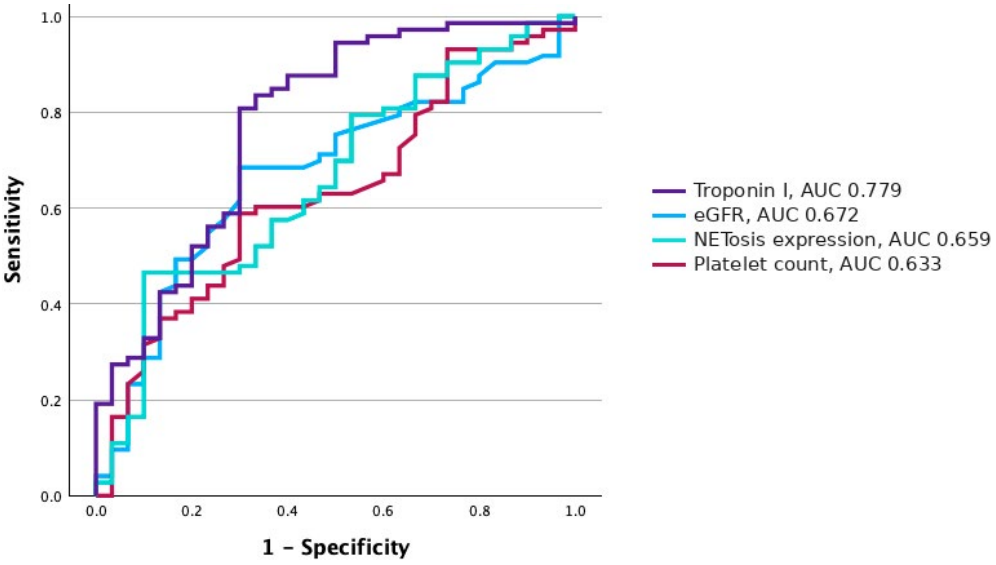

Fig. 4.2.5. *ROC curves for troponin I, eGFR, NETosis expression, and platelet count in the identification of microvascular obstruction presence (n = 103)*

AUC – area under the curve; eGFR – estimated glomerular filtration rate; MVO – microvascular obstruction; NETosis – neutrophil extracellular trap formation; ROC – receiver operating characteristic.

Table 4.2.8. *Diagnostic performance of selected laboratory and biomarker variables for MVO presence*

Variable	Cut-off value	AUC	95% CI	p-value	Sensitivity (%)	Specificity (%)
Troponin I, µg/L	≥ 18.56	0.779	0.674–0.883	< 0.001	80.8	70.0
eGFR, mL/min/1.73 m²	≤ 97.2	0.672	0.560–0.783	0.003	68.5	70.0
NETosis expression, mU/mL	≥ 62.1	0.659	0.544–0.774	0.007	46.6	90.0
Platelet count, ×10⁹/L	≤ 214.0	0.633	0.518–0.748	0.024	58.9	70.0

AUC – area under the curve; CI – confidence interval; eGFR – estimated glomerular filtration rate; MVO – microvascular obstruction; NETosis – neutrophil extracellular trap formation. Cut-off values were selected using the Youden index. For eGFR and platelet count, lower values indicated higher probability of MVO presence.

4.3. Global myocardial healing at 6 months

Analyses in this section were performed in the paired-CMR cohort of 93 patients with baseline and 6-month follow-up CMR.

4.3.1. Global LV structural and functional changes at 6 months

Significant improvement in global LV systolic function was observed over 6 months. LVEF increased from 49.0 [40.7–52.4]% to 55.8 [47.9–59.9]% ($p < 0.001$), and LVESVi decreased from 45.9 [37.2–57.3] mL/m² to 39.9 [31.5–51.1] mL/m² ($p = 0.005$). In contrast, LVEDVi did not change significantly during follow-up. Indexed LV stroke volume increased from 42.1 (9.4) mL/m² to 48.0 (10.1) mL/m² ($p < 0.001$), and LV mass index decreased from 56.2 [49.3–65.3] g/m² to 49.4 [42.9–54.9] g/m² ($p < 0.001$). GLS improved from −20.4 (4.4)% to −23.5 (5.6)% and GCS from −27.7 (6.7)% to −30.4 (8.1)% (both $p < 0.001$).

Global tissue characterization parameters also changed during follow-up. Mean native T1 decreased from 1352.1 [1298.6–1396.5] ms to 1275.0 [1248.3–1311.8] ms ($p < 0.001$), mean post-contrast T1 increased from 353.8 [290.7–394.9] ms to 403.9 [374.5–444.9] ms ($p < 0.001$), and mean T2 decreased from 44.2 [42.1–46.6] ms to 42.9 [41.1–45.0] ms ($p < 0.001$). Mean ECV did not change significantly during follow-up (29.5 [26.8–33.1]% vs. 29.0 [25.9–32.6]%, $p = 0.292$).

IS decreased from 30.9 [18.9–45.5]% to 18.8 [11.2–31.1]% ($p < 0.001$). MVO, present in 65 of 93 patients at baseline, was no longer detectable on follow-up CMR in any patient. Global CMR changes between baseline and 6-month follow-up are presented in Table 4.3.1.

Table 4.3.1. *Global CMR changes from baseline to 6 months*

Parameter	n	Baseline	6-month follow-up	p-value
LVEDV, mL	93	177.2 [149.5–210.0]	178.3 [146.5–214.5]	0.274
LVEDVi, mL/m²	93	90.3 [78.4–100.2]	90.2 [74.5–103.3]	0.262
LVESV, mL	93	91.8 [75.1–113.8]	80.8 [61.9–108.3]	**0.005**
LVESVi, mL/m²	93	45.9 [37.2–57.3]	39.9 [31.5–51.1]	**0.005**
LVS.V, mL	93	84.4 (20.5)	96.2 (22.5)	**< 0.001**
LVS.Vi, mL/m²	93	42.1 (9.4)	48.0 (10.1)	**< 0.001**
LV mass, g	93	114.7 [97.7–132.3]	97.2 [84.8–117.0]	**< 0.001**
LV mass index, g/m²	93	56.2 [49.3–65.3]	49.4 [42.9–54.9]	**< 0.001**
LVEF, %	93	49.0 [40.7–52.4]	55.8 [47.9–59.9]	**< 0.001**
LV GLS, %	92	−20.4 (4.4)	−23.5 (5.6)	**< 0.001**
LV GCS, %	92	−27.7 (6.7)	−30.4 (8.1)	**< 0.001**
Mean native T1, ms	92	1352.1 [1298.6–1396.5]	1275.0 [1248.3–1311.8]	**< 0.001**
Mean post-contrast T1, ms	86	353.8 [290.7–394.9]	403.9 [374.5–444.9]	**< 0.001**
Mean ECV, %	86	29.5 [26.8–33.1]	29.0 [25.9–32.6]	0.292
Mean T2, ms	86	44.2 [42.1–46.6]	42.9 [41.1–45.0]	**< 0.001**
Infarct size, %	93	30.9 [18.9–45.5]	18.8 [11.2–31.1]	**< 0.001**
MVO size, %	93	2.6 [0.0–5.9]	Not detectable	—

CMR – cardiovascular magnetic resonance; ECV – extracellular volume; GCS – global circumferential strain; GLS – global longitudinal strain; IQR – interquartile range; LV – left ventricle/left ventricular; LVEDV – left ventricular end-diastolic volume; LVEDVi – left ventricular end-diastolic volume index; LVEF – left ventricular ejection fraction; LVESV – left ventricular end-systolic volume; LVESVi – left ventricular end-systolic volume index; LVS.V – left ventricular stroke volume; LVS.Vi – left ventricular stroke volume index; MVO – microvascular obstruction; SD – standard deviation; T1 – T1 relaxation time; T2 – T2 relaxation time. Values are presented as median [IQR] or mean (SD), as appropriate.

4.3.2. Infarct shrinkage and residual infarct size

Infarct healing was assessed using two related measures: IS shrinkage, reflecting the reduction in infarct burden from baseline to follow-up, and residual IS, reflecting the remaining scar burden at 6 months. In the paired-CMR cohort, median IS shrinkage was 9.6 [3.0–16.1]%, and median residual IS at 6-month follow-up was 18.8 [11.2–31.1]% of LV mass.

Residual IS at 6 months was strongly associated with baseline CMR-defined injury severity. It showed a strong positive correlation with baseline IS ($r_s = 0.837$, $p < 0.001$) and a moderate positive correlation with baseline MVO size ($r_s = 0.590$, $p < 0.001$). Residual IS was also associated with biochemical markers of myocardial injury, showing a strong correlation

with troponin I (r_s = 0.746, p < 0.001) and moderate correlations with AST (r_s = 0.699, p < 0.001) and ALT (r_s = 0.572, p < 0.001).

Residual IS was also related to infarct territory and angiographic severity, correlating with MI localization, anterior MI, infarct-related artery, and lower pre-PCI TIMI flow (all $r_s \leq 0.36$, $p \leq 0.003$), and weakly with prior ventricular tachycardia or fibrillation. Weaker but significant correlations were observed with BNP, CRP, hs-CRP, glycemia, NLR, urea, eGFR, and platelet count (all $|r_s| \leq 0.33$). No significant correlations were observed with the specialized biomarkers (20-HETE, 15(S)-HETE, NETosis expression; all p > 0.24). Detailed coefficients are presented in Figure 4.3.1.

Variable	Residual IS *r (p-value)*	IS shrinkage *r (p-value)*
Baseline infarct size	0.837 (<0.001)	0.579 (<0.001)
Baseline MVO size	0.590 (<0.001)	0.100 (0.338)
Troponin I	0.746 (<0.001)	0.215 (0.039)
AST	0.699 (<0.001)	0.287 (0.005)
ALT	0.572 (<0.001)	0.301 (0.003)
BNP	0.329 (0.001)	0.180 (0.087)
CRP	0.320 (0.002)	0.038 (0.718)
hs-CRP	0.306 (0.003)	0.080 (0.448)
Glycemia	0.269 (0.009)	0.009 (0.929)
Neutrophil-to-lymphocyte ratio	0.262 (0.011)	0.010 (0.928)
Urea	0.238 (0.022)	0.118 (0.261)
eGFR	-0.226 (0.029)	-0.184 (0.078)
Platelet count	-0.222 (0.032)	-0.199 (0.056)
20-HETE	-0.123 (0.241)	0.064 (0.543)
15(S)-HETE	0.029 (0.783)	0.072 (0.498)
NETosis	0.101 (0.335)	0.061 (0.563)

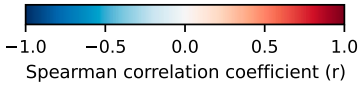

Fig. 4.3.1. *Correlations of residual IS and IS shrinkage with baseline CMR parameters, laboratory markers, and biomarkers in the paired-CMR cohort (n = 93)*

Cell color indicates the direction and strength of the Spearman correlation. Values within cells are Spearman correlation coefficients (r_s) and p-values. ALT – alanine aminotransferase;

AST – aspartate aminotransferase; BNP – B-type natriuretic peptide; CMR – cardiovascular magnetic resonance; CRP – C-reactive protein; eGFR – estimated glomerular filtration rate; HETE – hydroxyeicosatetraenoic acid; hs-CRP – high-sensitivity C-reactive protein; MVO – microvascular obstruction; NETosis – neutrophil extracellular trap formation.

Relative IS shrinkage showed weaker positive correlations with markers of acute myocardial injury, including troponin I (r_s = 0.215, p = 0.039), ALT (r_s = 0.301, p = 0.003), and AST (r_s = 0.287, p = 0.005). No significant correlations were observed between IS shrinkage and specialized biomarkers, including 20-HETE, 15(S)-HETE, and NETosis expression.

Overall, residual IS at 6 months was more consistently related to acute CMR-defined injury severity, infarct territory, and conventional biochemical markers of myocardial injury than IS shrinkage. In contrast, the investigated specialized biomarkers were not associated with infarct shrinkage or residual IS.

4.4. Regional myocardial phenotype and healing

Regional analyses of myocardial tissue characteristics (native T1, post-contrast T1, ECV, T2) and of longitudinal strain (LS) and circumferential strain (CS) were performed segmentally in infarcted, adjacent, and remote myocardium. The number of patients with available data varied by parameter and is shown in Tables 4.4.1 and 4.4.2.

4.4.1. Baseline regional tissue characteristics and strain in infarcted, adjacent, and remote myocardium

At baseline, segmental analysis revealed a stepwise pattern of impairment across infarcted, adjacent, and remote myocardium, both for myocardial deformation and for tissue characterization parameters (Table 4.4.1 and Figure 4.4.1).

Table 4.4.1. *Baseline regional myocardial tissue characteristics and strain in infarcted, adjacent, and remote segments*

Parameter (n)	Infarcted	Adjacent	Remote	p-value (I vs. A)	p-value (I vs. R)	p-value (A vs. R)	p-value (Overall)
Native T1, ms (100)	1433.7 [1383.0–1484.2]	1303.0 [1263.1–1345.4]	1269.7 [1237.6–1318.3]	**< 0.001**	**< 0.001**	**0.001**	**< 0.001**
Post-contrast T1, ms (99)	322.4 [261.5–367.1]	380.8 [318.5–430.7]	387.3 [325.7–439.3]	**< 0.001**	**< 0.001**	**0.004**	**< 0.001**
ECV, % (99)	36.1 [30.8–41.5]	26.4 [24.0–29.2]	24.7 [23.2–27.2]	**< 0.001**	**< 0.001**	**< 0.001**	**< 0.001**
T2, ms (96)	47.9 [44.3–50.6]	42.7 [40.5–43.8]	41.3 [40.0–43.3]	**< 0.001**	**< 0.001**	**1.000**	**< 0.001**
LS, % (98)	−17.1 [−20.4 to −13.7]	−22.3 [−26.1 to −17.8]	−21.2 [−25.5 to −17.8]	**< 0.001**	**< 0.001**	1.000	**< 0.001**
CS, % (99)	−24.7 [−30.3 to −19.6]	−27.2 [−32.6 to −23.7]	−30.2 [−35.8 to −25.9]	**0.028**	**< 0.001**	**0.011**	**< 0.001**

I – infarcted; A – adjacent; R – remote; ECV – extracellular volume; LS – longitudinal strain; CS – circumferential strain; T1 – T1 relaxation time; T2 – T2 relaxation time. Values are median [IQR]. Number in parentheses next to each parameter indicates the analytic n. Overall p-values were calculated using the Friedman test; pairwise comparisons used Wilcoxon signed-rank tests with Bonferroni correction.

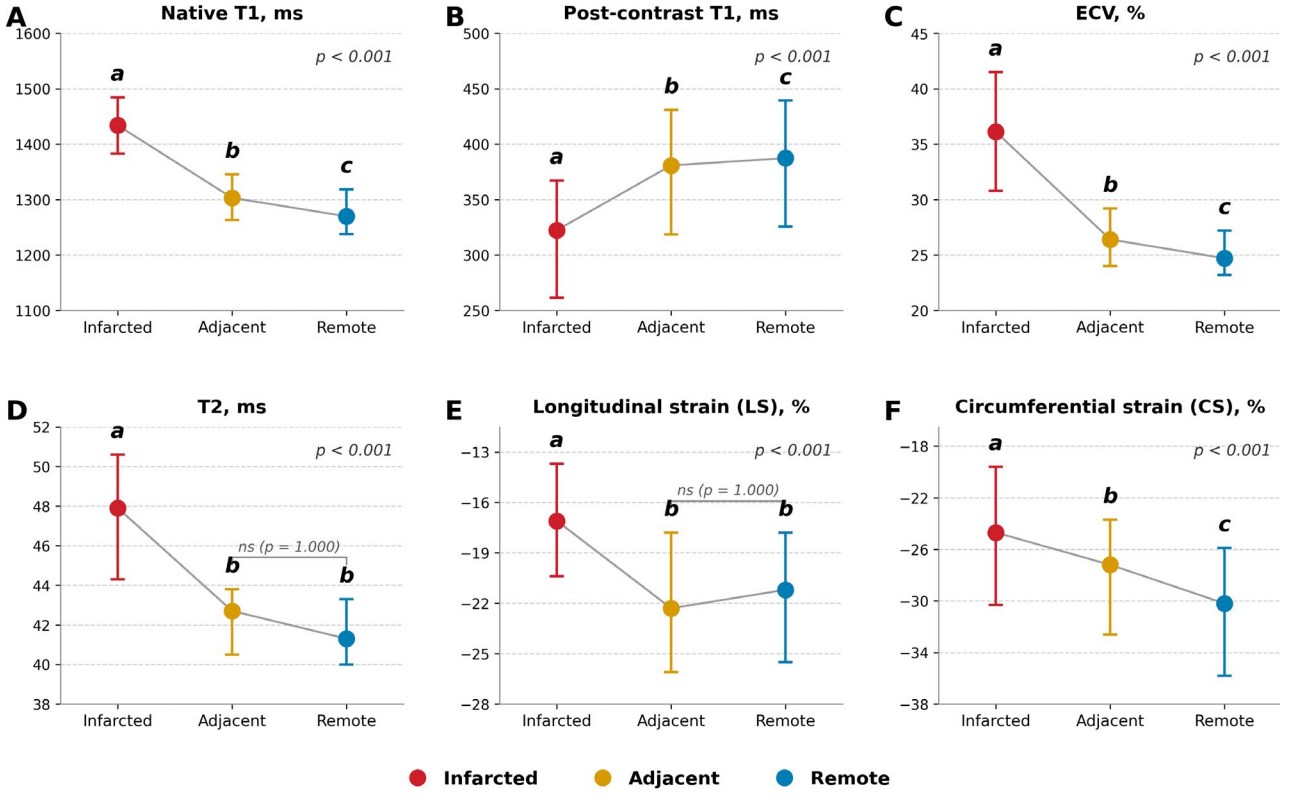

Fig. 4.4.1. *Regional myocardial tissue characteristics – native T1 (A), post-contrast T1 (B), ECV (C), T2 (D) – and strain, LS (E) and CS (F), in infarcted, adjacent, and remote segments at baseline*

Data are median with interquartile range. The p-value in each panel is the overall Friedman test; pairwise comparisons used Wilcoxon signed-rank tests with Bonferroni correction. Groups not sharing a common letter (a, b, c) differ significantly ($p < 0.05$); ns – not significant. CS – circumferential strain; ECV – extracellular volume; LS – longitudinal strain; T1 – T1 relaxation time; T2 – T2 relaxation time.

Infarcted segments exhibited the most pronounced contractile dysfunction, with median LS of −17.1% [−20.4 to −13.7] and CS of −24.7% [−30.3 to −19.6]. For CS, a stepwise gradient was observed, with intermediate values in adjacent segments (CS −27.2% [−32.6 to −23.7]) and the most preserved values in remote myocardium (CS −30.2% [−35.8 to −25.9]). LS was likewise most impaired in infarcted segments, whereas adjacent (LS −22.3% [−26.1 to −17.8]) and remote myocardium (LS −21.2% [−25.5 to −17.8]) showed similar, more preserved values. Pairwise comparisons confirmed significantly impaired CS in infarcted segments relative to both adjacent ($p = 0.028$) and remote myocardium ($p < 0.001$), and in adjacent relative to remote myocardium ($p = 0.011$). LS was significantly impaired in infarcted segments relative to both adjacent and remote myocardium (both $p < 0.001$), whereas adjacent and remote myocardium did not differ ($p = 1.000$).

Tissue characterization showed a parallel regional gradient. Relative to remote myocardium, infarcted segments had higher native T1 (1433.7 ms [1383.0–1484.2] vs. 1269.7 ms [1237.6–1318.3]; $p < 0.001$), higher ECV (36.1% [30.8–41.5] vs. 24.7% [23.2–27.2]; $p < 0.001$), longer T2 (47.9 ms [44.3–50.6] vs. 41.3 ms [40.0–43.3]; $p < 0.001$), and shorter post-contrast T1 (322.4 ms [261.5–367.1] vs. 387.3 ms [325.7–439.3]; $p < 0.001$).

When infarcted segments were compared with adjacent myocardium, differences of comparable magnitude were observed in native T1 (1433.7 ms [1383.0–1484.2] vs. 1303.0 ms [1263.1–1345.4]; $p < 0.001$), ECV (36.1% [30.8–41.5] vs. 26.4% [24.0–29.2]; $p < 0.001$), T2 (47.9 ms [44.3–50.6] vs. 42.7 ms [40.5–43.8]; $p < 0.001$), and post-contrast T1 (322.4 ms [261.5–367.1] vs. 380.8 ms [318.5–430.7]; $p < 0.001$).

Adjacent segments also differed from remote myocardium, with higher native T1 (1303.0 ms [1263.1–1345.4] vs. 1269.7 ms [1237.6–1318.3]; $p = 0.001$), higher ECV (26.4% [24.0–29.2] vs. 24.7% [23.2–27.2]; $p < 0.001$), and shorter post-contrast T1 (380.8 ms [318.5–430.7] vs. 387.3 ms [325.7–439.3]; $p = 0.004$). T2 values were similar between adjacent and remote myocardium (42.7 ms [40.5–43.8] vs. 41.3 ms [40.0–43.3]; $p = 1.000$).

4.4.2. Regional tissue and strain changes from baseline to 6 months

Between baseline and 6-month follow-up, regional myocardial deformation changed differently across the three myocardial regions, with the largest improvement in infarcted segments (Table 4.4.2 and Figure 4.4.2). In infarcted segments, LS improved from −17.2% [−20.6 to −14.5] to −21.9% [−26.3 to −17.5] ($p < 0.001$), and CS improved from −25.3% [−30.3 to −19.8] to −29.3% [−33.7 to −21.6] ($p < 0.001$). In adjacent segments, CS improved from −27.2% [−32.2 to −23.7] to −30.1% [−35.7 to −25.7] ($p = 0.002$), whereas

the change in LS did not reach statistical significance (p = 0.091). In remote segments, LS improved from −21.3% [−25.4 to −18.0] to −25.0% [−28.9 to −21.1] (p < 0.001), while CS did not change significantly (p = 0.067).

Table 4.4.2. Regional myocardial tissue characteristics and strain at baseline and 6-month follow-up in infarcted, adjacent, and remote segments

Segment and Parameter	Baseline	6-month follow-up	p-value
Infarcted segments (n):			
LS, % (91)	−17.2 [−20.6 to −14.5]	−21.9 [−26.3 to −17.5]	**< 0.001**
CS, % (91)	−25.3 [−30.3 to −19.8]	−29.3 [−33.7 to −21.6]	**< 0.001**
Native T1, ms (91)	1429.1 [1384.1–1482.6]	1312.8 [1272.5–1360.1]	**< 0.001**
Post-contrast T1, ms (86)	317.0 [254.8–356.7]	371.7 [331.3–410.6]	**< 0.001**
ECV, % (86)	35.9 [30.3–41.3]	34.3 [29.5–41.3]	0.219
T2, ms (89)	47.8 [44.3–50.6]	43.1 [41.5–46.2]	**< 0.001**
Adjacent segments (n):			
LS, % (90)	−21.9 [−26.5 to −17.6]	−23.6 [−29.4 to −19.3]	0.091
CS, % (91)	−27.2 [−32.2 to −23.7]	−30.1 [−35.7 to −25.7]	**0.002**
Native T1, ms (91)	1302.1 [1259.7–1344.7]	1262.6 [1234.3–1305.3]	**< 0.001**
Post-contrast T1, ms (86)	370.5 [303.5–429.5]	423.3 [395.8–474.1]	**< 0.001**
ECV, % (86)	26.1 [23.8–28.8]	26.0 [23.7–28.8]	0.602
T2, ms (89)	42.8 [40.3–43.9]	42.1 [39.8–44.0]	0.396
Remote segments (n):			
LS, % (89)	−21.3 [−25.4 to −18.0]	−25.0 [−28.9 to −21.1]	**< 0.001**
CS, % (89)	−30.2 [−36.0 to −26.0]	−32.3 [−39.7 to −27.8]	0.067
Native T1, ms (89)	1262.7 [1235.2–1311.7]	1253.6 [1223.2–1293.4]	**0.021**
Post-contrast T1, ms (84)	375.6 [323.0–432.8]	429.4 [397.5–471.2]	**< 0.001**
ECV, % (84)	24.8 [22.4–27.2]	25.3 [23.1–27.2]	**0.002**
T2, ms (87)	41.3 [40.0–43.3]	42.5 [39.9–44.4]	**0.036**

ECV – extracellular volume; CS – circumferential strain; LS – longitudinal strain; T1 – T1 relaxation time; T2 – T2 relaxation time. Values are median [IQR]. Number in parentheses next to each parameter indicates the analytic n. Within-region baseline-vs.-follow-up comparisons were performed using the Wilcoxon signed-rank test. Baseline values differ slightly from those in Table 4.4.1 because this paired analysis includes only patients with both baseline and 6-month follow-up CMR (n = 84–91).

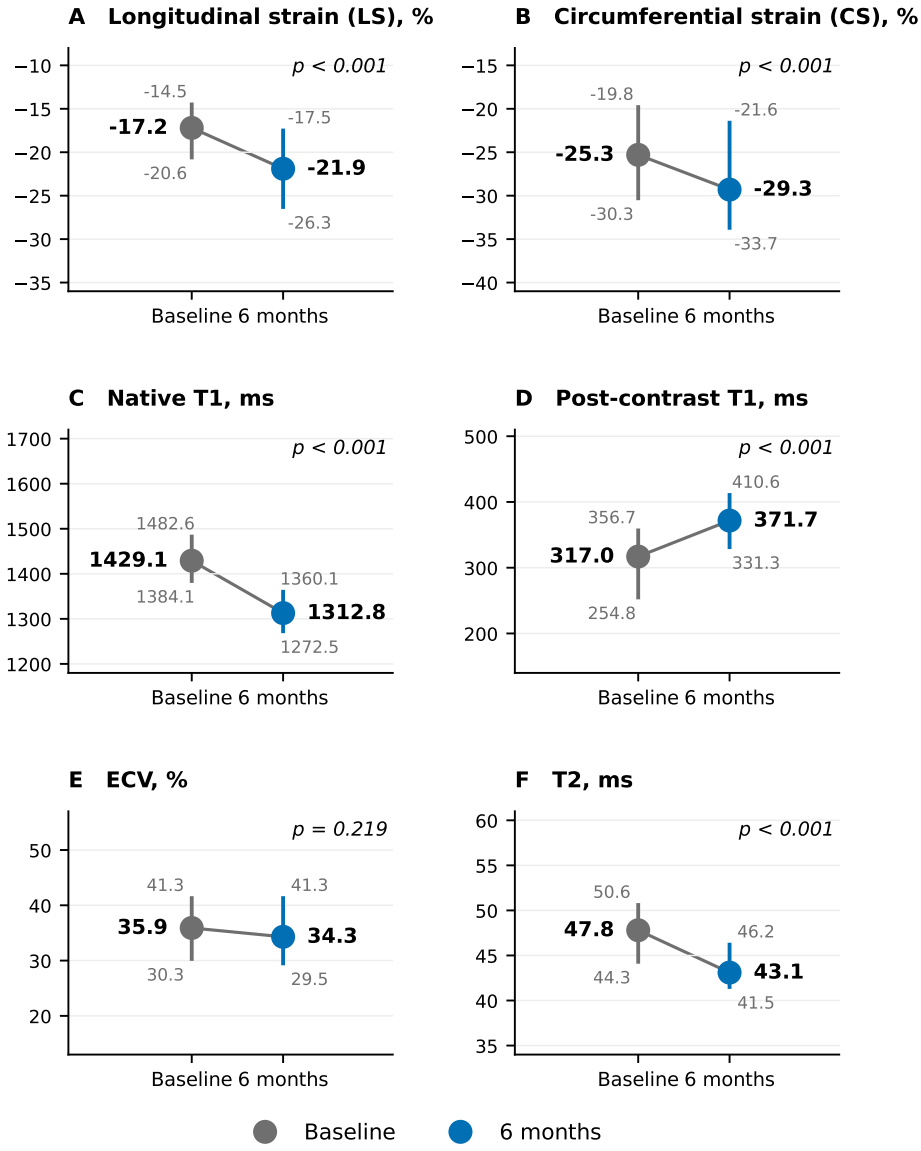

Fig. 4.4.2. *Regional myocardial tissue characteristics and strain at baseline and 6-month follow-up in infarcted myocardium*

The figure shows longitudinal changes in infarcted-segment myocardial deformation and tissue characteristics from baseline to 6-month follow-up. Values are median [IQR]. ECV – extracellular volume; LS – longitudinal strain; CS – circumferential strain; T1 – T1 relaxation time; T2 – T2 relaxation time.

Mapping parameters showed similar regional patterns. In infarcted segments, native T1 decreased from 1429.1 ms [1384.1–1482.6] to 1312.8 ms

[1272.5–1360.1] ($p < 0.001$), and post-contrast T1 increased from 317.0 ms [254.8–356.7] to 371.7 ms [331.3–410.6] ($p < 0.001$), whereas ECV did not change significantly ($p = 0.219$). Adjacent segments showed similar changes, with a decrease in native T1 from 1302.1 ms [1259.7–1344.7] to 1262.6 ms [1234.3–1305.3] ($p < 0.001$), and an increase in post-contrast T1 from 370.5 ms [303.5–429.5] to 423.3 ms [395.8–474.1] ($p < 0.001$), while ECV did not change significantly ($p = 0.602$). In remote myocardium, native T1 decreased from 1262.7 ms [1235.2–1311.7] to 1253.6 ms [1223.2–1293.4] ($p = 0.021$), post-contrast T1 increased from 375.6 ms [323.0–432.8] to 429.4 ms [397.5–471.2] ($p < 0.001$), and ECV increased from 24.8% [22.4–27.2] to 25.3% [23.1–27.2] ($p = 0.002$).

T2 changes also differed by region. T2 decreased in infarcted segments from 47.8 ms [44.3–50.6] to 43.1 ms [41.5–46.2] ($p < 0.001$), did not change significantly in adjacent segments ($p = 0.396$), and increased slightly in remote myocardium from 41.3 ms [40.0–43.3] to 42.5 ms [39.9–44.4] ($p = 0.036$).

4.5. Functional recovery

Functional recovery was evaluated using left ventricular ejection fraction at 6-month follow-up CMR. Patients were classified according to a clinically defined dichotomous outcome, and baseline clinical, laboratory, and CMR predictors of impaired functional recovery were assessed using descriptive comparisons, logistic regression, and ROC analysis.

4.5.1. Definition and frequency of impaired functional outcome

Impaired functional outcome was defined as LVEF < 50% at 6-month follow-up CMR. Among 93 patients with paired baseline and follow-up CMR data, 28 patients (30.1%) had impaired functional outcome, whereas 65 patients (69.9%) had follow-up LVEF ≥ 50%.

4.5.2. Baseline clinical, laboratory, and CMR characteristics according to follow-up LV functional outcome

Compared with patients with follow-up LVEF ≥ 50%, patients with follow-up LVEF < 50% were older ($p = 0.047$), had lower BMI ($p = 0.046$), and were more frequently current smokers (19/28 [67.9%] vs. 29/65 [44.6%]; $p = 0.045$). Sex, diabetes mellitus, arterial hypertension, and family history of CAD did not differ significantly between groups; dyslipidemia showed a borderline difference ($p = 0.051$). Patients with impaired follow-up LV function had longer door-to-balloon time ($p = 0.043$), more often presented with anterior myocardial infarction (16/28 [57.1%] vs. 22/65 [33.8%];

p = 0.042), and more frequently had pre-PCI TIMI flow 0–1 (25/28 [89.3%] vs. 42/65 [64.6%]; p = 0.015). Symptom-to-balloon time and Killip class ≥ 2 did not differ significantly between groups.

Among laboratory and biomarker variables, troponin I (52.9 [35.4–92.7] vs. 21.6 [9.4–35.7] µg/L; p < 0.001), AST (312.0 [182.5–433.0] vs. 131.0 [75.5–190.5] IU/L; p < 0.001), and BNP (p = 0.037) were higher in patients with impaired follow-up LV function. Platelet count was numerically lower in this group, although the difference did not reach statistical significance (p = 0.084). Urea, eGFR, and the specialized biomarkers – 20-HETE, 15(S)-HETE, and NETosis expression – did not differ significantly between groups.

Baseline LVEF was lower in patients with impaired follow-up LV function (38.5 [33.4–41.8] vs. 50.6 [46.7–55.9]%; p < 0.001). LVEDVi (p < 0.001) and LVESVi (p < 0.001) were larger, GLS (p = 0.012) and GCS (−22.4 [−26.7 to −18.6] vs. −29.5 [−33.4 to −25.9]%; p < 0.001) were worse, and IS was larger (47.2 [33.4–68.1] vs. 26.6 [14.9–38.0]%; p < 0.001) in this group. Baseline LV thrombus was also more frequent (8/28 [28.6%] vs. 2/65 [3.1%]; p = 0.042). Among the 65 MVO-positive patients with paired CMR data, MVO size was greater in those with impaired functional outcome (n = 21) than in those with preserved LVEF (n = 44; 7.1% [3.3–10.3] vs. 3.5% [2.0–5.9]; p = 0.006).

Among regional CMR parameters, infarcted-region circumferential strain was worse (−20.1 [−23.7 to −13.5] vs. −27.7 [−32.7 to −23.6]%; p < 0.001) and infarcted-region post-contrast T1 was lower (p = 0.044) in patients with follow-up LVEF < 50%. Infarcted-region ECV was numerically higher in this group, with a borderline difference (p = 0.058). Infarcted-region longitudinal strain, native T1, and T2 did not differ significantly between groups. Baseline characteristics according to follow-up LV functional outcome are presented in Table 4.5.1.

Table 4.5.1. *Baseline clinical, laboratory, and CMR characteristics according to follow-up LV functional outcome*

Variable	Follow-up LVEF ≥ 50% (n = 65)	Follow-up LVEF < 50% (n = 28)	p-value
Demographics and risk factors			
Age, years	60.5 [54.0–64.5]	65.0 [57.0–69.5]	**0.047**
Male sex, n (%)	48 (73.8)	24 (85.7)	0.209
BMI, kg/m²	28.4 [25.8–30.9]	26.8 [23.6–29.2]	**0.046**
Diabetes mellitus, n (%)	11 (16.9)	1 (3.6)	0.099
Arterial hypertension, n (%)	55 (84.6)	21 (75.0)	0.271
Dyslipidemia, n (%)	62 (95.4)	23 (82.1)	0.051
Current smoking, n (%)	29 (44.6)	19 (67.9)	**0.045**

Table 4.5.1 cont.

Variable	Follow-up LVEF ≥ 50% (n = 65)	Follow-up LVEF < 50% (n = 28)	p-value
Family history of CAD, n (%)	25 (38.5)	9 (32.1)	0.562
Clinical and procedural characteristics			
Symptom-to-balloon time, min	310.0 [152.5–545.0]	365.0 [207.5–510.0]	0.612
Door-to-balloon time, min	41.0 [31.5–59.0]	58.0 [44.5–74.0]	**0.043**
Anterior MI, n (%)	22 (33.8)	16 (57.1)	**0.042**
Pre-PCI TIMI flow 0–1, n (%)	42 (64.6)	25 (89.3)	**0.015**
Killip class ≥ 2, n (%)	14 (21.5)	8 (28.6)	0.464
Laboratory and biomarker parameters			
Platelet count, ×10⁹/L	222.0 [190.0–242.0]	207.5 [167.3–242.8]	0.084
Troponin I, µg/L	21.6 [9.4–35.7]	52.9 [35.4–92.7]	**< 0.001**
BNP, ng/L	143.7 [82.4–236.8]	218.3 [134.3–271.8]	**0.037**
AST, IU/L	131.0 [75.5–190.5]	312.0 [182.5–433.0]	**< 0.001**
Urea, mmol/L	5.1 [4.2–6.4]	5.8 [4.5–7.6]	0.194
eGFR, mL/min/1.73 m²	96.0 [82.7–102.5]	93.1 [79.4–98.8]	0.215
20-HETE, ng/mL	28.5 [4.0–99.1]	19.7 [1.4–101.8]	0.409
15(S)-HETE, ng/mL	0.4 [0.2–1.3]	0.6 [0.2–2.4]	0.124
NETosis expression, mU/mL	53.6 [42.6–74.6]	52.5 [44.5–67.0]	0.877
Baseline CMR parameters			
LVEF, %	50.6 [46.7–55.9]	38.5 [33.4–41.8]	**< 0.001**
LVEDVi, mL/m²	84.0 [72.1–96.7]	95.9 [90.5–113.7]	**< 0.001**
LVESVi, mL/m²	41.7 [36.3–51.1]	58.1 [52.8–72.9]	**< 0.001**
GLS, %	−21.1 [−23.7 to −18.4]	−18.6 [−21.8 to −15.2]	**0.012**
GCS, %	−29.5 [−33.4 to −25.9]	−22.4 [−26.7 to −18.6]	**< 0.001**
Infarct size, %	26.6 [14.9–38.0]	47.2 [33.4–68.1]	**< 0.001**
MVO size, %	3.5 [2.0–5.9]	7.1 [3.3–10.3]	**0.006**
Baseline LV thrombus, n (%)	2 (3.1)	8 (28.6)	**0.042**
Infarcted-region CMR parameters			
Longitudinal strain, %	−17.4 [−20.2 to −15.0]	−15.8 [−20.7 to −12.5]	0.287
Circumferential strain, %	−27.7 [−32.7 to −23.6]	−20.1 [−23.7 to −13.5]	**< 0.001**
Native T1, ms	1429.1 [1368.2–1483.6]	1420.3 [1385.2–1472.7]	0.893
Post-contrast T1, ms	327.0 [284.1–381.4]	288.1 [242.6–338.1]	**0.044**
ECV, %	35.0 [30.7–39.2]	40.3 [29.7–47.1]	0.058
T2, ms	47.5 [44.3–49.5]	48.5 [44.1–54.7]	0.259

AST – aspartate aminotransferase; BMI – body mass index; BNP – B-type natriuretic peptide; CAD – coronary artery disease; CMR – cardiovascular magnetic resonance; ECV – extracellular volume; eGFR – estimated glomerular filtration rate; GCS – global circumferential strain; GLS – global longitudinal strain; HETE – hydroxyeicosatetraenoic acid; IQR – interquartile range; LV – left ventricle/left ventricular; LVEDVi – left ventricular end-diastolic volume index; LVEF – left ventricular ejection fraction; LVESVi – left ventricular end-sys-

tolic volume index; MI – myocardial infarction; MVO – microvascular obstruction; NETosis – neutrophil extracellular trap formation; PCI – percutaneous coronary intervention; T1 – T1 relaxation time; T2 – T2 relaxation time; TIMI – Thrombolysis in Myocardial Infarction. Values are presented as median [IQR] or n (%), as appropriate. Continuous variables were compared using the Mann–Whitney U test. Categorical variables were compared using the chi-square test or Fisher's exact test, as appropriate.

4.5.3. Logistic regression analysis of predictors of impaired follow-up LV function

Among demographic and risk-factor variables, current smoking was associated with impaired follow-up LV function (OR 2.62, 95% CI 1.03–6.65; p = 0.043), while dyslipidemia showed an apparent protective association of borderline significance (OR 0.22, 95% CI 0.05–1.01; p = 0.051). Age, sex, BMI, diabetes mellitus, arterial hypertension, and family history of CAD were not associated with impaired follow-up LV function.

Among clinical and procedural variables, anterior MI (OR 2.61, 95% CI 1.05–6.46; p = 0.039) and pre-PCI TIMI flow 0–1 (OR 4.56, 95% CI 1.24–16.76; p = 0.022) were associated with impaired follow-up LV function, whereas symptom-to-balloon time, door-to-balloon time, and Killip class ≥ 2 were not.

Among laboratory and biomarker variables, higher troponin I (OR 1.035, 95% CI 1.017–1.053; p < 0.001), AST (p < 0.001), and BNP (p = 0.033), and lower platelet count (p = 0.041) were associated with impaired follow-up LV function. Urea, eGFR, and the specialized biomarkers – 20-HETE, 15(S)-HETE, and NETosis expression – were not associated with impaired follow-up LV function. Univariable predictors are presented in Table 4.5.2.

Table 4.5.2. *Univariable binary logistic regression analysis of predictors of impaired follow-up LV function*

Variable	OR	95% CI	p-value
Demographics and risk factors			
Age, years	1.036	0.985–1.090	0.172
Male sex	2.125	0.644–7.015	0.216
BMI, kg/m²	0.895	0.794–1.008	0.068
Diabetes mellitus	0.182	0.022–1.483	0.111
Arterial hypertension	0.545	0.184–1.621	0.275
Dyslipidemia	0.223	0.049–1.007	0.051
Current smoking	2.621	1.032–6.654	**0.043**
Family history of CAD	0.758	0.297–1.935	0.562

Table 4.5.2 cont.

Variable	OR	95% CI	p-value
Clinical and procedural characteristics			
Symptom-to-balloon time, min	1.000	0.998–1.002	0.840
Door-to-balloon time, min	1.001	0.993–1.008	0.839
Anterior MI	2.606	1.051–6.460	**0.039**
Pre-PCI TIMI flow 0–1	**4.563**	**1.242–16.762**	**0.022**
Killip class ≥ 2	**1.457**	**0.530–4.004**	**0.465**
Laboratory and biomarker parameters			
Platelet count, ×10⁹/L	0.989	0.979–1.000	**0.041**
Troponin I, µg/L	1.035	1.017–1.053	**< 0.001**
BNP, ng/L	1.004	1.000–1.007	**0.033**
AST, IU/L	1.009	1.005–1.013	**< 0.001**
Urea, mmol/L	1.248	0.968–1.608	0.087
eGFR, mL/min/1.73 m²	0.987	0.961–1.014	0.351
20-HETE, ng/mL	1.000	0.997–1.002	0.755
15(S)-HETE, ng/mL	1.194	0.863–1.652	0.285
NETosis expression, mU/mL	0.993	0.979–1.007	0.342
Baseline CMR parameters			
LVEF, %	0.806	0.734–0.885	**< 0.001**
LVEDVi, mL/m²	1.047	1.018–1.075	**0.001**
LVESVi, mL/m²	1.120	1.061–1.182	**< 0.001**
GLS, %	1.158	1.033–1.298	**0.012**
GCS, %	1.267	1.134–1.416	**< 0.001**
Infarct size, %	1.080	1.043–1.117	**< 0.001**
MVO size, %	1.174	1.051–1.311	**0.004**
Baseline LV thrombus	12.600	2.471–64.251	**0.002**
Infarcted-region CMR parameters			
Longitudinal strain, %	1.047	0.955–1.148	0.327
Circumferential strain, %	1.211	1.108–1.323	**< 0.001**
Native T1, ms	1.001	0.995–1.006	0.779
Post-contrast T1, ms	0.993	0.987–1.000	0.058
ECV, %	1.074	1.014–1.138	**0.015**
T2, ms	1.077	0.982–1.182	0.116

AST – aspartate aminotransferase; BMI – body mass index; BNP – B-type natriuretic peptide; CAD – coronary artery disease; CI – confidence interval; CMR – cardiovascular magnetic resonance; ECV – extracellular volume; eGFR – estimated glomerular filtration rate; GCS – global circumferential strain; GLS – global longitudinal strain; HETE – hydroxyeicosatetraenoic acid; LV – left ventricle/left ventricular; LVEDVi – left ventricular end-diastolic volume index; LVEF – left ventricular ejection fraction; LVESVi – left ventricular end-systolic volume index; MI – myocardial infarction; MVO – microvascular obstruction; NETosis – neutrophil extracellular trap formation; OR – odds ratio; PCI – percutaneous coronary intervention; T1 – T1 relaxation time; T2 – T2 relaxation time; TIMI – Thrombolysis in Myocardial Infarction. Values are odds ratios with 95% confidence intervals.

4.5.4. Multivariable regression analysis of predictors of impaired follow-up LV function

Variable selection for the multivariable analysis was based on three considerations: clinical relevance, the degree of correlation among candidate predictors, and the limited number of events available (28 patients with impaired follow-up LV function). Several univariable predictors showed strong intercorrelation – most notably troponin I with AST (r_s = 0.801) and with baseline IS (r_s = 0.738), and baseline LVEF with both GCS (r_s = −0.775) and infarcted-region CS (r_s = −0.734); GCS and infarcted-region CS were also closely related (r_s = 0.844). To avoid multicollinearity, strongly correlated variables were not entered simultaneously into the primary model.

Demographic, clinical, and procedural univariable predictors – current smoking, anterior MI, and pre-PCI TIMI flow 0–1 – were not entered into the primary model. These variables likely act through the acute injury captured by imaging. This was confirmed in an exploratory model: when pre-PCI TIMI flow 0–1 was added to the imaging variables, it did not retain independent significance (OR 3.13, 95% CI 0.50–19.64; p = 0.223), while baseline LVEF remained the only independent predictor (p = 0.024). Dyslipidemia was not considered for multivariable analysis given the small number of patients without dyslipidemia in the impaired-LVEF group (n = 5).

Among blood markers, troponin I was selected for the primary model. AST, BNP, and platelet count were excluded because they did not retain independent significance alongside troponin I in an exploratory analysis.

Among CMR parameters, GLS and GCS were excluded because of their close correlation with infarcted-region CS. The variables ultimately retained – baseline LVEF, baseline IS, and infarcted-region CS – were chosen to represent three distinct dimensions of acute injury: global systolic function, structural infarct burden, and regional infarcted-region mechanics. Infarcted-region ECV, despite a significant univariable association, was not included after a preliminary analysis confirmed that it added no independent contribution alongside the retained variables (p = 0.397).

The primary multivariable model therefore included baseline LVEF, troponin I, baseline IS, and infarcted-region circumferential strain. Of these, only baseline LVEF remained independently associated with impaired follow-up LV function (OR 0.859, 95% CI 0.758–0.973; p = 0.017). Troponin I (p = 0.080), baseline IS (p = 0.387), and infarcted-region circumferential strain (p = 0.583) lost their univariable associations once baseline LVEF was accounted for.

A sensitivity analysis was performed to examine whether infarct burden and regional mechanics retained their associations when baseline LVEF

was not included in the model. In this analysis, both larger baseline IS (OR 1.054, 95% CI 1.015–1.095; p = 0.006) and more impaired infarcted-region circumferential strain (OR 1.145, 95% CI 1.033–1.269; p = 0.010) were independently associated with impaired follow-up LV function. Multivariable results are presented in Table 4.5.3.

Table 4.5.3. *Multivariable binary logistic regression analyses of predictors of impaired follow-up LV function*

Variable	Primary model, OR (95% CI)	p-value	Sensitivity model, OR (95% CI)	p-value
Baseline LVEF, %	0.859 (0.758–0.973)	**0.017**	—	—
Troponin I, µg/L	1.018 (0.998–1.038)	**0.080**	—	—
Baseline infarct size, %	1.020 (0.975–1.067)	0.387	1.054 (1.015–1.095)	0.006
Infarcted-region CS, %	1.037 (0.911–1.181)	0.583	1.145 (1.033–1.269)	0.010

CI – confidence interval; CS – circumferential strain; LVEF – left ventricular ejection fraction; OR – odds ratio. Values are odds ratios with 95% confidence intervals.

4.5.5. Discriminatory performance of selected baseline markers for impaired follow-up LV function

ROC analysis was performed to assess the discriminatory performance of four baseline markers for impaired follow-up LV function: troponin I, baseline LVEF, baseline IS, and infarcted-region circumferential strain. These were selected to represent biochemical injury, global systolic function, structural infarct burden, and regional infarcted-region mechanics, respectively. The analysis was considered exploratory because of the limited number of impaired functional outcome events; its purpose was to describe discrimination rather than to develop a definitive prediction model. The discriminatory performance of these markers is presented in Table 4.5.4 and Figure 4.5.1.

All four markers showed good discriminatory performance, with AUC values ranging from 0.810 (troponin I) to 0.854 (baseline LVEF). Baseline LVEF showed the highest specificity (90.8%) for identifying impaired follow-up LV function, while infarcted-region CS showed the highest sensitivity (85.7%).

Table 4.5.4. *Discriminatory performance of selected baseline markers for impaired follow-up LV function*

Variable	Cut-off value	AUC	95% CI	p-value	Sensitivity (%)	Specificity (%)
Troponin I, µg/L	≥ 33.30	0.810	0.715–0.906	**< 0.001**	82.1	72.3
Baseline LVEF, %	≤ 41.3	0.854	0.762–0.946	**< 0.001**	75.0	90.8
Baseline infarct size, %	≥ 42.3	0.813	0.719–0.907	**< 0.001**	67.9	84.6
Infarcted-region CS, %	≥ −24.7	0.818	0.724–0.911	**< 0.001**	85.7	67.7

LVEF – left ventricular ejection fraction; AUC – area under the curve; CI – confidence interval; CS – circumferential strain. Impaired follow-up LV function was defined as follow-up LVEF < 50%. Cut-off values were selected using the Youden index.

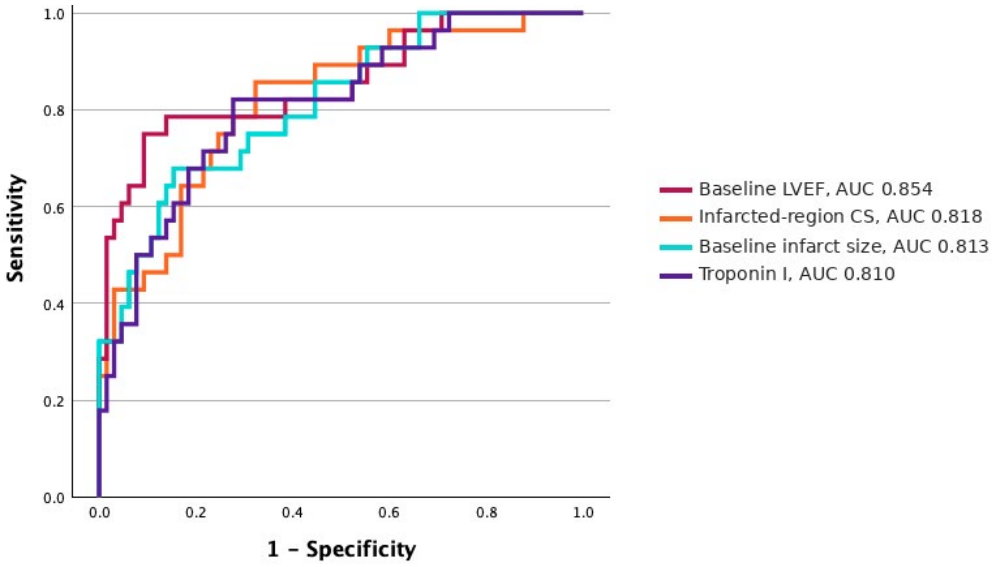

Fig. 4.5.1. *ROC curves of selected baseline markers for impaired follow-up LV function*

AUC – area under the curve; CS – circumferential strain; LVEF – left ventricular ejection fraction; ROC – receiver operating characteristic. ROC curves are shown for troponin I, baseline LVEF, baseline IS, and infarcted-region CS.

4.6. Adverse left ventricular remodeling phenotype

Adverse left ventricular remodeling was evaluated as a late structural outcome at 6-month follow-up CMR. Baseline clinical, laboratory, biomarker, and CMR characteristics associated with adverse remodeling were assessed using descriptive comparisons, logistic regression, and ROC analysis.

4.6.1. Definition and frequency of adverse left ventricular remodeling

Adverse left ventricular remodeling was defined as a ≥ 12% increase in both left ventricular end-diastolic volume and left ventricular end-systolic volume at 6-month follow-up compared with baseline CMR. Among 93 patients with paired baseline and follow-up CMR data, 19 patients (20.4%) met the criteria for ALVR, whereas 74 patients (79.6%) did not.

4.6.2. Baseline characteristics according to ALVR status

Compared with patients without ALVR, patients who developed ALVR more frequently had anterior myocardial infarction (12/19 [63.2%] vs. 26/74 [35.1%]; p = 0.027). Pre-hospital medication use was also more frequent in the ALVR group, including beta-blockers (10/19 [52.6%] vs. 20/74 [27.0%]; p = 0.033), angiotensin-converting enzyme (ACE) inhibitors or angiotensin receptor blockers (13/19 [68.4%] vs. 31/74 [41.9%]; p = 0.039), and calcium channel blockers (5/19 [26.3%] vs. 6/74 [8.1%]; p = 0.028). Patients who developed ALVR had a lower platelet count (191.0 [181.0–233.0] vs. 222.0 [196.5–245.8] $\times 10^9$/L; p = 0.022) and lower circulating 20-HETE concentrations (6.2 [0.1–32.4] vs. 37.1 [6.8–124.1] ng/mL; p = 0.004) than patients without ALVR. Urea was higher in the ALVR group, with a borderline difference (6.1 [4.8–7.7] vs. 5.2 [4.2–6.5] mmol/L; p = 0.067). Troponin I, BNP, AST, eGFR, 15(S)-HETE, and NETosis expression did not differ significantly between groups.

On baseline CMR, patients with ALVR had higher non-indexed LVESV (102.1 [91.5–133.4] vs. 89.0 [70.5–110.1] mL; p = 0.029), with a borderline trend toward higher non-indexed LVEDV (197.8 [164.1–224.0] vs. 175.6 [148.3–201.4] mL; p = 0.092). Baseline LVEF, IS, and GCS did not differ significantly between groups, while GLS showed a borderline trend (−17.6 [−22.9 to −15.7] vs. −20.9 [−23.2 to −18.4]%; p = 0.077). Among the 65 MVO-positive patients with paired CMR data, MVO size did not differ significantly according to ALVR status (3.8 [1.6–5.8] vs. 4.3 [2.7–8.0]%; p = 0.269). Among infarcted-region CMR parameters, patients with ALVR had higher native T1 (1466.6 [1417.3–1538.5] vs. 1416.6 [1364.2–1468.4] ms; p = 0.009) and lower post-contrast T1 (274.5 [232.3–337.4] vs. 323.7 [285.1–383.1] ms; p = 0.010), whereas regional strain measures, ECV, and T2 did not differ between groups. Baseline characteristics according to ALVR status are presented in Table 4.6.1.

Table 4.6.1. *Baseline clinical, procedural, laboratory, biomarker, and CMR characteristics according to adverse left ventricular remodeling status*

Variable	No ALVR (n = 74)	ALVR (n = 19)	p-value
Demographics and cardiovascular risk factors			
Age, years	61.0 [53.0–67.3]	61.0 [57.0–71.0]	0.407
Male sex, n (%)	56 (75.7)	16 (84.2)	0.548
BMI, kg/m²	28.0 [24.7–30.5]	28.4 [25.8–32.4]	0.214
Diabetes mellitus, n (%)	9 (12.2)	3 (15.8)	0.705
Arterial hypertension, n (%)	59 (79.7)	17 (89.5)	0.509
Dyslipidemia, n (%)	68 (91.9)	17 (89.5)	0.664
Current smoking, n (%)	36 (48.6)	12 (63.2)	0.259
Pre-hospital medications, n (%)			
Beta-blockers	20 (27.0)	10 (52.6)	**0.033**
ACE inhibitors or ARBs	31 (41.9)	13 (68.4)	**0.039**
Calcium channel blockers	6 (8.1)	5 (26.3)	**0.028**
Thiazide/thiazide-like diuretics	9 (12.2)	5 (26.3)	0.124
Statins	7 (9.5)	1 (5.3)	0.561
Clinical and procedural characteristics			
Symptom-to-balloon time, min	364.0 [203.8–576.3]	275.0 [170.0–440.0]	0.341
Door-to-balloon time, min	49.0 [31.0–68.8]	49.0 [40.0–63.0]	0.819
Anterior MI, n (%)	26 (35.1)	12 (63.2)	**0.027**
Pre-PCI TIMI flow 0–1, n (%)	54 (73.0)	13 (68.4)	0.922
Post-PCI TIMI flow 3, n (%)	68 (91.9)	19 (100.0)	0.439
Killip class ≥ 2, n (%)	17 (23.0)	5 (26.3)	0.767
Laboratory and biomarker parameters			
Platelet count, ×10⁹/L	222.0 [196.5–245.8]	191.0 [181.0–233.0]	**0.022**
Troponin I, µg/L	26.6 [11.2–47.9]	25.4 [17.7–41.1]	0.523
BNP, ng/L	154.8 [93.5–245.1]	157.1 [94.8–319.3]	0.407
AST, IU/L	155.5 [84.0–268.3]	167.0 [121.0–301.0]	0.539
Urea, mmol/L	5.2 [4.2–6.5]	6.1 [4.8–7.7]	0.067
eGFR, mL/min/1.73 m²	95.0 [85.5–101.6]	89.0 [78.0–100.0]	0.177
20-HETE, ng/mL	37.1 [6.8–124.1]	6.2 [0.1–32.4]	**0.004**
15(S)-HETE, ng/mL	0.4 [0.2–1.4]	0.8 [0.5–1.7]	0.141
NETosis expression, mU/mL	54.1 [42.6–68.5]	57.5 [45.0–105.3]	0.257
Baseline CMR parameters			
LVEF, %	50.2 [41.0–52.9]	45.0 [39.4–49.3]	0.107
LVEDV, mL	175.6 [148.3–201.4]	197.8 [164.1–224.0]	0.092
LVEDVi, mL/m²	88.7 [75.0–100.0]	90.7 [83.7–104.6]	0.253
LVESV, mL	89.0 [70.5–110.1]	102.1 [91.5–133.4]	**0.029**
LVESVi, mL/m²	45.0 [36.9–54.8]	52.9 [41.8–62.8]	0.088
GLS, %	−20.9 [−23.2 to −18.4]	−17.6 [−22.9 to −15.7]	0.077
GCS, %	−27.6 [−31.2 to −24.1]	−26.1 [−31.4 to −20.4]	0.402

Table 4.6.1 cont.

Variable	No ALVR (n = 74)	ALVR (n = 19)	p-value
LV thrombus, n (%)	7 (9.5)	3 (15.8)	0.421
Infarct size, %	28.5 [17.1–45.4]	39.5 [28.2–53.7]	0.101
MVO size, %	4.3 [2.7–8.0]	3.8 [1.6–5.8]	0.269
Infarcted-region CMR parameters			
Longitudinal strain, %	−17.8 [−20.7 to −14.1]	−16.2 [−17.4 to −13.5]	0.205
Circumferential strain, %	−26.4 [−30.8 to −20.4]	−22.2 [−30.3 to −18.0]	0.228
Native T1, ms	1416.6 [1364.2–1468.4]	1466.6 [1417.3–1538.5]	**0.009**
Post-contrast T1, ms	323.7 [285.1–383.1]	274.5 [232.3–337.4]	**0.010**
ECV, %	34.7 [30.1–41.0]	38.3 [35.1–42.2]	0.184
T2, ms	47.6 [44.2–49.8]	49.2 [44.3–52.2]	0.319

ACE – angiotensin-converting enzyme; ALVR – adverse left ventricular remodeling; ARB – angiotensin receptor blocker; AST – aspartate aminotransferase; BMI – body mass index; BNP – B-type natriuretic peptide; CMR – cardiovascular magnetic resonance; ECV – extracellular volume; eGFR – estimated glomerular filtration rate; GCS – global circumferential strain; GLS – global longitudinal strain; HETE – hydroxyeicosatetraenoic acid; IQR – interquartile range; LV – left ventricle/left ventricular; LVEDV – left ventricular end-diastolic volume; LVEDVi – left ventricular end-diastolic volume index; LVEF – left ventricular ejection fraction; LVESV – left ventricular end-systolic volume; LVESVi – left ventricular end-systolic volume index; MI – myocardial infarction; MVO – microvascular obstruction; NETosis – neutrophil extracellular trap formation; PCI – percutaneous coronary intervention; T1 – T1 relaxation time; T2 – T2 relaxation time; TIMI – Thrombolysis in Myocardial Infarction. Values are presented as median [IQR] or n (%), as appropriate.

4.6.3. Logistic regression analysis of predictors of adverse left ventricular remodeling

Baseline predictors of ALVR were first evaluated using univariable binary logistic regression. Anterior MI (OR 3.17, 95% CI 1.11–9.02; p = 0.031), lower platelet count (OR 0.99, 95% CI 0.97–1.00; p = 0.029), and higher urea (OR 1.34, 95% CI 1.02–1.78; p = 0.039) were associated with ALVR, while lower 20-HETE showed a borderline association (OR 0.98, 95% CI 0.96–1.00; p = 0.091). Among CMR parameters, no global volume, function, or strain measure was significantly associated with ALVR. Among infarcted-region parameters, higher native T1 (OR 1.01, 95% CI 1.00–1.01; p = 0.028) and lower post-contrast T1 (OR 0.99, 95% CI 0.98–1.00; p = 0.008) were associated with ALVR, while regional strain measures, ECV, and T2 were not. Univariable predictors are presented in Table 4.6.2.

Table 4.6.2. *Univariable binary logistic regression analysis of predictors of adverse left ventricular remodeling*

Variable	OR	95% CI	p-value
Clinical and laboratory variables			
Age, years	1.03	0.98–1.09	0.275
BMI, kg/m²	1.06	0.95–1.18	0.332
Symptom-to-balloon time, min	1.00	1.00–1.00	0.396
Door-to-balloon time, min	1.00	0.98–1.01	0.488
Anterior MI	3.17	1.11–9.02	**0.031**
Infarct-related artery	1.07	0.53–2.16	0.852
Pre-PCI TIMI flow 0–1	0.80	0.27–2.40	0.694
Thrombolysis before PCI	2.06	0.35–12.19	0.426
Manual thrombus aspiration during PCI	0.75	0.15–3.77	0.730
Platelet count, ×10⁹/L	0.99	0.97–1.00	**0.029**
Troponin I, µg/L	1.00	0.99–1.01	0.616
BNP, ng/L	1.00	1.00–1.01	0.309
Urea, mmol/L	1.34	1.02–1.78	**0.039**
AST, IU/L	1.00	1.00–1.00	0.642
20-HETE, ng/mL	0.98	0.96–1.00	0.091
15(S)-HETE, ng/mL	1.04	0.71–1.52	0.849
NETosis expression, mU/mL	1.01	1.00–1.02	0.172
Baseline CMR parameters			
LVEF, %	0.98	0.93–1.03	0.342
LVEDV, mL	1.01	1.00–1.02	0.118
LVEDVi, mL/m²	1.01	0.99–1.04	0.348
LVESV, mL	1.01	1.00–1.02	0.161
LVESVi, mL/m²	1.01	0.99–1.04	0.337
GLS, %	1.10	0.97–1.24	0.130
GCS, %	1.03	0.95–1.11	0.477
Infarct size, %	1.02	0.99–1.05	0.138
MVO size, %	0.98	0.88–1.10	0.732
Baseline LV thrombus	1.80	0.42–7.72	0.432
Infarcted-region parameters in baseline CMR			
LS, %	1.05	0.95–1.17	0.357
CS, %	1.04	0.98–1.11	0.217
Native T1, ms	1.01	1.00–1.01	**0.028**
Post-contrast T1, ms	0.99	0.98–1.00	**0.008**
ECV, %	1.02	0.96–1.08	0.581
T2, ms	1.04	0.94–1.15	0.451

AST – aspartate aminotransferase; BMI – body mass index; BNP – B-type natriuretic peptide; CI – confidence interval; CMR – cardiovascular magnetic resonance; CS – circumferential strain; ECV – extracellular volume; GCS – global circumferential strain; GLS – global longitudinal strain; HETE – hydroxyeicosatetraenoic acid; LS – longitudinal strain;

LVEDV – left ventricular end-diastolic volume; LVEDVi – left ventricular end-diastolic volume index; LVEF – left ventricular ejection fraction; LVESV – left ventricular end-systolic volume; LVESVi – left ventricular end-systolic volume index; MI – myocardial infarction; MVO – microvascular obstruction; NETosis – neutrophil extracellular trap formation; OR – odds ratio; PCI – percutaneous coronary intervention; T1 – T1 relaxation time; T2 – T2 relaxation time; TIMI – Thrombolysis in Myocardial Infarction. Values are odds ratios with 95% confidence intervals.

4.6.4. Multivariable logistic regression analysis of predictors of adverse left ventricular remodeling

Multivariable logistic regression was performed using two parallel models, given the limited number of ALVR events (n = 19). Anterior MI, although a univariable predictor (Table 4.6.2), did not retain independent significance in multivariable models adjusted for tissue-level imaging markers and was therefore not included in the final models. Model A (prespecified) included 20-HETE, urea, and platelet count. Model B (exploratory) replaced urea with post-contrast T1, the strongest imaging predictor in univariable analysis (Table 4.6.2), to evaluate the joint contribution of imaging and biomarker variables.

In Model A, lower platelet count (OR 0.981, 95% CI 0.965–0.996; p = 0.015) and lower 20-HETE (OR 0.985, 95% CI 0.970–1.000; p = 0.047) were independently associated with ALVR. Urea showed a borderline association (OR 1.380, 95% CI 0.998–1.907; p = 0.051).

In Model B, lower post-contrast T1 (OR 0.990, 95% CI 0.981–0.999; p = 0.033) and lower platelet count (OR 0.980, 95% CI 0.965–0.996; p = 0.015) remained independently associated with ALVR, while 20-HETE was borderline (OR 0.990, 95% CI 0.978–1.001; p = 0.076). Multivariable predictors of ALVR are presented in Table 4.6.3.

Table 4.6.3. *Multivariable logistic regression analysis of biomarker and combined biomarker–imaging predictors of adverse left ventricular remodeling*

Variable	OR	95% CI	p-value
Model A: Prespecified biomarker model			
20-HETE, ng/mL	0.985	0.970–1.000	**0.047**
Urea, mmol/L	1.380	0.998–1.907	0.051
Platelet count, ×10⁹/L	0.981	0.965–0.996	**0.015**
Model B: Exploratory combined model			
Post-contrast T1, ms	0.990	0.981–0.999	**0.033**
20-HETE, ng/mL	0.990	0.978–1.001	0.076
Platelet count, ×10⁹/L	0.980	0.965–0.996	**0.015**

20-HETE – 20-hydroxyeicosatetraenoic acid; CI – confidence interval; OR – odds ratio; T1 – T1 relaxation time. Values are odds ratios with 95% confidence intervals. Significant p-values (< 0.05) are shown in bold.

4.6.5. Discriminatory performance of selected biomarkers for adverse left ventricular remodeling

ROC analysis was performed to assess the discriminatory performance of four baseline biomarkers for adverse left ventricular remodeling: 20-HETE, post-contrast T1, platelet count, and urea. These were selected as the variables included in the multivariable models (Table 4.6.3). The analysis was considered exploratory because of the limited number of ALVR events; its purpose was to describe discrimination rather than to develop a definitive prediction model. The discriminatory performance of these markers is presented in Table 4.6.4 and Figure 4.6.1.

Three markers showed significant discriminatory ability for ALVR: 20-HETE (AUC 0.713, 95% CI 0.594–0.833; $p < 0.001$), post-contrast T1 (AUC 0.692, 95% CI 0.564–0.819; $p = 0.003$), and platelet count (AUC 0.670, 95% CI 0.546–0.794; $p = 0.007$), while urea showed borderline discriminatory ability (AUC 0.637, 95% CI 0.498–0.775; $p = 0.054$). 20-HETE showed the highest sensitivity (94.7%), with values ≤ 39.75 ng/mL identifying patients at risk of ALVR. Post-contrast T1 showed the highest specificity (77.0%) among the four markers, with values ≤ 283.8 ms supporting the identification of ALVR. Platelet count and urea showed more balanced sensitivity–specificity profiles.

Table 4.6.4. *Discriminatory performance of selected biomarkers for adverse left ventricular remodeling*

Variable	Cut-off value	AUC	95% CI	p-value	Sensitivity (%)	Specificity (%)
20-HETE, ng/mL	≤ 39.75	0.713	0.594–0.833	**< 0.001**	94.7	48.6
Post-contrast T1, ms	≤ 283.8	0.692	0.564–0.819	**0.003**	63.2	77.0
Platelet count, ×10⁹/L	≤ 209.0	0.670	0.546–0.794	**0.007**	68.4	66.2
Urea, mmol/L	≥ 6.1	0.637	0.498–0.775	0.054	52.6	71.6

AUC – area under the curve; CI – confidence interval; HETE – hydroxyeicosatetraenoic acid; T1 – T1 relaxation time. Cut-off values were selected using the Youden index. Significant p-values (< 0.05) are shown in bold.

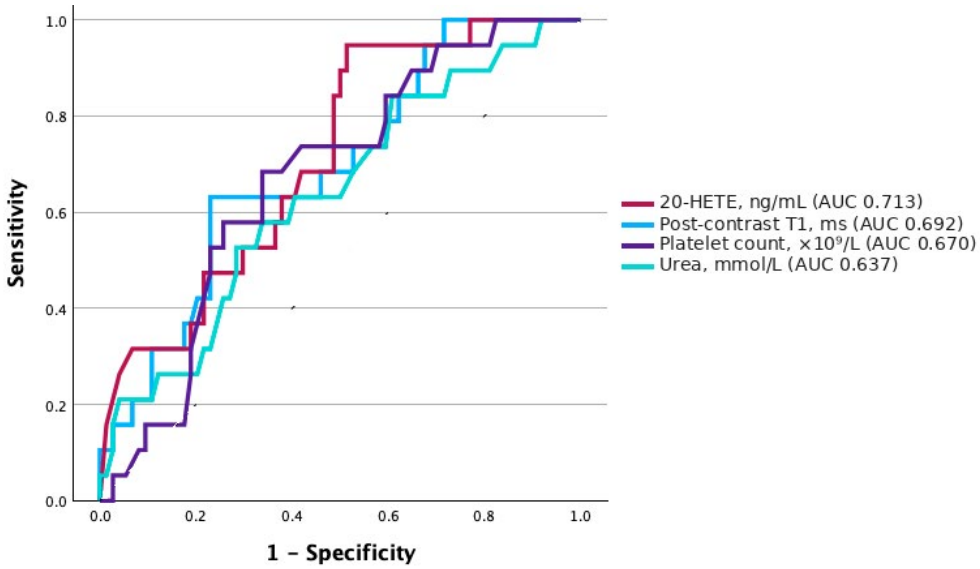

Fig. 4.6.1. *Receiver operating characteristic curves of selected biomarkers for adverse left ventricular remodeling*

ROC curves are shown for 20-HETE, post-contrast T1, platelet count, and urea. AUC – area under the curve; HETE – hydroxyeicosatetraenoic acid; ROC – receiver operating characteristic; T1 – T1 relaxation time.

5. DISCUSSION

5.1. Acute CMR-defined myocardial injury phenotype

The present CMR-based study focused on five components of post-STEMI myocardial injury and recovery: acute IS, MVO, regional myocardial tissue and strain, functional recovery, and ALVR. The main findings were that acute IS was primarily associated with pre-PCI TIMI flow 0–1 and peak troponin I, whereas MVO was additionally associated with renal function and NETosis expression. Later functional and structural outcomes showed different predictor profiles: impaired functional recovery was mainly related to baseline LV function, baseline IS, and infarcted-region CS, while adverse LV remodeling was associated with lower 20-HETE, lower platelet count, and shorter infarcted-region post-contrast T1. Overall, these findings suggest that IS, although important, captures only part of the post-STEMI injury profile.

Current smoking was frequent in this cohort (51.4%), exceeding the prevalence reported in a large Polish primary-PCI STEMI registry and in a pooled analysis of primary-PCI STEMI trials [94, 95].

5.1.1. Acute infarct size

In the present study, the mean IS on baseline CMR was 34.2 (19.4)% of LV mass. This value appears higher than reported in most reperfused STEMI cohorts assessed by CMR, where IS is generally smaller [43, 84, 96]. The proportion of patients with pre-PCI TIMI flow 0–1 (71%), the frequency of anterior or LAD-related infarction (41%), and the timing of baseline CMR (median 3 [2–5] days after primary PCI) were within the range reported in comparable CMR-STEMI studies [43, 84, 96], indicating that the higher IS cannot be attributed to enrichment for these established predictors or to differences in CMR timing. Imaging was performed at 3T, whereas other studies used 1.5T machines, although field strength is not expected to systematically affect quantified IS [97]. Therefore, the larger IS observed in our cohort most likely reflects longer symptom-to-balloon time and the inclusion of unselected patients, who are often excluded from randomized trials.

Large acute IS, defined as the upper tertile of IS (≥ 41.91% of LV mass), was independently associated with pre-PCI TIMI flow 0–1 and higher peak troponin I. Both predictors are biologically coherent: impaired pre-PCI flow reflects the severity of coronary occlusion before reperfusion, while peak troponin I captures the extent of cardiomyocyte necrosis. These associations are consistent with previous CMR-based studies showing that impaired pre-

PCI culprit-vessel flow and higher cardiac biomarkers are associated with larger IS after primary PCI [98–100].

Patients with pre-PCI TIMI flow 0–1 had substantially larger infarcts than patients with pre-PCI TIMI flow 2–3 (38.5 (18.9)% vs. 23.6 (16.5)% of LV mass), and this association remained independent after multivariable adjustment.

Larger infarcts were also observed in anterior STEMI, LAD-territory infarction, and in patients with acute-phase ventricular tachycardia or ventricular fibrillation. However, anterior MI was not independently associated with large IS after adjustment for pre-PCI TIMI flow and peak troponin I. This suggests that the effect of infarct location was largely captured by more direct markers of injury severity, particularly impaired coronary flow before PCI and the extent of cardiomyocyte necrosis. This is consistent with previous CMR studies identifying infarct location and impaired reperfusion markers as determinants of IS and MVO [43]. The association between acute-phase ventricular tachycardia or ventricular fibrillation and IS is also plausible, as larger infarcts create a substrate for malignant arrhythmias. However, recent translational evidence suggests that the relationship between ventricular fibrillation and IS is complex and may not simply reflect larger infarcts causing arrhythmia [101].

In contrast, 20-HETE, 15(S)-HETE, and NETosis expression were not associated with acute IS. This negative finding suggests that these specialized biomarkers did not primarily reflect the extent of cardiomyocyte necrosis in this cohort. Their relevance may instead relate more strongly to microvascular or remodeling phenotypes, which is supported by the separate association between NETosis expression and MVO.

Taken together, acute CMR-defined IS in this cohort mainly reflected the severity of coronary occlusion before reperfusion and was closely mirrored by peak troponin I concentration. Clinical and anatomical features such as anterior infarction, LAD involvement, and acute ventricular arrhythmias identified patients with larger infarcts in univariable analyses, but their effects were largely explained by pre-PCI coronary flow and biochemical evidence of cardiomyocyte necrosis.

5.1.2. Microvascular obstruction

Among the 103 patients with available MVO analysis, MVO was identified in 73 patients, representing approximately 71% of the cohort. This rate is higher than that reported in recent CMR studies of reperfused STEMI, in which MVO or microvascular injury has typically been observed in approximately 50–60% of patients [50, 54]. The longer ischemic time in this

cohort, with a median symptom-to-balloon time of 342 minutes compared to approximately 180 minutes in the cohorts of Lechner et al. and Troger et al. [50, 54], likely accounts for this difference. Accordingly, MVO was analyzed both as a binary variable and by its extent among patients with MVO. The partially divergent results indicate that the determinants of MVO occurrence and those influencing its burden may differ.

Pre-PCI TIMI 0–1 flow was independently associated with the presence of MVO (odds ratio 3.97, $p = 0.017$). This association is clinically anticipated, as absent or severely impaired antegrade flow prior to PCI indicates a longer and more complete ischemic insult in the infarct-related territory. Previous CMR studies have similarly linked impaired pre-PCI TIMI flow with larger IS and greater MVO following STEMI [99]. This relationship likely reflects both more severe ischemic injury before reperfusion and subsequent microvascular damage after restoration of epicardial artery patency.

Peak troponin I concentration was also independently associated with the presence of MVO (odds ratio 1.029 per µg/L, $p = 0.015$), supporting a close relationship between IS and microvascular injury. Larger infarcts are more frequently accompanied by endothelial swelling, distal embolization, leukocyte–platelet plugging, and microvascular thrombosis, all of which contribute to MVO [6]. Previous CMR studies have demonstrated that higher troponin I concentrations correlate with IS and MVO after STEMI [66, 67, 102], and additional studies have identified peak troponin as an independent marker of CMR-defined MVO following primary PCI [71, 103]. In this cohort, troponin I remained associated with MVO after adjustment for pre-PCI flow, eGFR, and NETosis expression, indicating that IS is an important, but not exclusive, determinant of MVO.

Lower eGFR was independently associated with the presence of MVO (odds ratio 0.963 per mL/min/1.73 m^2, $p = 0.038$). Although renal function is not a direct indicator of coronary microvascular injury, this association is biologically plausible. Reduced eGFR is linked to endothelial dysfunction, inflammation, platelet activation, impaired vasodilatory reserve, and more advanced vascular disease [6, 104]. Previous STEMI studies have demonstrated that reduced eGFR predicts angiographic slow flow or no-reflow, as well as impaired ST-segment resolution, after primary PCI [69, 105]. While these outcomes are not identical to CMR-defined MVO, they reflect the same clinical issue: failed tissue-level reperfusion despite successful epicardial artery reopening. In this cohort, eGFR remained associated with MVO after adjustment for pre-PCI flow, troponin I, and NETosis expression, suggesting that renal dysfunction may indicate a systemic microvascular vulnerability not fully explained by coronary flow or IS.

Higher NETosis expression was independently associated with MVO (odds ratio 1.025 per mU/mL, p = 0.020), suggesting a link between MVO and the inflammatory response following STEMI. NETs promote endothelial activation, platelet adhesion, fibrin deposition, and small-vessel obstruction. Evidence from STEMI cohorts supports this association: culprit-site extracellular DNA has been linked to CMR-defined MVO and reduced ejection fraction [26], while circulating NET components have been associated with IS, left ventricular function, clinical outcomes, and MVO-related injury [79]. Mechanistic studies further demonstrate that NETs at the culprit site can activate coronary endothelial cells and amplify local inflammation [28]. The association in this model persisted after adjustment for pre-PCI flow, troponin I, and eGFR, suggesting that NETosis reflects a thromboinflammatory component of MVO not captured by standard clinical markers.

When platelet count was included in the model, the association between NETosis expression and MVO was attenuated. This finding is consistent with the close relationship between NETosis and platelet activation. NETs facilitate platelet adhesion and fibrin deposition, while activated platelets can induce NET release [27]. Therefore, platelet count may partially overlap with NETosis expression as an indicator of the same thromboinflammatory process.

The diagnostic performance of individual markers for MVO varied. Pre-PCI TIMI 0–1 flow was excluded from the ROC analysis due to its binary angiographic nature. Peak troponin I demonstrated the highest discrimination (AUC 0.78), with a cutoff of ≥ 18.56 μg/L providing 81% sensitivity and 70% specificity. This finding aligns with previous CMR-STEMI studies, indicating that higher troponin concentrations are associated with MVO and may help identify patients at increased risk after primary PCI. eGFR and NETosis expression exhibited moderate discrimination (AUC 0.67 and 0.66, respectively), while platelet count showed lower discrimination (AUC 0.63). NETosis expression ≥ 62.1 mU/mL demonstrated high specificity but limited sensitivity, suggesting that markedly elevated NETosis may identify a smaller high-risk subgroup rather than serve as a general screening marker. As these cutoffs were derived from the present cohort using the Youden index, they should be considered exploratory and require external validation.

5.2. Global myocardial healing and residual infarct burden at 6 months

In the present study, global myocardial healing was evaluated in 93 patients with paired baseline and 6-month CMR data. The main findings were: (a) global LV systolic function improved, mainly because LV end-systolic volume decreased while end-diastolic volume did not change significantly;

(b) global longitudinal and circumferential strain improved; (c) native T1 and T2 decreased and post-contrast T1 increased, whereas ECV did not change significantly; and (d) IS decreased from 30.9% to 18.8% of LV mass, and MVO was no longer detectable at follow-up. Overall, these findings indicate a predominantly favorable global healing during the first 6 months after reperfused STEMI.

5.2.1. Global LV functional and volumetric changes

In the overall cohort, serial CMR showed improved global LV systolic function 6 months after STEMI. This included a significant increase in LVEF and stroke volume index, a reduction in LVESVi, and improvements in both GLS and GCS. LVEDVi did not change significantly, indicating improved systolic emptying rather than an increase in LV chamber size at the cohort level.

These findings align with previous CMR studies reporting favorable functional changes after STEMI. Podlesnikar et al. found improved LVEF, reduced LVESV, and better LV GCS from the early post-STEMI phase to 6 months [106]. Cui et al. also reported increased LVEF and reduced LVESV at 6 months after STEMI [107]. The pattern in our cohort is consistent with post-STEMI functional recovery described in recent CMR studies. However, these cohort-level changes do not represent uniform recovery, as individual trajectories vary; ALVR and limited LV functional improvement, which occurred in some patients, are discussed separately.

5.2.2. Residual infarct size and tissue characterization

In the paired-CMR cohort, infarct healing was observed by 6 months. The median IS decreased by 9.6 [3.0–16.1] percentage points, with a median residual IS of 18.8 [11.2–31.1]% of LV mass. IS decreased from 30.9 [18.9–45.5]% at baseline to 18.8 [11.2–31.1]% at follow-up. MVO was present in 65 of 93 patients at baseline and was undetectable in all patients at 6 months. These findings indicate infarct maturation, residual scar formation, and resolution of acute MVO during healing.

This pattern aligns with the established progression of IS after STEMI, though the magnitude of change differed from that observed in previous serial CMR studies. Mayr et al. reported a smaller baseline IS (13.8% of LV mass) and a modest reduction to 10.0% by 4 months [55]. In our cohort, the baseline infarct was larger and showed greater shrinkage over a similar period. This difference is likely due to the larger initial infarct burden rather than methodological differences, as a larger scar has more potential for reduction during healing.

In our cohort, MVO was no longer detectable at 6 months. This suggests that MVO was mainly an acute-phase microvascular injury. This distinction is clinically important, as persistent MVO is associated with worse post-STEMI outcomes. Troger et al. found that patients with persistent MVO had larger infarcts, reduced left ventricular function, and more frequent adverse cardiac events [54].

Global mapping parameters also reflected myocardial healing. Both native T1 and T2 values decreased from baseline to 6 months, consistent with the resolution of acute myocardial edema. The reduction in LV mass index further supports this, as it suggests decreased edema rather than loss of viable myocardium [108]. Post-contrast T1 increased, reflecting reduced gadolinium retention after the resolution of acute edema and tissue injury. Global ECV remained unchanged, indicating that diffuse extracellular expansion did not predominantly affect the entire LV during follow-up. Previous studies have reported a similar decrease in global LV native T1 in serial 3T CMR cohorts following STEMI [15]. However, direct comparison with published data is challenging because most CMR studies after STEMI report regional rather than global mapping values. Changes within specific myocardial zones are discussed in the next section.

5.3. Regional myocardial phenotype and healing

5.3.1. Regional differences in myocardial deformation and tissue characteristics

5.3.1.1. Overview of regional impairment across infarcted, adjacent, and remote myocardium

Acute CMR segmental analysis showed a stepwise pattern of impairment across infarcted, adjacent, and remote myocardium, affecting both myocardial deformation and tissue characterization parameters. Infarcted segments exhibited the most pronounced abnormalities, while remote myocardium was least affected. Adjacent segments demonstrated intermediate values for native T1, ECV, and CS. These findings indicate that post-STEMI injury is not limited to the LGE-positive infarct core but may also involve the surrounding border zone.

However, not all parameters captured this three-zone gradient equally. LS and T2 values differentiated infarcted segments from non-infarcted myocardium but did not distinguish adjacent from remote segments. In contrast, native T1, ECV, post-contrast T1, and circumferential strain differentiated all three regions. These results suggest that mapping-based parameters and CS are more sensitive to subtle regional myocardial involvement than T2

or LS. Wamil et al. conducted a similar three-zone analysis in the OxAMI cohort, defining infarcted, adjacent, and remote segments based on LGE, and demonstrated that both native T1 and CS were progressively impaired from remote to infarcted myocardium. Erley et al. also reported persistent impairment of regional CS in LGE-positive segments [60].

5.3.1.2. Tissue and functional differences across infarcted, adjacent, and remote zones

Infarcted segments exhibited the most significant tissue and functional abnormalities, characterized by increased native T1, ECV, and T2, as well as reduced post-contrast T1 and impaired LS and CS. This pattern is consistent with the substrate of acute reperfused infarction, which includes cardiomyocyte necrosis, intra- and extracellular edema, expansion of the extracellular space, microvascular injury, and impaired contractile integrity [109].

Adjacent segments demonstrated similar, though less severe, abnormalities, suggesting peri-infarct myocardial involvement even in the absence of visible LGE. In the context of acute reperfused STEMI, edema, inflammatory changes, and microvascular dysfunction can extend beyond the visually enhanced infarct core [58]. Deformation abnormalities observed in adjacent segments may be partially attributable to the mechanical influence of the infarcted myocardium, rather than direct necrosis within the adjacent tissue itself [15].

Carrick et al. identified a broader myocardial response extending beyond the infarcted-region, demonstrating that early elevation of remote-zone native T1 was associated with inflammation, LV remodeling, and adverse clinical outcomes following STEMI [56].

5.3.1.3. Longitudinal versus circumferential strain in border-zone myocardium

A notable finding was the different behavior of longitudinal and circumferential strain in the peri-infarct region. While both strain components were impaired in infarcted segments, only CS distinguished adjacent from remote myocardium, whereas LS did not differ between these two regions.

This result can be explained by the transmural fiber architecture and regional mechanics of the left ventricle. LS primarily reflects subendocardial fiber function, while CS depends more on mid-wall fibers and short-axis mechanics [61]. In reperfused STEMI, LS impairment likely results from infarct-core involvement, where subendocardial injury is most severe. In visually LGE-negative adjacent segments, the lack of detectable infarct enhancement may account for LS values like those in remote zones.

CS may be more sensitive to peri-infarct mechanical dysfunction, such as altered mid-wall shortening and interactions with adjacent infarcted segments. This view aligns with previous CMR studies that found a stronger association between circumferential deformation and segmental abnormalities in infarct-related segments. Erley et al. reported that segmental CS was the most effective feature-tracking parameter for distinguishing LGE-positive from LGE-negative segments after STEMI [60]. Similarly, Wong et al. showed that CMR-derived CS added value in predicting early segmental contractile recovery after STEMI, highlighting the importance of circumferential mechanics in post-infarction assessment [82].

5.3.1.4. Regional differences in tissue mapping parameters

A similar pattern was observed among the tissue mapping parameters. Native T1, ECV, and post-contrast T1 demonstrated significant differences between adjacent and remote myocardium, while T2 did not differ significantly between these two regions.

This dissociation reflects the distinct biological factors underlying each mapping index. T2 mapping primarily detects increased myocardial water content and serves as a marker of acute edema [14]. Native T1 is also affected by edema but can indicate a broader range of tissue changes, including extracellular expansion, necrosis, inflammation, and alterations in tissue composition. ECV more directly reflects expansion of the extracellular compartment, whereas post-contrast T1 depends on gadolinium distribution within that compartment [110]. Thus, higher native T1 and ECV, along with lower post-contrast T1 in adjacent segments, despite no significant difference in T2, suggest that peri-infarct abnormalities in this cohort were not explained only by T2-detectable edema.

Bulluck et al. also reported increased ECV in remote myocardium early after reperfused STEMI, which was associated with later adverse LV remodeling [58]. Without a corresponding T2 increase, the elevated ECV was interpreted as indicating extracellular or matrix-related changes rather than edema alone. In our cohort, a similar dissociation between ECV and T2 in adjacent segments suggests that the peri-infarct border zone may involve extracellular or interstitial changes not fully detected by T2 mapping.

5.3.1.5. Regional CMR abnormalities in non-infarcted myocardium

Overall, our findings show that acute post-STEMI myocardium has a graded regional pattern that extends beyond the LGE-defined infarct core. Adjacent and remote regions display measurable, parameter-specific changes, though these are less pronounced than in infarcted tissue. Previous studies

suggest that abnormalities in non-infarcted myocardium may have prognostic significance. Early native T1 elevation in non-infarcted myocardium is independently associated with major adverse cardiac events after STEMI [57, 64]. Recent data also link elevated non-infarct T2 and dynamic remote-zone T1 changes to long-term outcomes [111, 112].

These regional findings provide the basis for the longitudinal analysis in the next section, which examines how they progress from baseline to 6-month follow-up.

5.3.2. Follow-up changes in regional CMR parameters

5.3.2.1. Overview of longitudinal changes across myocardial regions

From baseline to 6-month follow-up, regional myocardial deformation and tissue characteristics varied across infarcted, adjacent, and remote segments (Table 4.4.2 and Figure 4.4.2). Infarcted segments demonstrated the most consistent changes, including significant improvements in LS and CS, reductions in native T1 and T2, and an increase in post-contrast T1. ECV remained unchanged.

In adjacent segments, CS improved and native T1 decreased, with an increase in post-contrast T1. LS, ECV, and T2 did not change significantly. In remote myocardium, LS improved, native T1 decreased slightly, and post-contrast T1 increased. ECV and T2 showed small but significant increases, while CS remained unchanged.

These findings show that recovery was most pronounced in infarcted myocardium, whereas changes in non-infarcted regions were more selective and parameter-specific.

5.3.2.2. Follow-up changes in infarcted myocardium

Follow-up changes in infarcted segments were most pronounced, aligning with the expected progression of reperfused infarction. Improvements in LS and CS indicate partial recovery of regional contractile function, consistent with previous CMR feature-tracking data after STEMI [106]. The parallel decrease in native T1 and T2 supports resolution of acute-phase tissue changes, especially myocardial edema. Tahir et al. also demonstrated that native T1 and T2 values differ significantly between acute and chronic myocardial infarction, supporting their use in distinguishing recent from chronic infarction [113]. The increase in post-contrast T1 may reflect changes in contrast distribution as acute injury progresses to a chronic infarct substrate. In contrast, ECV did not change significantly in infarcted segments in our cohort. This may indicate persistent extracellular space expansion at 6

months despite improvements in edema-sensitive and functional parameters. This contrasts with Garg et al., who observed region-dependent ECV changes after reperfused STEMI, including a modest reduction in infarct-segment ECV between acute CMR performed 24–72 hours after STEMI and 3-month follow-up [63]. The discrepancy may be due to differences in imaging timing, as our baseline CMR was performed slightly later, at a median of 3 [2–5] days after primary PCI, and follow-up at 6 months rather than 3 months.

5.3.2.3. Follow-up changes in adjacent myocardium

In adjacent segments, follow-up changes were less pronounced than in infarcted myocardium. However, improved CS and reduced native T1 suggest partial recovery of reversibly injured peri-infarct myocardium. This most likely reflects regression of edema and functional stunning rather than resolution of fixed structural damage [113]. The smaller magnitude of change is consistent with less severe baseline injury and suggests preserved recovery potential in the peri-infarct zone [15].

5.3.2.4. Follow-up changes in remote myocardium

In remote segments, LS improved, aligning with overall functional recovery following STEMI. Nevertheless, small but statistically significant increases in ECV and T2 values (ECV 24.8% to 25.3%, $p = 0.002$; T2 41.3 to 42.5 ms, $p = 0.036$) indicate a subtle, diffuse tissue response in non-infarcted myocardium. These alterations should not be interpreted simply as persistent residual inflammation. They may represent early signs of reactive fibrosis and extracellular matrix expansion resulting from increased wall stress and altered loading conditions after infarction [63, 114]. Garg et al. also reported a similar modest increase in ECV within normal or non-infarcted myocardium after reperfused STEMI, associating this pattern with extracellular expansion and impaired regional contractile function [63]. Together with studies demonstrating the prognostic significance of non-infarcted myocardial T1 and T2 abnormalities after STEMI [57, 64], these findings indicate that post-STEMI remodeling extends beyond infarcted or adjacent tissue and may involve subtle structural changes in remote myocardium, even when functional improvement is observed.

5.4. Predictors of impaired LV functional recovery

Impaired LV functional recovery was defined as LVEF < 50% at 6-month follow-up CMR and was observed in 28 of 93 patients (30.1%) with paired baseline and follow-up CMR data. The main finding of this analysis was that

impaired functional recovery was primarily related to the severity of the acute ischemic injury and the degree of early LV systolic impairment. Patients with impaired follow-up LV function had lower baseline LVEF, larger baseline LV volumes, larger infarct and MVO size, more impaired global and infarcted-region strain, and higher circulating markers of cardiomyocyte injury. In contrast, the specialized circulating biomarkers – 20-HETE, 15(S)-HETE, and NETosis expression – were not associated with impaired follow-up LV function. These findings suggest that structural and functional CMR markers assessed in the acute infarct phase, together with troponin I, were stronger predictors of persistent LV dysfunction than the analyzed specialized biomarkers.

5.4.1. Clinical, procedural, and biomarker predictors

Univariable analyses showed that current smoking, anterior MI, and pre-PCI TIMI flow 0–1 were associated with impaired follow-up LV function. These findings are expected, as anterior MI usually involves a larger myocardial territory, while pre-PCI TIMI flow 0–1 reflects absent or severely reduced antegrade flow before reperfusion. In this cohort, however, their relationship with impaired follow-up LV function appeared to be largely explained by the degree of early LV dysfunction seen on baseline CMR. This is consistent with previous CMR-based STEMI studies showing that acute IS and early LV functional impairment provide stronger prognostic information than clinical or procedural variables alone [43, 81].

Among routine laboratory markers, elevated troponin I, AST, and BNP levels, as well as reduced early platelet count, were associated with impaired follow-up LV function in univariable analyses. This pattern indicates more severe acute myocardial injury and greater early hemodynamic stress in patients who subsequently developed persistent LV dysfunction. In this cohort, troponin I demonstrated a strong correlation with both AST and baseline IS, supporting the interpretation that these markers primarily reflected the same acute injury burden. However, AST, BNP, and platelet count did not retain independent significance when analyzed alongside troponin I in an exploratory analysis, and troponin I itself was no longer independently associated with impaired follow-up LV function after baseline LVEF was included in the primary model. Therefore, the prognostic information provided by routine circulating markers substantially overlapped with early CMR-derived LV systolic function. In contrast, 20-HETE, 15(S)-HETE, and NETosis expression were not associated with impaired follow-up LV function, even in univariable analysis.

5.4.2. Baseline LV function and infarct burden

Among baseline CMR parameters, early LV systolic function was the dominant predictor of impaired follow-up LV function. Patients with impaired recovery showed lower baseline LVEF, larger LV volumes, greater IS, increased MVO extent, worse global and infarcted-region deformation, and more frequent LV thrombus. In the primary multivariable model, only baseline LVEF was independently associated with impaired follow-up LV function. This finding is expected, as early LVEF after STEMI reflects the combined effects of IS, regional contractile dysfunction, myocardial stunning, microvascular injury, and acute loading conditions. Previous CMR-based STEMI studies have also shown that early LVEF, IS, MVO, and myocardial strain are closely related to later LV recovery and post-infarction prognosis [10, 107]. When baseline LVEF was excluded from the sensitivity model, larger IS and worse circumferential strain in the infarcted-region became independent predictors. These markers reflect the structural and regional mechanical basis of persistent LV dysfunction.

5.4.3. Infarcted-region mechanics and tissue characterization

When baseline LVEF was excluded, the predictors that emerged – larger IS and more impaired infarcted-region CS – point to the structural and mechanical state of the infarct itself as the substrate of persistent dysfunction. Infarcted-region CS was the strongest of these regional markers. As discussed earlier, circumferential shortening depends on mid-wall fibers that fail mainly in transmural injury, so it reflects the depth of irreversible damage and residual contractile reserve more specifically than LS. This is consistent with results of previous studies, where infarct-region CS predicted segmental and global recovery beyond IS [82, 83], whereas LS, although sensitive to early injury, discriminates injury severity less well.

Infarcted-region post-contrast T1 was also lower in patients with impaired recovery ($p = 0.044$), reflecting expanded extracellular space from necrosis and early fibrosis [115]. Its association was weaker, however – only borderline in univariable analysis – suggesting that it may describe infarct severity rather than adding a distinct dimension of risk, consistent with the reported dependence of mapping parameters on infarct extent [62]. Taken together, these findings indicate that infarcted-region deformation captures aspects of viable but dysfunctional myocardium – contractile reserve and fiber integrity – that tissue characterization alone does not fully reflect, supporting a complementary rather than redundant role for regional mechanics in predicting functional recovery.

5.5. Predictors of adverse left ventricular remodeling

ALVR was defined as a 12% or greater increase in both LVEDV and LVESV at 6 months, and was observed in 19 of 93 patients (20.4%) with paired CMR data. While impaired functional recovery was primarily associated with baseline LV function and markers of infarct severity, ALVR showed a different profile of predictors.

5.5.1. Clinical, biomarker, and imaging predictors

Three variables independently predicted ALVR: lower platelet count, lower 20-HETE, and abnormal infarcted-region tissue characteristics. Anterior STEMI was more frequent in ALVR patients but lost independent significance once these predictors entered the multivariable model.

CMR-based STEMI studies have identified larger IS, MVO, reduced myocardial salvage, lower baseline LVEF, and impaired strain as predictors of ALVR [10, 116, 117]. In the present cohort, these markers – along with GCS, troponin I, BNP, and pre-PCI TIMI flow – did not independently predict ALVR. The discrepancy likely reflects the small number of ALVR events (n = 19) and the stricter ALVR definition, which required simultaneous increases in both LVEDV and LVESV.

5.5.2. Platelet count

Lower platelet count on the morning after PCI was independently associated with ALVR in both multivariable models. Both groups stayed within the normal range, but ALVR patients had values at the lower end (191 [181–233] vs. 222 [196.5–245.8] × 10^9/L; $p = 0.022$). Procedural antithrombotic interventions that can lower platelet count – pre-PCI thrombolysis and manual thrombus aspiration – did not differ between groups (all $p > 0.10$). Lower values in this early phase may reflect platelet consumption at sites of coronary and microvascular injury, or a stronger inflammatory response in the first hours after the infarct [27].

Direct evidence linking early post-PCI platelet count to CMR-defined ALVR remains limited. Lower admission platelet count has been associated with worse clinical outcomes in acute coronary syndromes [16]. Both lower and higher admission platelet counts have been linked to larger IS and higher mortality in primary-PCI STEMI [118]. ALVR has more often been linked to higher on-treatment platelet reactivity than to platelet count [88]. In experimental studies, platelet infiltration into infarcted myocardium amplified local inflammation and contributed to adverse remodeling [119].

Platelet count is a useful but non-specific marker that may be underrecognized as a predictor of post-STEMI remodeling.

5.5.3. The 20-HETE and eicosanoid pathway

In this cohort, lower circulating 20-HETE was independently associated with ALVR (OR 0.985, p = 0.047). This is in apparent contradiction with most clinical and experimental data. 20-HETE is a cytochrome P450-derived arachidonic acid metabolite (CYP4A and CYP4F families) involved in vascular tone, endothelial function, oxidative stress, and inflammation [17, 18]. Elevated 20-HETE has been linked to arterial hypertension, ischemic stroke, and incident MI in stable CAD [80], and in experimental ischemia–reperfusion models 20-HETE production aggravates acute myocardial injury, whereas its inhibition reduces IS and oxidative stress, supporting a deleterious role during the acute reperfusion phase [17, 20].

The direction of the association observed in our study is consistent with recent human data from the acute setting. In patients with acute coronary syndrome, circulating 20-HETE concentrations were markedly lower than in patients with stable coronary artery disease and in controls (6.13 vs. 27.20 vs. 52.66 ng/mL; p < 0.001), and 20-HETE distinguished acute coronary syndrome from stable disease with an AUC of 0.91 [120]. The authors suggested that this reduction reflected altered synthesis, local consumption, redistribution, and degradation during acute endothelial stress, inflammation, and thrombosis, rather than a protective decrease in 20-HETE production. This may help explain the apparent difference from experimental ischemia–reperfusion studies, which usually capture a transient increase in local 20-HETE production shortly after reperfusion [17, 20]. In patients with STEMI, however, circulating concentrations measured over the following days may be lower because of increased consumption at sites of endothelial and microvascular injury. Thus, lower early 20-HETE concentrations in our cohort may indicate more severe acute vascular stress and greater dysregulation of the eicosanoid pathway, which could link it to the adverse remodeling observed here.

Beyond these effects, 20-HETE activates endothelial cells and promotes von Willebrand factor release, platelet adhesion, and thrombosis [19], providing a mechanistic link between the eicosanoid pathway and platelet-related biology relevant to the present cohort, in which both lower 20-HETE and lower early post-PCI platelet count were independently associated with adverse remodeling.

The finding that lower circulating 20-HETE was associated with adverse remodeling in this cohort should therefore not be interpreted simplistically.

Two further considerations are worth noting. First, deficient 20-HETE signaling itself is not biologically neutral: human polymorphisms in CYP4F2 and CYP4A11 that reduce 20-HETE production are associated with arterial hypertension and end-organ vulnerability, indicating that low 20-HETE in some contexts reflects a maladaptive rather than a protective phenotype [121]. Second, plasma 20-HETE concentrations in STEMI patients change dynamically in the days and weeks after primary PCI [29]; a single early measurement, as obtained in the present study, may therefore capture only one phase of a complex temporal response. The present association between low early 20-HETE and later remodeling should accordingly be regarded as hypothesis-generating, requiring confirmation in studies with serial sampling.

5.5.4. Infarcted-region tissue characterization

Among regional CMR markers, infarcted-region native T1 was higher and post-contrast T1 was shorter at baseline in patients who later developed ALVR, whereas ECV and T2 did not differ between groups. Post-contrast T1 retained independent significance in the combined biomarker–imaging model. These parameters reflect related but distinct aspects of acute tissue injury. Higher native T1 is consistent with greater edema and interstitial expansion, while shorter post-contrast T1 reflects greater gadolinium retention within an expanded extracellular space, suggesting more severe acute interstitial injury [14]. Their convergence in patients who later developed ALVR suggests that infarcted-region tissue characteristics, rather than IS alone, were associated with subsequent adverse structural remodeling.

The absence of corresponding differences in ECV and T2 is also relevant. ECV is derived from native and post-contrast T1 together with hematocrit, and this combined calculation may be less sensitive to between-group differences seen in raw mapping values. In the present study, hematocrit was not measured on the day of CMR, a methodological limitation because ECV calculation requires hematocrit correction and the timing of hematocrit assessment can influence ECV precision [122]. T2 mainly reflects free-water content and may be less specific for the interstitial and contrast-distribution abnormalities captured by native and post-contrast T1. Overall, these findings support the value of acute-phase CMR mapping as a tissue-level marker of post-MI remodeling risk, while also highlighting the need for cautious interpretation of individual mapping parameters [13].

Taken together, patients in this cohort who subsequently developed left ventricular dilatation were characterized by lower platelet counts, lower circulating 20-HETE, and more pronounced infarcted-region mapping abnormalities in the acute phase after STEMI. These observations are

consistent with a remodeling phenotype reflecting systemic and tissue-level processes during the early post-infarction period, and partly distinct from the determinants of functional recovery.

CONCLUSIONS

1. Independent predictors of large acute infarct size (≥ 41.91% of LV myocardial mass) were pre-PCI TIMI flow 0–1 (OR 8.08; $p = 0.017$) and higher troponin I concentration ($p < 0.001$). Independent predictors of MVO were pre-PCI TIMI flow 0–1 (OR 3.97; $p = 0.017$), higher troponin I concentration ($p = 0.015$), lower eGFR ($p = 0.038$), and higher NETosis expression (OR 1.03 per 1 mU/mL; $p = 0.020$). 20-HETE and 15(S)-HETE were not associated with acute myocardial injury.
2. At 6 months after MI, LVEF improved, infarct size decreased, and MVO was no longer detected on follow-up CMR. Residual infarct size was strongly associated with baseline infarct size ($r_s = 0.84$; $p < 0.001$) and troponin I concentration ($r_s = 0.75$; $p < 0.001$), and moderately with baseline MVO extent ($r_s = 0.59$; $p < 0.001$), but was not associated with 20-HETE, 15(S)-HETE, or NETosis expression.
3. Injury involved all three myocardial zones: in the acute phase the infarcted myocardium was the most impaired, while the adjacent myocardium differed significantly from the remote in circumferential strain, native and post-contrast T1 relaxation times, and extracellular volume (all $p < 0.05$), but not in longitudinal strain or T2. Over 6 months, recovery was uneven – most pronounced in the infarcted zone and only partial in the adjacent zone.
4. Impaired LV systolic function recovery at 6 months (LVEF < 50%) occurred in 30.1% of patients. Lower baseline LVEF was independently associated with this outcome (OR 0.86; $p = 0.017$; AUC = 0.85). In a sensitivity analysis excluding baseline LVEF, the independent predictors were larger baseline infarct size ($p = 0.006$) and worse infarcted-region circumferential strain ($p = 0.010$). The specialized biomarkers were not associated with impaired LV functional recovery.
5. Adverse LV remodeling at 6 months (≥ 12% increase in LV end-diastolic and end-systolic volumes) occurred in 20.4% of patients. The independent predictors were lower platelet count (OR 0.981; $p = 0.015$), lower 20-HETE concentration (OR 0.985; $p = 0.047$), and shorter infarcted-region post-contrast T1 relaxation time (OR 0.990; $p = 0.033$).

LIMITATIONS OF THE STUDY

Several limitations should be considered when interpreting these findings. First, this was a single-center observational study with a relatively small baseline cohort (n = 105) and paired-CMR cohort (n = 93), which limits the generalizability of the results to broader patient populations.

Second, the small number of outcome events (impaired LV functional recovery in 28 of 93 patients; adverse LV remodeling in 19 of 93) constrained the multivariable analyses and increased the risk of chance associations. The events-per-variable ratio was below the recommended threshold of 10, and the resulting wide confidence intervals reflect this instability. The ROC-derived cutoff values were determined in the same cohort and should therefore be regarded as exploratory and require validation in independent cohorts.

Third, the follow-up period was 6 months, so longer-term remodeling changes and the associations of the identified predictors with clinical outcomes such as heart failure or mortality were not assessed.

Fourth, the circulating biomarkers were measured only once during the acute phase, so temporal changes in 20-HETE, 15(S)-HETE, and NETosis expression could not be evaluated.

Finally, myocardial segments were classified as infarcted on the basis of any detectable LGE, without a transmurality threshold, and whole-segment strain and mapping values were included in the infarcted-region averages.

PRACTICAL RECOMMENDATIONS

1. In patients after a first STEMI, assessment of NETosis expression during the acute phase may be considered as an additional marker in the comprehensive evaluation of myocardial injury risk. Higher NETosis expression (≥ 62.1 mU/mL) may help identify patients with a higher risk of MVO. Because of its high specificity and lower sensitivity, this marker is more suitable for identifying higher-risk patients than for ruling out MVO.
2. In patients after first STEMI with baseline CMR-derived LVEF ≤ 41.3%, closer clinical follow-up and repeated assessment of LV function at 6 months should be considered. Baseline infarct size ≥ 42.3% of LV mass and infarcted-region circumferential strain (≥ −24.7%) may be used as additional risk markers for impaired LV systolic function recovery.
3. A lower platelet count (≤ 209.0 × 10^9/L), measured during the acute phase after first STEMI, may be considered as an additional, easily accessible marker of adverse LV remodeling risk. Assessment of 20-HETE concentration, as an exploratory biomarker, could also provide additional information on the risk of adverse LV remodeling.

SANTRAUKA

SANTRUMPOS

15(S)-HETE – 15(S)-hidroksieikozatetraeno rūgštis
20-HETE – 20-hidroksieikozatetraeno rūgštis
AHA – Amerikos širdies asociacija (angl. *American Heart Association*)
ALT – alaninaminotransferazė
AST – aspartataminotransferazė
AUC – plotas po kreive (angl. *area under the curve*)
AVB – atrioventrikulinė blokada
BNP – B tipo natriurezinis peptidas (angl. *B-type natriuretic peptide*)
CRB – C reaktyvusis baltymas
ECV – užląstelinis tūris (angl. *extracellular volume*)
EKG – elektrokardiografija
GCS – bendroji apsukinė įtampa (angl. *global circumferential strain*)
GFG – glomerulų filtracijos greitis
GLS – bendroji išilginė įtampa (angl. *global longitudinal strain*)
HbA1c – glikuotasis hemoglobinas
IŠL – išeminė širdies liga
KMI – kūno masės indeksas
KS – kairysis skilvelis
KSGDT – kairiojo skilvelio galinis diastolinis tūris
KSGDTi – kairiojo skilvelio galinio diastolinio tūrio indeksas
KSGST – kairiojo skilvelio galinis sistolinis tūris
KSGSTi – kairiojo skilvelio galinio sistolinio tūrio indeksas
KSIF – kairiojo skilvelio išstūmio frakcija
LGE – vėlyvasis gadolinio kaupimasis (angl. *late gadolinium enhancement*)
LSMUL KK – Lietuvos sveikatos mokslų universiteto ligoninė Kauno klinikos
MI – miokardo infarktas
MVO – mikrovaskulinė obstrukcija (angl. *microvascular obstruction*)

NADPH – nikotinamido adenino dinukleotido fosfatas (angl. *nicotinamide adenine dinucleotide phosphate*)
NET – neutrofilų užląsteliniai tinklai (angl. *neutrophil extracellular traps*)
NETozė – neutrofilų užląstelinių tinklų susidarymas (angl. *NETosis*)
NLS – neutrofilų ir limfocitų santykis
PI – pasikliautinasis intervalas
PVAI – perkutaninė vainikinių arterijų intervencija
$\mathbf{r_s}$ – Spearmano koreliacijos koeficientas
SCMR – Širdies magnetinio rezonanso draugija (angl. *Society for Cardiovascular Magnetic Resonance*)
SN – standartinis nuokrypis
ŠKL – širdies ir kraujagyslių ligos
ŠMRT – širdies magnetinio rezonanso tyrimas
ŠS – šansų santykis
TIMI – angl. *Thrombolysis In Myocardial Infarction*
TKI – tarpkvartilinis intervalas
ŪMIkSTP – ūminis miokardo infarktas, kai ST segmentas pakilęs
VAA – vainikinių arterijų angiografija
VAL – vainikinių arterijų liga

ĮVADAS

Širdies ir kraujagyslių ligos (ŠKL) išlieka pagrindine sergamumo ir mirštamumo priežastimi pasaulyje. Viena dažniausių ŠKL formų yra išeminė širdies liga (IŠL), o viena sunkiausių jos klinikinių išraiškų – ūminis miokardo infarktas (MI) [1, 2]. Pagal 2021 m. Europos kardiologų draugijos ŠKL profilaktikos gaires Lietuva vis dar priskiriama labai didelės ŠKL rizikos regionui [3].

Ūminis miokardo infarktas, kai ST segmentas pakilęs (ŪMIkSTP), dažniausiai išsivysto dėl ūminės vainikinės arterijos okliuzijos ar subokliuzijos. Pirminė perkutaninė vainikinių arterijų intervencija (PVAI) yra pagrindinis reperfuzinio gydymo metodas. Laiku atlikta PVAI mažina mirštamumą, pakartotinio miokardo infarkto ir insulto riziką [4]. Net ir po sėkmingos reperfuzijos daliai pacientų nustatoma reikšminga išemijos ir reperfuzijos pažaida. Eksperimentiniai duomenys rodo, kad išemija sukelia tik nedidelius mikrocirkuliacijos pokyčius, o ryški mikrovaskulinė pažaida dažniausiai išryškėja prasidėjus reperfuzijai [5]. Šiai pažaidai svarbūs du tarpusavyje susiję mechanizmai: mikrokraujagyslių spindžio obstrukcija ir suspaudimas iš išorės. Mi-

krokraujagyslių spindžio obstrukciją gali lemti distalinė tromboembolizacija, kraujo ląstelių sankaupos, vietinė trombozė ir vazospazmas. Kompresija iš išorės dažniausiai susijusi su intersticine ir ląsteline edema, intramiokardine hemoragija ir padidėjusiu kairiojo skilvelio (KS) prisipildymo spaudimu [5]. Viena svarbiausių šios pažaidos išraiškų yra mikrovaskulinė obstrukcija (MVO), kai, atkūrus epikardinę kraujotaką, smulkiosiose miokardo kraujagyslėse perfuzija išlieka sutrikusi. MVO siejama su didesne infarkto apimtimi, blogesniu KS funkcijos atsistatymu, nepalankiu KS remodeliavimusi ir blogesne prognoze [6, 7].

KS remodeliavimasis po ūminio miokardo infarkto sukelia KS dydžio, geometrijos, masės ir funkcijos pokyčius. Nepalanki šio proceso eiga susijusi su išliekančia KS disfunkcija, širdies nepakankamumu ir blogesnėmis ilgalaikėmis baigtimis [8–10]. Šių pokyčių mastą lemia ne vien infarkto apimtis, bet ir padidėjusi miokardo sienelės įtampa dėl pakitusio prieškrūvio ir pokrūvio, renino, angiotenzino ir aldosterono bei simpatinės nervų sistemos suaktyvėjimas, uždegimo procesai ir tarpląstelinio audinio persitvarkymas, progresuojanti fibrozė [8]. Po MI miokardas skirtingose zonose gyja nevienodai: ryškiausi struktūriniai ir funkciniai pokyčiai vyksta infarktinėje zonoje, tačiau pokyčių nustatoma ir periinfarktiniame bei nutolusiame miokarde. Šie regioniniai gijimo skirtumai gali iš dalies paaiškinti, kodėl net ir panašios infarkto apimties pacientų KS funkcijos atsistatymas ir remodeliavimosi eiga skiriasi [10].

Širdies magnetinio rezonanso tyrimas (ŠMRT) laikomas neinvaziniu KS tūrių, masės ir išstūmio frakcijos vertinimo aukso standartu. Skirtingų tyrėjų tyrimo rezultatai sutampa, todėl ŠMRT tinka KS struktūrinių ir funkcinių pokyčių stebėsenai po miokardo infarkto [11, 12]. Vieno tyrimo metu ŠMRT galima įvertinti ne tik KS funkciją, bet ir infarkto apimtį bei MVO, nustatomą vėlyvojo gadolinio kaupimosi (angl. *late gadolinium enhancement*, LGE) vaizduose [13]. Parametriniai miokardo žemėlapiai – nekontrastinio (natyvinio) ir pokontrastinio T1, T2 bei užląstelinio tūrio (ECV) – suteikia informacijos apie audinio savybes: edemą, užląstelinio tarpo pokyčius ir fibrozę. Miokardo deformacijos (įtampos) analizės metu papildomai galima kiekybiškai įvertinti regioninę miokardo mechaniką – išilginę ir apsukinę įtampas [14]. Šie parametrai padeda atskirti infarktinę, periinfarktinę ir nutolusiąją miokardo zonas bei įvertinti regioninius miokardo gijimo ypatumus [15]. Sujungiant parametrinių miokardo žemėlapių ir deformacijos analizę į vieną tyrimą, galima nuosekliai stebėti struktūrinius, funkcinius ir audinio pokyčius ūminiu ir vėlesniu laikotarpiais bei susieti juos su miokardo gijimu ir KS remodeliavimusi [10].

Neatsižvelgiant į pažangių vaizdinių tyrimų galimybes, vis dar sudėtinga anksti įvertinti sutrikusio KS funkcijos atsistatymo ir nepalankaus remodelia-

vimosi riziką. Įprastiniai klinikiniai, angiografiniai ir laboratoriniai rodikliai tik iš dalies paaiškina individualius miokardo pažaidos, gijimo ir funkcijos atsistatymo skirtumus. Papildomos informacijos gali suteikti kraujo rodikliai, susiję su uždegiminiais ir trombozinias procesais, bei eikozanoidų apykaitos produktai. Šiame tyrime vertintas trombocitų skaičius [16], NETozės raiška – neutrofilų užląstelinių tinklų (angl. neutrophil extracellular traps, NET) susidarymas – ir eikozanoidai: 20-hidroksieikozatetraeno rūgštis (20-HETE) bei 15(S)-hidroksieikozatetraeno rūgštis (15(S)-HETE).

20-HETE susidaro iš arachidono rūgšties, veikiant CYP4A ir CYP4F fermentams. 20-HETE reguliuoja kraujagyslių tonusą ir skatina smulkiųjų kraujagyslių vazokonstrikciją [17, 18], endotelio aktyvaciją ir trombocitų adheziją prie kraujagyslės sienelės [19]. Šis metabolitas taip pat aktyvina nikotinamido adenino dinukleotido fosfato (NADPH) oksidazę, didina reaktyviųjų deguonies formų susidarymą ir oksidacinį stresą, todėl gali prisidėti prie endotelio disfunkcijos ir mikrovaskulinės pažaidos [20].

15(S)-HETE susidaro iš arachidono rūgšties, veikiant 12/15-lipoksigenazei. Žmogaus išeminiame miokarde nustatyta padidėjusi 15(S)-HETE koncentracija, o eksperimentiniuose tyrimuose šis metabolitas skatino trombų formavimąsi [21]. Be to, 15(S)-HETE skatina fibroblastų virtimą miofibroblastais, todėl gali stiprinti miokardo fibrozę [22]. Iš eksperimentinio miokardo infarkto modelio pašalinus 12/15-lipoksigenazės geną, sumažėjo fibrozė ir nepalankus KS remodeliavimasis [23]. Šie duomenys leidžia manyti, kad 15(S)-HETE gali būti susijęs su miokardo gijimu ir KS remodeliavimusi po infarkto.

NETozės metu aktyvinti neutrofilai išskiria dekondensuotą chromatiną, histonus ir granulių baltymus, iš kurių susidaro NET [24]. Jie suriša trombocitus, fibriną ir krešėjimo faktorius, pažeidžia endotelį ir gali užkimšti kapiliarus, todėl skatina trombų formavimąsi smulkiosiose kraujagyslėse ir didina mikrovaskulinę pažaidą po reperfuzijos [25–28].

Šių kraujo žymenų reikšmė vertinant ūminę miokardo pažaidą, vėlesnį miokardo gijimą ir KS remodeliavimąsi po pirmojo ŪMIkSTP iki šiol nėra pakankamai ištirta [29, 30]. Bendras ŠMRT rodiklių ir kraujo biologinių žymenų vertinimas gali suteikti papildomos informacijos apie KS funkcijos atsistatymą ir remodeliavimąsi po ŪMIkSTP.

DARBO TIKSLAS IR UŽDAVINIAI

Darbo tikslas

Širdies magnetinio rezonanso tyrimu įvertinti miokardo išemijos ir reperfuzijos pažaidos požymius, miokardo gijimą, kairiojo skilvelio funkcijos ki-

timą bei remodeliavimosi ypatumus pacientams po pirmojo ūminio miokardo infarkto, kai ST segmentas pakilęs, bei taikyto reperfuzinio gydymo. Nustatyti pradinius klinikinius, biologinių žymenų ir širdies magnetinio rezonanso tyrimo prognozinius veiksnius, susijusius su ūmine miokardo pažaida, sutrikusia kairiojo skilvelio sistoline funkcija ir nepalankiu remodeliavimusi po 6 mėnesių.

Darbo uždaviniai

1. ŠMRT įvertinti ūminio miokardo infarkto apimtį ir mikrovaskulinę obstrukciją bei nustatyti jų sąsajas su klinikiniais, angiografiniais, laboratoriniais rodikliais ir specializuotais biologiniais žymenimis.
2. Įvertinti KS sistolinės funkcijos ir infarktinio audinio pokyčius per 6 mėnesius po MI bei nustatyti liekamojo infarkto dydžio sąsajas su pradiniais ŠMRT rodikliais ir kraujo žymenimis.
3. Palyginti ŠMRT miokardo charakteristikas ir įtampos rodiklius infarktinėje, periinfarktinėje ir nutolusiojoje zonose ūminiu laikotarpiu ir praėjus 6 mėnesiams po miokardo infarkto.
4. Nustatyti pradinius klinikinius, angiografinius, laboratorinius, biologinių žymenų ir ŠMRT rodiklius, susijusius su sutrikusiu KS sistolinės funkcijos atsistatymu po 6 mėnesių, ir įvertinti prognozinę jų vertę.
5. Nustatyti pradinius klinikinius, angiografinius, laboratorinius, biologinių žymenų ir ŠMRT rodiklius, susijusius su nepalankiu KS remodeliavimusi po 6 mėnesių, ir įvertinti prognozinę jų vertę.

Tyrimo naujumas ir aktualumas

Šiame tyrime pacientams po pirmojo ŪMIkSTP vertinti ne tik įprastiniai ŠMRT rodikliai – KS tūriai, KSIF, infarkto dydis ir MVO, bet ir regioniniai audinių charakterizavimo bei deformacijos parametrai (nekontrastinis ir pokontrastinis T1, T2 relaksacijos laikai, ECV, išilginė ir apsukinė miokardo įtampa) infarktinėje, periinfarktinėje ir nutolusiojoje miokardo zonose.

Šis tyrimas yra vienas pirmųjų, kuriame pacientams po pirmojo ŪMIkSTP vertintos cirkuliuojančių biologinių žymenų sąsajos su pradinio ir pakartotinio ŠMRT rodikliais, ir pirmasis tokio pobūdžio tyrimas Lietuvoje. Kartu analizuoti trys cirkuliuojantys biologiniai žymenys – 20-HETE, 15(S)-HETE ir NETozės raiška, susieti su pažangiais ŠMRT audinių charakterizavimo ir deformacijos rodikliais.

Gauti rezultatai rodo, kad po ŪMIkSTP baigtys turi skirtingą prognozinių veiksnių profilį. Ūminę miokardo pažaidą ir MVO labiau atspindi angiografiniai, miokardo nekrozės ir NETozės raiškos rodikliai, sutrikusį KS funkcijos atsistatymą – pradinė KSIF, infarkto dydis ir infarktinės zonos apsukinė

įtampa, o nepalankų KS remodeliavimąsi – trombocitų skaičius, 20-HETE koncentracija ir infarktinės zonos pokontrastinis T1 relaksacijos laikas. Šie duomenys pabrėžia kompleksinio ŠMRT ir kraujo biologinių žymenų vertinimo svarbą individualiai paciento rizikai įvertinti ir individualizuotai stebėsenai po reperfuzinio gydymo pagrįsti.

DARBO METODIKA

Tiriamųjų kontingentas

Atliktas perspektyvusis, stebimasis, vieno centro tyrimas Lietuvos sveikatos mokslų universiteto ligoninės Kauno klinikų (LSMUL KK) Kardiologijos klinikoje. 2020-09–2022-01 laikotarpiu į tyrimą įtraukti pacientai, kuriems diagnozuotas pirmasis ŪMIkSTP. Diagnozė nustatyta remiantis Ketvirtuoju universaliuoju miokardo infarkto apibrėžimu [65]: angiografija patvirtinta ūminė vainikinės arterijos okliuzija pacientui, turinčiam išemijos simptomų, ST segmento pakilimą EKG ir troponino I koncentraciją, viršijančią 0,04 µg/l ribą. Į tyrimą įtraukti pacientai, kuriems MI išemija truko ne ilgiau nei 24 val. ir buvo taikytas reperfuzinis gydymas. Iš 112 įtrauktų pacientų 104 atlikta pirminė PVAI, 8 pacientams prieš PVAI taikyta fibrinolizė. Visiems pacientams taikytas gairėmis pagrįstas gydymas pagal Europos kardiologų draugijos rekomendacijas [89]. ŠMRT atliktas 105 pacientams praėjus 3 paroms [TKI 2–5] po PVAI, o pakartotinis ŠMRT – 93 pacientams praėjus 6 mėnesiams (±11 parų) po pradinio ŠMRT (1 pav.).

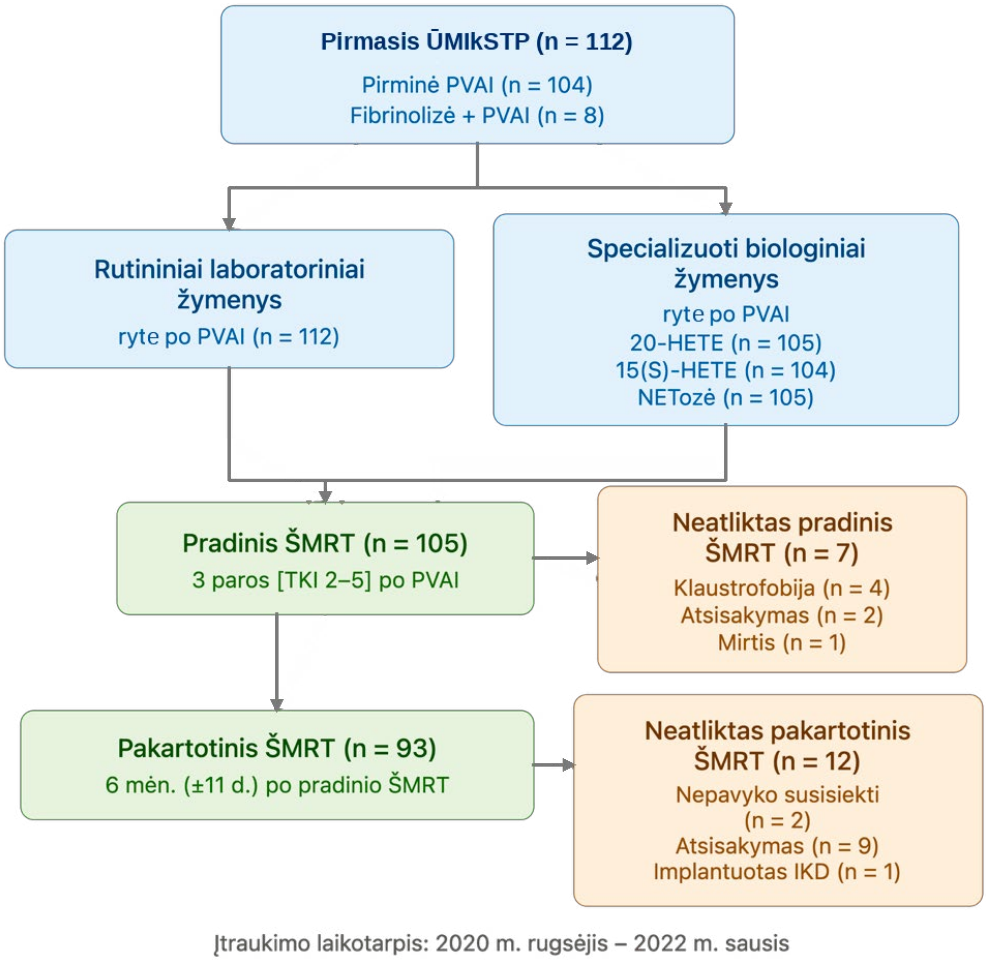

1 pav. *Tiriamųjų atrankos ir tyrimo eigos schema*

ŪMIkSTP – ūminis miokardo infarktas, kai ST segmentas pakilęs; PVAI – perkutaninė vainikinių arterijų intervencija; ŠMRT – širdies magnetinio rezonanso tyrimas; IKD – implantuojamasis kardioverteris-defibriliatorius; TKI – tarpkvartilinis intervalas.

Įtraukimo ir neįtraukimo kriterijai

Į tyrimą įtraukti vyresni nei 18 metų pacientai, kuriems diagnozuotas pirmasis ŪMIkSTP. Pacientai neįtraukti, jei anamnezėje diagnozuota IŠL (persirgtas MI, ankstesnė PVAI ar vainikinių arterijų jungčių operacija), vidutinio ar sunkaus laipsnio vožtuvų liga, persirgtas miokarditas, aktyvi onkologinė liga, inkstų funkcijos sutrikimas, jei apskaičiuotasis glomerulų filtracijos greitis (GFG) < 30 ml/min./1,73 m², ar nėštumas. Taip pat neįtraukti pacientai, turintys ŠMRT kontraindikacijų, ir pacientai, kuriems įtraukimo metu nu-

statytas prieširdžių virpėjimas. Tyrimas atliktas laikantis Helsinkio deklaracijos ir patvirtintas Kauno regioninio biomedicininių tyrimų etikos komiteto (leidimo Nr. BE-2-6, 2020-02-05). Visi pacientai pasirašė Informuoto asmens sutikimo formą.

Klinikiniai, angiografiniai ir procedūrų duomenys

Klinikiniai duomenys surinkti iš medicininės dokumentacijos (stacionarinio gydymo ligos istorijų): amžius, lytis, gretutinės ligos, širdies ir kraujagyslių ligų rizikos veiksniai, vartoti medikamentai bei antropometriniai duomenys. Apskaičiuotas kūno paviršiaus plotas (*Du Bois* formule) ir kūno masės indeksas (KMI). Vainikinių arterijų angiografijos (VAA) ir PVAI metu vertinta: priežastinė vainikinė arterija, TIMI (angl. *Thrombolysis In Myocardial Infarction*) kraujo tėkmė prieš PVAI ir po jos, daugiagyslė vainikinių arterijų liga (VAL), manualinė trombo aspiracija, glikoproteino IIb/IIIa inhibitorių skyrimas. Registruotos hospitalizacijos ŪMIkSTP komplikacijos: Kilipo klasė, prieširdžių virpėjimas ar plazdėjimas, skilvelinė tachikardija ar virpėjimas, antrojo ar trečiojo laipsnio atrioventrikulinė blokada (AVB).

Rutininiai kraujo žymenys

Veninio kraujo mėginiai paimti kitą rytą po PVAI, nevalgius. Rutininiai laboratoriniai rodikliai (bendrasis kraujo tyrimas su trombocitų skaičiumi, neutrofilų ir limfocitų santykiu (NLS), troponinas I, B tipo natriurezinis peptidas (BNP), kreatininas ir GFG, šlapalas, gliukozė, glikuotasis hemoglobinas (HbA1c), elektrolitai, lipidų profilis, kepenų fermentai bei C reaktyvusis baltymas (CRB)) nustatyti LSMUL KK Centrinėje laboratorijoje standartiniais metodais.

Specializuoti biožymenys

20-HETE ir 15(S)-HETE koncentracijos nustatytos plazmoje. Eikozanoidai iš plazmos išskirti organine ekstrakcija. Surinkta viršutinė organinė fazė išgarinta iki sausumo azoto srove 40 °C temperatūroje (*Multivap Nitrogen Evaporator*, Organomation Associates, Berlin, MA, JAV). 20-HETE ir 15(S)-HETE koncentracijos nustatytos komerciniais konkurenciniais imunofermentiniais (ELISA) rinkiniais (*Abcam, Cambridge*, JK; kat. Nr. ab175817 ir ab133035). Optinis tankis matuotas mikroplokštelių skaitytuvu *Infinite M Plex* (*Tecan, Männedorf*, Šveicarija) ties 450 nm (20-HETE) ir ties 405 nm su 590 nm referentiniu bangos ilgiu (15(S)-HETE). NETozės raiška serume vertinta kolorimetriniu neutrofilų elastazės tyrimo rinkiniu (Abcam, JK; kat. Nr. ab235979).

Širdies magnetinio rezonanso tyrimas

Visi ŠMRT atlikti tuo pačiu 3,0 T skeneriu (*Magnetom Skyra*, *Siemens Healthineers*, Erlangenas, Vokietija), naudojant 18 kanalų kūno ritę kartu su stuburo rite, sinchronizuojant su EKG. Pradiniam ir kontroliniam tyrimui taikytas vienodas standartizuotas protokolas. Atliktos judesio vaizdų sekos (dviejų, trijų, keturių kamerų ir trumposios ašies, apimančios visą kairįjį skilvelį nuo pamato iki viršūnės) bei nekontrastinio ir pokontrastinio T1 ir T2 žemėlapių sekos. LGE skenavimas atliktas 10–15 min. po gadobutrolio (0,2 mmol/kg) suleidimo. Tyrimas atliktas pagal Širdies magnetinio rezonanso draugijos (angl. Society for Cardiovascular Magnetic Resonance, SCMR) rekomendacijas [11, 123].

Širdies magnetinio rezonanso tyrimo vaizdų analizė

Visus ŠMRT vaizdus analizavo vienas, daugiau nei 5 metų patirtį turintis tyrėjas, nežinodamas klinikinių ir baigčių duomenų. Analizė atlikta naudojant *Medis Suite* (3.2 versija, Medis Medical Imaging Systems, Leiden, Nyderlandai) programinę įrangą, pagal SCMR vaizdų analizės standartus [11]. KS galinis diastolinis ir galinis sistolinis tūriai (KSGDT, KSGST), KSIF, KS smūginis tūris ir KS miokardo masė apskaičiuoti iš trumposios ašies judesio vaizdų. Tūriai ir masė indeksuoti pagal kūno paviršiaus plotą. Infarkto dydis matuotas trumposios ašies LGE vaizduose. Hiperintensyvus miokardas apibrėžtas kaip sritis, kurios signalo intensyvumas buvo didesnis nei 5 standartiniai nuokrypiai virš nutolusiojo miokardo signalo intensyvumo [90, 91]. MVO apibrėžta kaip hipointensyvi šerdis hiperintensyvioje zonoje ir įtraukta į bendrą infarkto plotą. Infarkto dydis ir MVO išreikšti gramais ir procentine KS masės dalimi. Miokardas padalytas naudojant Amerikos širdies asociacijos (angl. American Heart Association, AHA) 16 segmentų modelį [92]. Segmentai, kuriuose stebėtas LGE signalas, priskirti infarktiniams, tiesiogiai su jais besiribojantys – periinfarktiniams, o visi kiti, be kaupimosi, – nutolusiesiems**.** Ta pati klasifikacija nuosekliai taikyta tiek įtampos, tiek žemėlapių analizėms.

Miokardo įtampa vertinta kontūrų žymėjimo (angl. *feature tracking*) metodu: bendroji išilginė įtampa (angl. *global longitudinal strain*, GLS) apskaičiuota iš ilgosios ašies (dviejų, trijų ir keturių kamerų) vaizdų, o bendroji apsukinė įtampa (angl. *global circumferential strain*, GCS) – iš trumposios ašies (pamatinio, vidurinio ir viršūninio) pjūvių. Žemėlapių analizėje matuoti nekontrastinis ir pokontrastinis T1 bei T2 rodikliai, taip pat apskaičiuotas ECV [14]. Visi šie rodikliai įvertinti pagal 16 segmentų modelį ir suvidurkinti infarktinėje, periinfarktinėje bei nutolusiojoje zonose.

Tyrimo baigtys

Tyrime vertintos 4 pagrindinės baigtys:

1. **Didelė ūminio miokardo infarkto apimtis** – kai infarkto dydis pateko į viršutinį tyrimo imties tercilį (≥ 41,91 proc. KS masės).
2. **MVO** – vertinta pradiniame ŠMRT, LGE vaizduose (nustatyta arba nenustatyta).
3. **Sutrikęs KS sistolinės funkcijos atsistatymas** – kai pakartotiniame ŠMRT KSIF buvo < 50 proc. [39, 124].
4. **Nepalankus KS remodeliavimasis** – nustatytas, kai kontroliniame ŠMRT tyrime KSGDT ir KSGST padidėjo ne mažiau kaip 12 proc., palyginti su pradiniu ŠMRT tyrimu [39].

Statistinė analizė

Statistinė duomenų analizė atlikta naudojant *IBM SPSS Statistics* (31.0 versiją, IBM *Corp*., *Armonk*, NY, JAV). Kiekybinių kintamųjų skirstinio normalumas vertintas Shapiro-Wilk testu. Normaliai pasiskirsčiusių kiekybinių kintamųjų pateiktas vidurkis ir standartinis nuokrypis (SN), o nenormaliai pasiskirsčiusių – mediana ir tarpkvartilinis intervalas (TKI). Kategoriniai kintamieji pateikti absoliučiaisiais skaičiais ir procentais. Skirtumams tarp nepriklausomų grupių įvertinti taikytas Mann-Whitney U testas arba Stjudento t testas, atsižvelgiant į duomenų skirstinį. Trims ir daugiau grupėms palyginti taikyta Kruskal-Wallis analizė arba vienfaktorė dispersinė analizė (ANOVA), atsižvelgiant į duomenų skirstinį, esant poreikiui – atliktas post hoc palyginimas. Poriniams duomenims taikytas porinis Wilcoxon testas, o skirtumams tarp infarktinės, gretimos ir nutolusiosios zonų įvertinti – Friedmano testas su poriniais Wilcoxon testais ir Bonferroni korekcija. Kategorinių kintamųjų sąsajos vertintos χ^2 testu, o kai tikėtini dažniai buvo maži – tiksliuoju Fišerio testu. Koreliacijos tarp tęstinių laboratorinių, biologinių žymenų ir ŠMRT rodiklių vertinti Spearmano koreliacijos koeficientu (r_s); koreliacijos stiprumas vertintas kaip nereikšmingas ($|r_s|$ 0,00–0,09), silpnas (0,10–0,39), vidutinis (0,40–0,69), stiprus (0,70–0,89) arba labai stiprus (0,90–1,00) [93]. Su iš anksto apibrėžtais binariniais tyrimo rodikliais susijusiems veiksniams nustatyti atlikta vienaveiksnė ir daugiaveiksnė binarinė logistinės regresijos analizė. Rezultatai pateikti kaip šansų santykiai (ŠS) su 95 proc. pasikliautinaisiais intervalais (PI). Šių rodiklių prognozinei reikšmei įvertinti taikyta ROC analizė, apskaičiuotas plotas po kreive (angl. *area under the curve*, AUC), o optimalios ribinės reikšmės nustatytos pagal Youden indeksą (J).

REZULTATAI

Tiriamųjų charakteristika

Galutinę tiriamųjų imtį sudarė 105 pacientai, kuriems atliktas pradinis ŠMRT tyrimas; iš jų 93 pacientams atliktas ir pakartotinis ŠMRT po 6 mėnesių. Tiriamųjų amžiaus vidurkis buvo 60,3 (10,0) metų, vyrai sudarė 81 (77,1 proc.). Priekinės KS sienelės MI diagnozuotas 43 (41,0 proc.) pacientams, TIMI 0–1 kraujo tėkmė prieš PVAI nustatyta 75 (71,4 proc.), o TIMI 3 kraujo tėkmė po PVAI pasiekta 98 (93,3 proc.) pacientams. Daugiagyslė VAL nustatyta 52 (49,5 proc.), Kilipo ≥ 2 klasė – 27 (25,7 proc.) pacientams. Maksimali troponino I koncentracija buvo 46,7 (52,6) µg/l. 20-HETE koncentracija buvo 122,6 (252,5) ng/ml, 15(S)-HETE – 1,1 (1,4) ng/ml, NETozės raiška – 62,5 (41,2) mU/ml. Tiriamųjų klinikinė, procedūrinė, laboratorinė ir biologinių žymenų charakteristika pateikta 1 lentelėje.

1 lentelė. *Tiriamųjų klinikinė, procedūrinė, laboratorinė ir biožymenų charakteristika*

Rodiklis	(n = 105)
Demografiniai duomenys ir rizikos veiksniai	
Amžius, metai	60,3 (10,0)
Vyriška lytis, n (proc.)	81 (77,1)
Cukrinis diabetas, n (proc.)	14 (13,3)
Arterinė hipertenzija, n (proc.)	84 (80,0)
Dislipidemija, n (proc.)	95 (90,5)
Rūkymas, n (proc.)	54 (51,4)
Miokardo infarkto ir procedūrų metu nustatyti duomenys	
Visas išemijos laikas, min.	424,8 (286,6)
Atvykimo – reperfuzijos laikas, min.	65,0 (63,9)
Fibrinolizė prieš PVAI, n (proc.)	8 (7,6)
Priekinės KS sienelės MI, n (proc.)	43 (41,0)
TIMI 0–1 kraujo tėkmė prieš PVAI, n (proc.)	75 (71,4)
TIMI 3 kraujo tėkmė po PVAI, n (proc.)	98 (93,3)
Daugiagyslė VAL, n (proc.)	52 (49,5)
Klinikinės komplikacijos ŪMIkSTP metu	
Kilipo klasė ≥ 2, n (proc.)	27 (25,7)
Skilvelinė tachikardija / virpėjimas, n (proc.)	9 (8,6)
Laboratoriniai rodikliai ir biologiniai žymenys	
Troponinas I, µg/l	46,7 (52,6)
BNP, ng/l	185,8 (127,2)
GFG, ml/min./1,73 m²	91,1 (17,7)
Trombocitai, ×10⁹/l	226,3 (59,2)

1 lentelės tęsinys

Rodiklis	(n = 105)
20-HETE, ng/ml	122,6 (252,5)
15(S)-HETE, ng/ml	1,1 (1,4)
NETozės raiška, mU/ml	62,5 (41,2)

KS – kairysis skilvelis; MI – miokardo infarktas; ŪMIkSTP – ūminis miokardo infarktas, kai ST segmentas pakilęs; VAL – vainikinių arterijų liga; PVAI – perkutaninė vainikinių arterijų intervencija; TIMI – angl. *Thrombolysis In Myocardial Infarction*; BNP – B tipo natriurezinis peptidas; GFG – glomerulų filtracijos greitis; HETE – hidroksieikozatetraeno rūgštis; NETozė – neutrofilų užląstelinių tinklų susidarymas. Vertės pateiktos kaip vidurkis (standartinis nuokrypis) arba n (proc.).

Ūminė miokardo pažaida: infarkto apimtis ir mikrovaskulinė obstrukcija

Vidutinė ūminio infarkto apimtis pradiniame ŠMRT tyrime buvo 34,2 (19,4) proc. KS masės. Didesnė infarkto apimtis nustatyta pacientams, kuriems diagnozuotas priekinės KS sienelės MI (42,0 (18,7) ir 28,6 (18,0) proc.; $p < 0,001$), TIMI 0–1 kraujo tėkmė prieš PVAI (38,5 (18,9) ir 23,6 (16,5) proc.; $p < 0,001$) ir skilvelinė tachikardija ar virpėjimas ūminiu laikotarpiu (54,3 (15,7) ir 32,3 (18,6) proc.; $p < 0,001$). Stebėta stipri teigiamoji infarkto dydžio koreliacija su troponino I ($r_s = 0,738$; $p < 0,001$) ir aspartataminotransferazės (AST; $r_s = 0,704$; $p < 0,001$) koncentracija bei vidutinė teigiamoji koreliacija su alaninaminotransferazės (ALT; $r_s = 0,602$; $p < 0,001$) koncentracija, tačiau su specializuotais biologiniais žymenimis (20-HETE, 15(S)-HETE, NETozės raiška) reikšmingų koreliacijų nestebėta. Daugiaveiksnėje analizėje nepriklausomi didelės ūminio infarkto apimties (≥ 41,91 proc. KS masės) veiksniai buvo TIMI 0–1 kraujo tėkmė prieš PVAI ir didesnė troponino I koncentracija (2 lentelė).

MVO pradiniame ŠMRT tyrime nustatyta 73 pacientams (70,9 proc.). MVO grupėje, palyginti su pacientais be MVO, nustatyta reikšmingai didesnė troponino I koncentracija (36,4 [21,4–77,3] ir 12,5 [4,3–33,6] μg/l; $p < 0,001$) ir didesnė NETozės raiška (56,4 [42,1–71,3] ir 48,7 [36,7–60,7] mU/ml; $p = 0,011$). Šioje grupėje taip pat nustatyta reikšmingai didesnė AST ir ALT koncentracija, mažesnis GFG ir mažesnis trombocitų skaičius. Specializuotų eikozanoidų – 20-HETE ir 15(S)-HETE – koncentracijos tarp grupių reikšmingai nesiskyrė. Daugiaveiksnėje analizėje nepriklausomi MVO veiksniai buvo: TIMI 0–1 kraujo tėkmė prieš PVAI, didesnė troponino I koncentracija, mažesnis GFG ir didesnė NETozės raiška (2 lentelė). ROC analizėje geriausią skiriamąją gebą MVO atžvilgiu turėjo troponinas I (AUC 0,78; jautrumas 80,8 proc., specifiškumas 70,0 proc.). GFG, NETozės raiška ir trombocitų

skaičius pasižymėjo silpnesne bendra skiriamąja geba; NETozės raiška, nors mažo jautrumo (46,6 proc.), pasižymėjo dideliu specifiškumu (90,0 proc.) (3 lentelė).

2 lentelė. *Nepriklausomi didelės ūminio miokardo infarkto apimties ir mikrovaskulinės obstrukcijos veiksniai*

Veiksnys	ŠS (95 proc. PI)	p
Didelė infarkto apimtis (≥ 41,91 proc. KS masės)		
TIMI 0–1 kraujo tėkmė prieš PVAI	8,08 (1,45–45,15)	0,017
Troponinas I (kas 10 µg/l)	1,28 (1,10–1,45)	< 0,001
Mikrovaskulinė obstrukcija		
TIMI 0–1 kraujo tėkmė prieš PVAI	3,97 (1,28–12,30)	0,017
Troponinas I (kas 1 µg/l)	1,03 (1,01–1,05)	0,015
GFG (kas 1 ml/min./1,73 m²)	0,96 (0,93–1,00)	0,038
NETozės raiška (kas 1 mU/ml)	1,03 (1,00–1,05)	0,020

ŠS – šansų santykis; PI – pasikliautinasis intervalas; KS – kairysis skilvelis; PVAI – perkutaninė vainikinių arterijų intervencija; TIMI – angl. *Thrombolysis In Myocardial Infarction*; GFG – glomerulų filtracijos greitis; NETozė – neutrofilų užląstelinių tinklų susidarymas. Pateikti nurodyto vienetų pokyčio kiekybinių rodiklių šansų santykiai.

3 lentelė. *Pasirinktų laboratorinių rodiklių ir biožymenų diagnostinė vertė nustatant mikrovaskulinę obstrukciją*

Rodiklis	Slenkstinė vertė	AUC	95 proc. PI	p	Jautrumas, proc.	Specifiškumas, proc.
Troponinas I, µg/l	≥ 18,56	0,779	0,674–0,883	< 0,001	80,8	70,0
GFG, ml/min./1,73 m²	≤ 97,2	0,672	0,560–0,783	0,003	68,5	70,0
NETozės raiška, mU/ml	≥ 62,1	0,659	0,544–0,774	0,007	46,6	90,0
Trombocitai, $\times 10^9$/l	≤ 214,0	0,633	0,518–0,748	0,024	58,9	70,0

AUC – plotas po kreive; PI – pasikliautinasis intervalas; GFG – glomerulų filtracijos greitis; NETozė – neutrofilų užląstelinių tinklų susidarymas. Slenkstinės vertės nustatytos pagal Youden indeksą.

Kairiojo skilvelio funkcijos ir infarktinio audinio pokyčiai po 6 mėnesių

Pakartotinis ŠMRT po 6 mėnesių atliktas 93 pacientams. Per stebėjimo laikotarpį nustatyta palanki KS funkcijos ir infarktinio audinio pokyčių dinamika: reikšmingai pagerėjo KSIF nuo 49,0 [40,7–52,4] iki 55,8 [47,9–59,9]

proc. (p < 0,001), o kairiojo skilvelio galinio sistolinio tūrio indeksas (KSGSTi) reikšmingai sumažėjo nuo 45,9 [37,2–57,3] iki 39,9 [31,5–51,1] ml/m² (p = 0,005). Kairiojo skilvelio galinio diastolinio tūrio indeksas (KSGDTi) reikšmingai nekito. Taip pat pagerėjo GLS ir GCS, sumažėjo KS masės indeksas.

Infarkto dydis per 6 mėnesius reikšmingai sumažėjo nuo 30,9 [18,9–45,5] iki 18,8 [11,2–31,1] proc. KS masės (p < 0,001). Pakartotinio ŠMRT metu MVO nenustatyta nė vienam pacientui. Miokardo struktūriniai rodikliai taip pat atspindėjo infarktinio audinio gijimą: reikšmingai sumažėjo vidutinės nekontrastinio T1 ir T2 relaksacijos laikų vertės, padidėjo pokontrastinio T1 relaksacijos laikas, o vidutinis ECV reikšmingai nekito. Pagrindiniai KS funkcijos, tūrių ir infarktinio audinio pokyčiai pateikti 4 lentelėje.

***4 lentelė**. KS funkcijos, tūrių ir infarktinio audinio pokyčiai per 6 mėnesius*

Rodiklis	n	Pradinis tyrimas	Po 6 mėn.	p
KSGDTi, ml/m²	93	90,3 [78,4–100,2]	90,2 [74,5–103,3]	0,262
KSGSTi, ml/m²	93	45,9 [37,2–57,3]	39,9 [31,5–51,1]	0,005
KS smūginio tūrio indeksas, ml/m²	93	42,1 (9,4)	48,0 (10,1)	< 0,001
KS masės indeksas, g/m²	93	56,2 [49,3–65,3]	49,4 [42,9–54,9]	< 0,001
KSIF, proc.	93	49,0 [40,7–52,4]	55,8 [47,9–59,9]	< 0,001
GLS, proc.	92	−20,4 (4,4)	−23,5 (5,6)	< 0,001
GCS, proc.	92	−27,7 (6,7)	−30,4 (8,1)	< 0,001
Nekontrastinis T1, ms	92	1352,1 [1298,6–1396,5]	1275,0 [1248,3–1311,8]	< 0,001
Pokontrastinis T1, ms	86	353,8 [290,7–394,9]	403,9 [374,5–444,9]	< 0,001
ECV, proc.	86	29,5 [26,8–33,1]	29,0 [25,9–32,6]	0,292
T2, ms	86	44,2 [42,1–46,6]	42,9 [41,1–45,0]	< 0,001
Infarkto dydis, proc. KS masės	93	30,9 [18,9–45,5]	18,8 [11,2–31,1]	< 0,001
MVO dydis, proc. KS masės	93	2,6 [0,0–5,9]	Nenustatyta	—

KS – kairysis skilvelis; KSGDTi – kairiojo skilvelio galinio diastolinio tūrio indeksas; KSGSTi – kairiojo skilvelio galinio sistolinio tūrio indeksas; KSIF – kairiojo skilvelio išstūmio frakcija; GLS – bendroji išilginė įtampa; GCS – bendroji apsukinė įtampa; ECV – užląstelinis tūris; MVO – mikrovaskulinė obstrukcija; T1, T2 – T1 ir T2 relaksacijos laikai. Tūriai ir masė indeksuoti pagal kūno paviršiaus plotą. Vertės pateiktos kaip mediana [TKI] arba vidurkis (SN).

Liekamasis infarkto dydis po 6 mėnesių buvo 18,8 [11,2–31,1] proc. KS masės, o infarkto apimties sumažėjimas – 9,6 [3,0–16,1] proc. KS masės. Stebėta stipri teigiamoji liekamosios infarkto apimties koreliacija su pradine infarkto apimtimi (r_s = 0,837; p < 0,001) ir maksimalia troponino I koncen-

tracija (r_s = 0,746; p < 0,001) bei vidutinė teigiamoji koreliacija su pradine MVO apimtimi (r_s = 0,590; p < 0,001), tačiau su specializuotais biologiniais žymenimis (20-HETE, 15(S)-HETE, NETozės raiška) reikšmingų koreliacijų nenustatyta. Infarkto apimties sumažėjimas su pradine MVO apimtimi bei specializuotais biologiniais žymenimis taip pat nekoreliavo.

Miokardo charakteristikos ir įtampos regioniniai skirtumai bei pokyčiai per 6 mėnesius

Pradiniame ŠMRT tyrime, atlikus segmentinę analizę, nustatytas laipsniškas miokardo pažaidos didėjimas nuo nutolusiosios iki infarktinės zonos. Ryškiausi pokyčiai nustatyti infarktinėje zonoje: joje išilginė ir apsukinė miokardo įtampos buvo labiausiai sumažėjusios, nekontrastinio T1, T2 relaksacijos laiko ir ECV vertės buvo didžiausios, o pokontrastinis T1 relaksacijos laikas – trumpiausias. Periinfarktinėje zonoje šie rodikliai buvo pakitę mažiau, o nutolusiojoje zonoje – mažiausiai. Lyginant periinfarktinę ir nutolusiąją zonas, reikšmingai skyrėsi apsukinė įtampa, nekontrastinis T1, ECV ir pokontrastinis T1, tačiau išilginė įtampa ir T2 relaksacijos laikas reikšmingai nesiskyrė (2 pav.). Pradinės regioninės ŠMRT rodiklių vertės pateiktos 2 paveiksle.

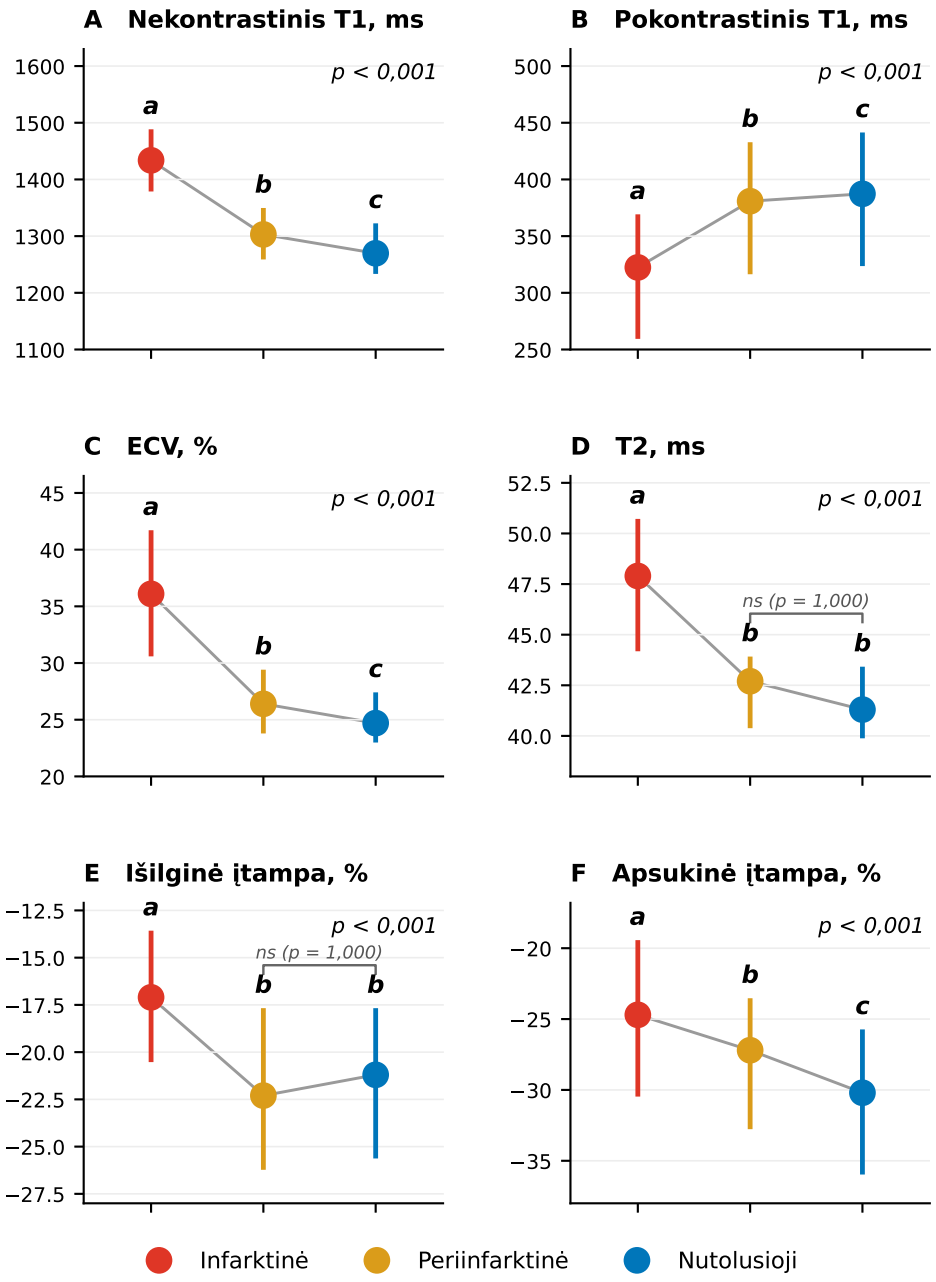

2 pav. *Miokardo charakteristikos ir įtampos rodikliai infarktinėje, periinfarktinėje ir nutolusiojoje zonose pradiniame ŠMRT tyrime*

Skirtingos raidės (a, b, c) žymi statistiškai reikšmingus skirtumus tarp zonų ($p < 0,05$); vienodos raidės ir „ns“ – statistiškai nereikšmingus skirtumus. ECV – užląstelinis tūris; T1, T2 – T1 ir T2 relaksacijos laikai.

Per 6 mėnesius regioniniai miokardo pokyčiai buvo nevienodi. Ryškiausias miokardo įtampos pagerėjimas nustatytas infarktinėje zonoje: išilginė miokardo įtampa pagerėjo nuo −17,2 [−20,6 iki −14,5] iki −21,9 [−26,3 iki −17,5] proc. ($p < 0,001$), o apsukinė įtampa – nuo −25,3 [−30,3 iki −19,8] iki −29,3 [−33,7 iki −21,6] proc. ($p < 0,001$). Šioje zonoje taip pat reikšmingai sumažėjo nekontrastinio T1 ir T2 relaksacijos laikas, padidėjo pokontrastinis T1 relaksacijos laikas, o ECV reikšmingai nepakito. Periinfarktinėje zonoje reikšmingai pagerėjo tik apsukinė įtampa, sumažėjo nekontrastinis T1 ir padidėjo pokontrastinis T1 relaksacijos laikas, o išilginė įtampa, ECV ir T2 reikšmingai nekito. Nutolusiojoje zonoje pagerėjo išilginė įtampa, sumažėjo nekontrastinis T1 ir padidėjo pokontrastinis T1 relaksacijos laikas. ECV ir T2 vertės šioje zonoje padidėjo neryškiai, tačiau statistiškai reikšmingai. Regioninių rodiklių pokyčiai pateikti 5 lentelėje.

***5 lentelė**. Miokardo charakteristikų ir įtampos regioniniai pokyčiai per 6 mėnesius*

Rodiklis	n	Pradinis tyrimas	Po 6 mėn.	p
Infarktinė zona				
Išilginė įtampa, proc.	91	−17,2 [−20,6 iki −14,5]	−21,9 [−26,3 iki −17,5]	< 0,001
Apsukinė įtampa, proc.	91	−25,3 [−30,3 iki −19,8]	−29,3 [−33,7 iki −21,6]	< 0,001
Nekontrastinis T1, ms	91	1429,1 [1384,1–1482,6]	1312,8 [1272,5–1360,1]	< 0,001
Pokontrastinis T1, ms	86	317,0 [254,8–356,7]	371,7 [331,3–410,6]	< 0,001
ECV, proc.	86	35,9 [30,3–41,3]	34,3 [29,5–41,3]	0,219
T2, ms	89	47,8 [44,3–50,6]	43,1 [41,5–46,2]	< 0,001
Periinfarktinė zona				
Išilginė įtampa, proc.	90	−21,9 [−26,5 iki −17,6]	−23,6 [−29,4 iki −19,3]	0,091
Apsukinė įtampa, proc.	91	−27,2 [−32,2 iki −23,7]	−30,1 [−35,7 iki −25,7]	0,002
Nekontrastinis T1, ms	91	1302,1 [1259,7–1344,7]	1262,6 [1234,3–1305,3]	< 0,001
Pokontrastinis T1, ms	86	370,5 [303,5–429,5]	423,3 [395,8–474,1]	< 0,001
ECV, proc.	86	26,1 [23,8–28,8]	26,0 [23,7–28,8]	0,602
T2, ms	89	42,8 [40,3–43,9]	42,1 [39,8–44,0]	0,396
Nutolusioji zona				
Išilginė įtampa, proc.	89	−21,3 [−25,4 iki −18,0]	−25,0 [−28,9 iki −21,1]	< 0,001
Apsukinė įtampa, proc.	89	−30,2 [−36,0 iki −26,0]	−32,3 [−39,7 iki −27,8]	0,067
Nekontrastinis T1, ms	89	1262,7 [1235,2–1311,7]	1253,6 [1223,2–1293,4]	0,021
Pokontrastinis T1, ms	84	375,6 [323,0–432,8]	429,4 [397,5–471,2]	< 0,001
ECV, proc.	84	24,8 [22,4–27,2]	25,3 [23,1–27,2]	0,002
T2, ms	87	41,3 [40,0–43,3]	42,5 [39,9–44,4]	0,036

ECV – užląstelinis tūris; T1, T2 – T1 ir T2 relaksacijos laikai. Vertės pateiktos kaip mediana [TKI]; n – į analizę įtrauktų pacientų skaičius.

Sutrikęs kairiojo skilvelio sistolinės funkcijos atsistatymas

Sutrikęs KS sistolinės funkcijos atsistatymas, atlikus pakartotinį ŠMRT, apibrėžtas kaip KSIF < 50 proc., nustatytas 28 iš 93 pacientų (30,1 proc.). Šiems pacientams, palyginti su pacientais, kurių KSIF po 6 mėnesių buvo ≥ 50 proc., nustatyta mažesnė pradinė KSIF (atitinkamai 38,5 [33,4–41,8] ir 50,6 [46,7–55,9] proc.; p < 0,001), didesnė infarkto apimtis (47,2 [33,4–68,1] ir 26,6 [14,9–38,0] proc. KS masės; p < 0,001), didesnė mikrovaskulinės obstrukcijos apimtis (7,1 [3,3–10,3] ir 3,5 [2,0–5,9] proc. KS masės; p = 0,006), didesnė maksimali troponino I ir AST koncentracija (abiejų p < 0,001) bei blogesnė infarktinės zonos apsukinė įtampa (p < 0,001). Specializuotų biologinių žymenų – 20-HETE, 15(S)-HETE ir NETozės raiškos – reikšmės tarp grupių reikšmingai nesiskyrė.

Pagrindiniame daugiaveiksniame modelyje nepriklausomu sutrikusio KS sistolinės funkcijos atsistatymo veiksniu išliko tik mažesnė pradinė KSIF (ŠS 0,859; 95 proc. PI 0,758–0,973; p = 0,017); infarkto apimtis, troponino I koncentracija ir infarktinės zonos apsukinė įtampa reikšmingumo neteko. Atlikus jautrumo analizę be pradinės KSIF, nepriklausomais veiksniais išliko didesnė pradinė infarkto apimtis (ŠS 1,054; 95 proc. PI 1,015–1,095; p = 0,006) ir blogesnė infarktinės zonos apsukinė įtampa (ŠS 1,145; 95 proc. PI 1,033–1,269; p = 0,010) (6 lentelė).

***6 lentelė**. Daugiaveiksnė logistinė regresija sutrikusio kairiojo skilvelio funkcijos atsistatymo veiksniams nustatyti*

Veiksnys	Pagrindinis modelis, ŠS (95 proc. PI)	p	Jautrumo modelis, ŠS (95 proc. PI)	p
Pradinė KSIF, proc.	0,859 (0,758–0,973)	0,017	–	–
Troponinas I, µg/l	1,018 (0,998–1,038)	0,080	–	–
Pradinė infarkto apimtis, proc.	1,020 (0,975–1,067)	0,387	1,054 (1,015–1,095)	0,006
Infarktinės zonos apsukinė įtampa, proc.	1,037 (0,911–1,181)	0,583	1,145 (1,033–1,269)	0,010

ŠS – šansų santykis; PI – pasikliautinasis intervalas; KSIF – kairiojo skilvelio išstūmio frakcija. Pateikti vieno vieneto pokyčio kiekybinių kintamųjų šansų santykiai.

ROC analizei visi keturi pradiniai žymenys turėjo gerą skiriamąją gebą (AUC 0,810–0,854). Didžiausiu specifiškumu pasižymėjo pradinė KSIF (90,8 proc.), o didžiausiu jautrumu – infarktinės zonos apsukinė įtampa (85,7 proc.) (7 lentelė).

*7 **lentelė**. Pradinių rodiklių geba prognozuoti sutrikusį kairiojo skilvelio funkcijos atsistatymą*

Rodiklis	Slenkstinė vertė	AUC	95 proc. PI	p	Jautrumas, proc.	Specifiškumas, proc.
Pradinė KSIF, proc.	≤ 41,3	0,854	0,762–0,946	< 0,001	75,0	90,8
Pradinis infarkto dydis, proc.	≥ 42,3	0,813	0,719–0,907	< 0,001	67,9	84,6
Infarktinės zonos apsukinė įtampa, proc.	≥ −24,7	0,818	0,724–0,911	< 0,001	85,7	67,7
Troponinas I, µg/l	≥ 33,30	0,810	0,715–0,906	< 0,001	82,1	72,3

AUC – plotas po ROC kreive; PI – pasikliautinasis intervalas; KSIF – kairiojo skilvelio išstūmio frakcija. Sutrikęs KS funkcijos atsistatymas apibrėžtas kaip pakartotinio tyrimo KSIF < 50 proc. Slenkstinės vertės nustatytos pagal Youden indeksą.

Nepalankus kairiojo skilvelio remodeliavimasis

Nepalankus KS remodeliavimasis, apibrėžtas kaip ≥ 12 proc. KSGDT ir KSGST tūrių padidėjimas po 6 mėnesių, nustatytas 19 iš 93 pacientų (20,4 proc.). Šie pacientai, palyginti su pacientais, kuriems nepalankus KS remodeliavimasis neišsivystė, dažniau buvo patyrę priekinės KS sienelės MI (atitinkamai 63,2 proc. ir 35,1 proc.; p = 0,027), jiems nustatytas mažesnis trombocitų skaičius (191,0 [181,0–233,0] ir 222,0 [196,5–245,8] $\times 10^9$/l; p = 0,022) ir mažesnė 20-HETE koncentracija (6,2 [0,1–32,4] ir 37,1 [6,8–124,1] ng/ml; p = 0,004). Vertinant infarktinės zonos audinio charakteristikų rodiklius, nepalankaus KS remodeliavimosi grupėje nustatytas didesnis nekontrastinio T1 ir trumpesnis pokontrastinio T1 relaksacijos laikas. Pradinė KSIF, infarkto ir MVO apimtis tarp grupių reikšmingai nesiskyrė.

Dėl riboto nepalankaus KS remodeliavimosi atvejų skaičiaus daugiaveiksnė analizė atlikta dviem modeliais. Naudojant biologinių žymenų modelį (A), su nepalankiu KS remodeliavimusi nepriklausomai buvo susijęs mažesnis trombocitų skaičius (ŠS 0,981; 95 proc. PI 0,965–0,996; p = 0,015) ir mažesnė 20-HETE koncentracija (ŠS 0,985; 95 proc. PI 0,970–1,000; p = 0,047). Naudojant bendrą biologinių žymenų ir vaizdinių rodiklių modelį (B), nepriklausomais veiksniais išliko trumpesnis pokontrastinio T1 relaksacijos laikas (ŠS 0,990; 95 proc. PI 0,981–0,999; p = 0,033) ir mažesnis trombocitų skaičius (ŠS 0,980; 95 proc. PI 0,965–0,996; p = 0,015) (8 lentelė). ROC analizėje didžiausią skiriamąją gebą turėjo 20-HETE (AUC 0,713), kuris pasižymėjo didžiausiu jautrumu (94,7 proc.), o pokontrastinis T1 relaksacijos laikas – didžiausiu specifiškumu (77,0 proc.) (9 lentelė).

***8 lentelė**. Daugiaveiksnė logistinė regresija nepalankaus kairiojo skilvelio remodeliavimosi veiksniams nustatyti*

Veiksnys	ŠS (95 proc. PI)	p
A modelis: pirminis biologinių žymenų modelis		
20-HETE, ng/ml	0,985 (0,970–1,000)	0,047
Šlapalas, mmol/l	1,380 (0,998–1,907)	0,051
Trombocitų skaičius, $\times 10^9$/l	0,981 (0,965–0,996)	0,015
B modelis: bendras biologinių žymenų ir vaizdinių rodiklių		
Pokontrastinis T1, ms	0,990 (0,981–0,999)	0,033
20-HETE, ng/ml	0,990 (0,978–1,001)	0,076
Trombocitų skaičius, $\times 10^9$/l	0,980 (0,965–0,996)	0,015

ŠS – šansų santykis; PI – pasikliautinasis intervalas; HETE – hidroksieikozatetraeno rūgštis; T1 – T1 relaksacijos laikas. A modelis – pirminis biologinių žymenų modelis; B modelis – bendras biologinių žymenų ir vaizdinių rodiklių modelis. Pateikti vieno vieneto pokyčio kiekybinių kintamųjų šansų santykiai.

***9 lentelė.** Pradinių rodiklių geba prognozuoti nepalankų kairiojo skilvelio remodeliavimąsi*

Rodiklis	Slenkstinė vertė	AUC	95 proc. PI	p	Jautrumas, proc.	Specifiš-kumas, proc.
20-HETE, ng/ml	≤ 39,75	0,713	0,594–0,833	< 0,001	94,7	48,6
Pokontrastinis T1, ms	≤ 283,8	0,692	0,564–0,819	0,003	63,2	77,0
Trombocitų skaičius, $\times 10^9$/l	≤ 209,0	0,670	0,546–0,794	0,007	68,4	66,2
Šlapalas, mmol/l	≥ 6,1	0,637	0,498–0,775	0,054	52,6	71,6

AUC – plotas po kreive; PI – pasikliautinasis intervalas; T1 – T1 relaksacijos laikas; HETE – hidroksieikozatetraeno rūgštis. Slenkstinės vertės nustatytos pagal Youden indeksą.

TYRIMO SILPNOSIOS SAVYBĖS

Šio tyrimo rezultatus reikėtų vertinti atsižvelgiant į kelis ribotumus. Pirma, tai buvo vieno centro stebimasis tyrimas su gana nedidele pradine imtimi (n = 105) ir porinių ŠMRT tyrimų imtimi (n = 93), todėl rezultatų pritaikomumas platesnei pacientų populiacijai yra ribotas.

Antra, nedidelis baigčių skaičius (sutrikęs KS funkcijos atsistatymas – 28 iš 93, nepalankus KS remodeliavimasis – 19 iš 93) ribojo daugiaveiksnės analizės galimybes ir didino atsitiktinių sąsajų riziką. ROC analizės slenkstinės vertės buvo nustatytos tos pačios imties tiriamiesiems, todėl jos turėtų

būti vertinamos kaip tiriamosios. Taip pat būtina slenkstines vertes patvirtinti tiriant nepriklausomas imtis.

Trečia, stebėsenos trukmė buvo 6 mėnesiai, todėl ilgesnio laikotarpio remodeliavimosi pokyčiai ir nustatytų prognozinių rodiklių sąsajos su klinikinėmis baigtimis, pvz., širdies nepakankamumas ar mirštamumas, nebuvo vertintos.

Ketvirta, biologiniai žymenys buvo vertinti tik vieną kartą ūminiu laikotarpiu, todėl nebuvo galima įvertinti 20-HETE, 15(S)-HETE ir NETozės raiškos pokyčių laiko požiūriu.

Penkta, segmentas buvo laikomas infarktiniu esant net minimaliam jame nustatytam LGE, netaikant transmuralumo slenksčio, o viso segmento įtampos ir parametrinių miokardo žemėlapių vertės buvo įtrauktos į infarktinės zonos vidurkius.

IŠVADOS

1. Nepriklausomi didelės ūminės infarkto apimties (≥ 41,91 proc. KS miokardo masės) prognoziniai veiksniai buvo prieš PVAI nustatyta TIMI 0–1 kraujo tėkmė (ŠS 8,08; p = 0,017) ir didesnė troponino I koncentracija (p < 0,001). Nepriklausomi MVO prognoziniai veiksniai buvo TIMI 0–1 kraujo tėkmė (ŠS 3,97; p = 0,017), didesnė troponino I koncentracija (p = 0,015), mažesnis GFG (p = 0,038) ir didesnė NETozės raiška (ŠS 1,03 kas 1 mU/ml; p = 0,020). 20-HETE ir 15(S)-HETE su ūmine miokardo pažaida nebuvo susiję.
2. Praėjus 6 mėnesiams po MI, KSIF pagerėjo, infarkto dydis sumažėjo, o MVO nebenustatyta. Liekamasis infarkto dydis buvo stipriai susijęs su pradiniu infarkto dydžiu (r_s = 0,84; p < 0,001) ir troponino I koncentracija (r_s = 0,75; p < 0,001), vidutiniškai – su pradine MVO apimtimi (r_s = 0,59; p < 0,001), tačiau nebuvo susijęs su 20-HETE, 15(S)-HETE ir NETozės raiška.
3. Pažaida apėmė visas tris miokardo zonas: ūminiu laikotarpiu infarktinis miokardas buvo labiausiai pažeistas, o periinfarktinis nuo nutolusiojo reikšmingai skyrėsi apsukine įtampa, nekontrastiniu ir pokontrastiniu T1 relaksacijos laiku bei ECV (visi p < 0,05), bet ne išilgine įtampa ir T2. Per 6 mėnesius miokardas atsistatė netolygiai – ryškiausiai infarktinėje zonoje, periinfarktinėje – tik iš dalies.
4. Po 6 mėnesių sutrikęs KS sistolinės funkcijos atsistatymas (KSIF < 50 proc.) nustatytas 30,1 proc. pacientų. Su šia baigtimi nepriklausomai buvo susijusi mažesnė pradinė KSIF (ŠS 0,86; p = 0,017; AUC = 0,85). Jautrumo analizėje, neįtraukus pradinės KSIF, nepriklau-

somi veiksniai buvo didesnis pradinis infarkto dydis (p = 0,006) ir blogesnė infarktinės zonos apsukinė įtampa (p = 0,010). Specializuoti biologiniai žymenys su sutrikusiu KS funkcijos atsistatymu nebuvo susiję.

5. Nepalankus KS remodeliavimasis po 6 mėnesių (≥ 12 proc. KSGDT ir KSGST padidėjimas) nustatytas 20,4 proc. pacientų. Nepriklausomi prognoziniai veiksniai buvo mažesnis trombocitų skaičius (ŠS 0,981; p = 0,015), mažesnė 20-HETE koncentracija (ŠS 0,985; p = 0,047) ir trumpesnis infarktinės zonos pokontrastinis T1 relaksacijos laikas (ŠS 0,990; p = 0,033).

PRAKTINĖS REKOMENDACIJOS

1. Pacientams po pirmojo ŪMIkSTP ūminiu laikotarpiu svarstytina NETozės raišką įtraukti kaip papildomą kompleksinio miokardo pažaidos rizikos vertinimo žymenį. Didesnė NETozės raiška (≥ 62,1 mU/ml) gali padėti nustatyti pacientus, turinčius didesnę MVO riziką. Dėl didelio specifiškumo ir mažesnio jautrumo šis žymuo labiau tinka didesnės rizikos pacientams nustatyti, o ne MVO atmesti.
2. Pacientams po pirmojo ŪMIkSTP, kuriems pradiniame ŠMRT nustatoma KSIF ≤ 41,3 proc., tikslinga svarstyti intensyvesnę klinikinę stebėseną bei pakartotinį KS funkcijos vertinimą po 6 mėnesių. Pradinė infarkto apimtis ≥ 42,3 proc. ir infarktinės zonos apsukinė įtampa (≥ −24,7 proc.) gali būti naudojami kaip papildomi sutrikusio KS sistolinės funkcijos atsistatymo rizikos rodikliai.
3. Mažesnį trombocitų skaičių (≤ 209,0 × 10^9/l), nustatytą ūminiu laikotarpiu po pirmojo ŪMIkSTP, tikslinga vertinti kaip papildomą, lengvai prieinamą nepalankaus KS remodeliavimosi rizikos rodiklį. 20-HETE koncentracijos vertinimas, kaip tiriamasis žymuo, galėtų suteikti papildomos informacijos apie nepalankaus KS remodeliavimosi riziką.

REFERENCES

[1] Mensah GA, Fuster V, Murray CJL, et al. Global Burden of Cardiovascular Diseases and Risks, 1990-2022. *J Am Coll Cardiol* 2023; 82: 2350–2473.

[2] Vaduganathan M, Mensah GA, Turco JV, et al. The Global Burden of Cardiovascular Diseases and Risk. *J Am Coll Cardiol* 2022; 80: 2361–2371.

[3] Visseren FLJ, Mach F, Smulders YM, et al. 2021 ESC Guidelines on cardiovascular disease prevention in clinical practice. *Eur Heart J* 2021; 42: 3227–3337.

[4] Byrne RA, Rossello X, Coughlan JJ, et al. 2023 ESC Guidelines for the management of acute coronary syndromes. *Eur Heart J* 2023; 44: 3720–3826.

[5] Sezer M, van Royen N, Umman B, et al. Coronary Microvascular Injury in Reperfused Acute Myocardial Infarction: A View From an Integrative Perspective. *J Am Heart Assoc* 2018; 7: e009949.

[6] Konijnenberg LSF, Damman P, Duncker DJ, et al. Pathophysiology and diagnosis of coronary microvascular dysfunction in ST-elevation myocardial infarction. *Cardiovasc Res* 2020; 116: 787–805.

[7] Niccoli G, Scalone G, Lerman A, et al. Coronary microvascular obstruction in acute myocardial infarction. *Eur Heart J* 2016; 37: 1024–1033.

[8] Frantz S, Hundertmark MJ, Schulz-Menger J, et al. Left ventricular remodelling post-myocardial infarction: pathophysiology, imaging, and novel therapies. *Eur Heart J* 2022; 43: 2549–2561.

[9] van der Bijl P, Abou R, Goedemans L, et al. Left Ventricular Post-Infarct Remodeling. *JACC Heart Fail* 2020; 8: 131–140.

[10] Gissler MC, Antiochos P, Ge Y, et al. Cardiac Magnetic Resonance Evaluation of LV Remodeling Post-Myocardial Infarction: Prognosis, Monitoring and Trial Endpoints. *JACC Cardiovasc Imaging* 2024; 17: 1366–1380.

[11] Schulz-Menger J, Bluemke DA, Bremerich J, et al. Standardized image interpretation and post-processing in cardiovascular magnetic resonance - 2020 update : Society for Cardiovascular Magnetic Resonance (SCMR): Board of Trustees Task Force on Standardized Post-Processing. *J Cardiovasc Magn Reson Off J Soc Cardiovasc Magn Reson* 2020; 22: 19.

[12] Bellenger NG, Davies LC, Francis JM, et al. Reduction in sample size for studies of remodeling in heart failure by the use of cardiovascular magnetic resonance. *J Cardiovasc Magn Reson Off J Soc Cardiovasc Magn Reson* 2000; 2: 271–278.

[13] Ibanez B, Aletras AH, Arai AE, et al. Cardiac MRI Endpoints in Myocardial Infarction Experimental and Clinical Trials: JACC Scientific Expert Panel. *J Am Coll Cardiol* 2019; 74: 238–256.

[14] Messroghli DR, Moon JC, Ferreira VM, et al. Clinical recommendations for cardiovascular magnetic resonance mapping of T1, T2, T2* and extracellular volume: A consensus statement by the Society for Cardiovascular Magnetic Resonance (SCMR) endorsed by the European Association for Cardiovascular Imaging (EACVI). *J Cardiovasc Magn Reson Off J Soc Cardiovasc Magn Reson* 2017; 19: 75.

[15] Wamil M, Borlotti A, Liu D, et al. Combined T1-mapping and tissue tracking analysis predicts severity of ischemic injury following acute STEMI—an Oxford Acute Myocardial Infarction (OxAMI) study. *Int J Cardiovasc Imaging*; 35. Epub ahead of print 1 July 2019. DOI: 10.1007/s10554-019-01542-8.

[16] Gresele P, Guglielmini G, Del Pinto M, et al. Low platelet count at admission has an adverse impact on outcome in patients with acute coronary syndromes: from the START Antiplatelet registry. *Sci Rep* 2024; 14: 14516.

[17] Rocic P, Schwartzman ML. 20-HETE in the regulation of vascular and cardiac function. *Pharmacol Ther* 2018; 192: 74–87.

[18] Pascale JV, Wolf A, Kadish Y, et al. 20-Hydroxyeicosatetraenoic acid (20-HETE): Bioactions, receptors, vascular function, cardiometabolic disease and beyond. *Adv Pharmacol* 2023; 97: 229–255.
[19] Wang J, Li H, He J, et al. 20-Hydroxyeicosatetraenoic acid involved in endothelial activation and thrombosis. *Am J Physiol-Heart Circ Physiol* 2015; 308: H1359–H1367.
[20] Han Y, Zhao H, Tang H, et al. 20-Hydroxyeicosatetraenoic Acid Mediates Isolated Heart Ischemia/Reperfusion Injury by Increasing NADPH Oxidase-Derived Reactive Oxygen Species Production. *Circ J* 2013; 77: 1807–1816.
[21] Lundqvist A, Sandstedt M, Sandstedt J, et al. The Arachidonate 15-Lipoxygenase Enzyme Product 15-HETE Is Present in Heart Tissue from Patients with Ischemic Heart Disease and Enhances Clot Formation. *PloS One* 2016; 11: e0161629.
[22] Chen X, Du Z, Guo D, et al. Activation of the Macrophage-Associated Inflammasome Exacerbates Myocardial Fibrosis Through the 15-HETE-Mediated Pathway in Acute Myocardial Infarction. *Engineering* 2024; 42: 143–156.
[23] Kain V, Ingle KA, Kabarowski J, et al. Genetic deletion of 12/15 lipoxygenase promotes effective resolution of inflammation following myocardial infarction. *J Mol Cell Cardiol* 2018; 118: 70–80.
[24] Brinkmann V, Reichard U, Goosmann C, et al. Neutrophil Extracellular Traps Kill Bacteria. *Science* 2004; 303: 1532–1535.
[25] Mangold A, Alias S, Scherz T, et al. Coronary Neutrophil Extracellular Trap Burden and Deoxyribonuclease Activity in ST-Elevation Acute Coronary Syndrome Are Predictors of ST-Segment Resolution and Infarct Size. *Circ Res* 2015; 116: 1182–1192.
[26] Mangold A, Ondracek AS, Hofbauer TM, et al. Culprit site extracellular DNA and microvascular obstruction in ST-elevation myocardial infarction. *Cardiovasc Res* 2022; 118: 2006–2017.
[27] Stark K, Massberg S. Interplay between inflammation and thrombosis in cardiovascular pathology. *Nat Rev Cardiol* 2021; 18: 666–682.
[28] Hofbauer TM, Ondracek AS, Mangold A, et al. Neutrophil Extracellular Traps Induce MCP-1 at the Culprit Site in ST-Segment Elevation Myocardial Infarction. *Front Cell Dev Biol* 2020; 8: 564169.
[29] Zhang L, Dai Z, Guo R, et al. Metabolomics reveal dynamic changes in eicosanoid profile in patients with ST-elevation myocardial infarction after percutaneous coronary intervention. *Clin Exp Pharmacol Physiol* 2021; 48: 463–470.
[30] Solati Z, Surendran A, Aukema HM, et al. Impact of Reperfusion on Plasma Oxylipins in ST-Segment Elevation Myocardial Infarction. *Metabolites* 2023; 14: 19.
[31] Chong B, Jayabaskaran J, Jauhari SM, et al. Global burden of cardiovascular diseases: projections from 2025 to 2050. *Eur J Prev Cardiol* 2025; 32: 1001–1015.
[32] Movs.isyan NK, Vinciguerra M, Medina-Inojosa JR, et al. Cardiovascular Diseases in Central and Eastern Europe: A Call for More Surveillance and Evidence-Based Health Promotion. *Ann Glob Health* 2020; 86: 21.
[33] Radisauskas R, Sileikiene L, Kranciukaite-Butylkiniene D, et al. Trends in Myocardial Infarction Morbidity and Mortality from Ischemic Heart Disease in Middle-Aged Lithuanian Population from 2000 to 2023: Data from Population-Based Kaunas Ischemic Heart Disease Register. *Medicina (Mex)* 2025; 61: 910.
[34] Reimer KA, Lowe JE, Rasmussen MM, et al. The wavefront phenomenon of ischemic cell death. 1. Myocardial infarct size vs. duration of coronary occlusion in dogs. *Circulation* 1977; 56: 786–794.
[35] Heusch G. Myocardial ischaemia-reperfusion injury and cardioprotection in perspective. *Nat Rev Cardiol* 2020; 17: 773–789.

[36] Hausenloy DJ, Yellon DM. Myocardial ischemia-reperfusion injury: a neglected therapeutic target. *J Clin Invest* 2013; 123: 92–100.
[37] Bolognese L, Neskovic AN, Parodi G, et al. Left Ventricular Remodeling After Primary Coronary Angioplasty. *Circulation* 2002; 106: 2351–2357.
[38] Legallois D, Hodzic A, Alexandre J, et al. Definition of left ventricular remodelling following ST-elevation myocardial infarction: a systematic review of cardiac magnetic resonance studies in the past decade. *Heart Fail Rev* 2020; 27: 37–48.
[39] Bulluck H, Go YY, Crimi G, et al. Defining left ventricular remodeling following acute ST-segment elevation myocardial infarction using cardiovascular magnetic resonance. *J Cardiovasc Magn Reson* 2016; 19: 26.
[40] Chalise U, Becirovic-Agic M, Lindsey ML. The cardiac wound healing response to myocardial infarction. *WIREs Mech Dis* 2023; 15: e1584.
[41] Lindsey ML, Oliver AF, Gaye A, et al. Cellular Interactions of Cardiac Repair After Myocardial Infarction. *Cells* 2025; 14: 1903.
[42] Kim RJ, Fieno DS, Parrish TB, et al. Relationship of MRI delayed contrast enhancement to irreversible injury, infarct age, and contractile function. *Circulation* 1999; 100: 1992–2002.
[43] Stone GW, Selker HP, Thiele H, et al. Relationship Between Infarct Size and Outcomes Following Primary PCI. *J Am Coll Cardiol* 2016; 67: 1674–1683.
[44] Bulluck H, Dharmakumar R, Arai AE, et al. Cardiovascular Magnetic Resonance in Acute ST-Segment–Elevation Myocardial Infarction. *Circulation* 2018; 137: 1949–1964.
[45] Burns RJ, Gibbons RJ, Yi Q, et al. The relationships of left ventricular ejection fraction, end-systolic volume index and infarct size to six-month mortality after hospital discharge following myocardial infarction treated by thrombolysis. *J Am Coll Cardiol* 2002; 39: 30–36.
[46] Shah V, Kalekar T, Gupta A, et al. Role of Late Gadolinium Enhancement in the Assessment of Myocardial Viability. *Cureus*. Epub ahead of print 4 March 2022. DOI: 10.7759/cureus.22844.
[47] Wu KC, Zerhouni EA, Judd RM, et al. Prognostic Significance of Microvascular Obstruction by Magnetic Resonance Imaging in Patients With Acute Myocardial Infarction. *Circulation* 1998; 97: 765–772.
[48] Köhler D, Leiss V, Beichert L, et al. Targeting Gαi2 in neutrophils protects from myocardial ischemia reperfusion injury. *Basic Res Cardiol* 2024; 119: 717–732.
[49] Carrick D, Haig C, Ahmed N, et al. Myocardial Hemorrhage After Acute Reperfused ST-Segment–Elevation Myocardial Infarction: Relation to Microvascular Obstruction and Prognostic Significance. *Circ Cardiovasc Imaging*; 9. Epub ahead of print January 2016. DOI: 10.1161/CIRCIMAGING.115.004148.
[50] Lechner I, Reindl M, Stiermaier T, et al. Clinical Outcomes Associated With Various Microvascular Injury Patterns Identified by CMR After STEMI. *J Am Coll Cardiol* 2024; 83: 2052–2062.
[51] Eitel I, de Waha S, Wöhrle J, et al. Comprehensive prognosis assessment by CMR imaging after ST-segment elevation myocardial infarction. *J Am Coll Cardiol* 2014; 64: 1217–1226.
[52] van Kranenburg M, Magro M, Thiele H, et al. Prognostic value of microvascular obstruction and infarct size, as measured by CMR in STEMI patients. *JACC Cardiovasc Imaging* 2014; 7: 930–939.
[53] de Waha S, Patel MR, Granger CB, et al. Relationship between microvascular obstruction and adverse events following primary percutaneous coronary intervention for ST-segment elevation myocardial infarction: an individual patient data pooled analysis from seven randomized trials. *Eur Heart J* 2017; 38: 3502–3510.

[54] Troger F, Pamminger M, Poskaite P, et al. Clinical Impact of Persistent Microvascular Obstruction in CMR After Reperfused STEMI. *Circ Cardiovasc Imaging* 2025; 18: e017645.
[55] Mayr A, Klug G, Reindl M, et al. Evolution of Myocardial Tissue Injury: A CMR Study Over a Decade After STEMI. *JACC Cardiovasc Imaging* 2022; 15: 1030–1042.
[56] Carrick D, Haig C, Rauhalammi S, et al. Pathophysiology of LV Remodeling in Survivors of STEMI. *JACC Cardiovasc Imaging* 2015; 8: 779–789.
[57] Reinstadler SJ, Stiermaier T, Liebetrau J, et al. Prognostic Significance of Remote Myocardium Alterations Assessed by Quantitative Noncontrast T1 Mapping in ST-Segment Elevation Myocardial Infarction. *JACC Cardiovasc Imaging* 2018; 11: 411–419.
[58] Bulluck H, Rosmini S, Abdel-Gadir A, et al. Automated Extracellular Volume Fraction Mapping Provides Insights Into the Pathophysiology of Left Ventricular Remodeling Post-Reperfused ST-Elevation Myocardial Infarction. *J Am Heart Assoc* 2016; 5: e003555.
[59] Amzulescu MS, De Craene M, Langet H, et al. Myocardial strain imaging: review of general principles, validation, and sources of discrepancies. *Eur Heart J - Cardiovasc Imaging* 2019; 20: 605–619.
[60] Erley J, Starekova J, Sinn M, et al. Cardiac magnetic resonance feature tracking global and segmental strain in acute and chronic ST-elevation myocardial infarction. *Sci Rep* 2022; 12: 22644.
[61] Smiseth OA, Rider O, Cvijic M, et al. Myocardial Strain Imaging. *JACC Cardiovasc Imaging* 2025; 18: 340–381.
[62] Chen H, Erley J, Muellerleile K, et al. Contrast-enhanced cardiac MRI is superior to non-contrast mapping to predict left ventricular remodeling at 6 months after acute myocardial infarction. *Eur Radiol* 2023; 34: 1863–1874.
[63] Garg P, Broadbent DA, Swoboda PP, et al. Extra-cellular expansion in the normal, non-infarcted myocardium is associated with worsening of regional myocardial function after acute myocardial infarction. *J Cardiovasc Magn Reson* 2016; 19: 73.
[64] Shanmuganathan M, Masi A, Burrage MK, et al. Acute Response in the Noninfarcted Myocardium Predicts Long-Term Major Adverse Cardiac Events After STEMI. *JACC Cardiovasc Imaging* 2023; 16: 46–59.
[65] Thygesen K, Alpert JS, Jaffe AS, et al. Fourth Universal Definition of Myocardial Infarction (2018). *Circulation* 2018; 138: e618–e651.
[66] Younger JF, Plein S, Barth J, et al. Troponin-I concentration 72 h after myocardial infarction correlates with infarct size and presence of microvascular obstruction. *Heart* 2007; 93: 1547–1551.
[67] Hallén J, Buser P, Schwitter J, et al. Relation of Cardiac Troponin I Measurements at 24 and 48 Hours to Magnetic Resonance–Determined Infarct Size in Patients With ST-Elevation Myocardial Infarction. *Am J Cardiol* 2009; 104: 1472–1477.
[68] Bruder O, Jensen C, Jochims M, et al. Relation of B-type natriuretic peptide (BNP) and infarct size as assessed by contrast-enhanced MRI. *Int J Cardiol* 2010; 144: 53–58.
[69] Kai T, Oka S, Hoshino K, et al. Renal Dysfunction as a Predictor of Slow-Flow/No-Reflow Phenomenon and Impaired ST Segment Resolution After Percutaneous Coronary Intervention in ST-Elevation Myocardial Infarction With Initial Thrombolysis in Myocardial Infarction Grade 0. *Circ J* 2021; 85: 1770–1778.
[70] Ota S, Tanimoto T, Orii M, et al. Association between hyperglycemia at admission and microvascular obstruction in patients with ST-segment elevation myocardial infarction. *J Cardiol* 2015; 65: 272–277.

[71] Feistritzer H-J, Reinstadler SJ, Klug G, et al. Multimarker approach for the prediction of microvascular obstruction after acute ST-segment elevation myocardial infarction: a prospective, observational study. *BMC Cardiovasc Disord* 2016; 16: 239.
[72] Ørn S, Manhenke C, Ueland T, et al. C-reactive protein, infarct size, microvascular obstruction, and left-ventricular remodelling following acute myocardial infarction. *Eur Heart J* 2009; 30: 1180–1186.
[73] Hong D, Choi KH, Song YB, et al. Prognostic implications of post-percutaneous coronary intervention neutrophil-to-lymphocyte ratio on infarct size and clinical outcomes in patients with acute myocardial infarction. *Sci Rep* 2019; 9: 9646.
[74] Massalha E, Oren D, Goitein O, et al. Post–ST-Segment–Elevation Myocardial Infarction Platelet Reactivity Is Associated With the Extent of Microvascular Obstruction and Infarct Size as Determined by Cardiac Magnetic Resonance Imaging. *J Am Heart Assoc* 2022; 11: e020973.
[75] Welt FGP, Batchelor W, Spears JR, et al. Reperfusion Injury in Patients With Acute Myocardial Infarction. *J Am Coll Cardiol* 2024; 83: 2196–2213.
[76] Frangogiannis NG. The inflammatory response in myocardial injury, repair, and remodelling. *Nat Rev Cardiol* 2014; 11: 255–265.
[77] Benkhoff M, Alde K, Ehreiser V, et al. Thromboinflammation is associated with clinical outcome after ST-elevation myocardial infarction. *Blood Adv* 2024; 8: 5581–5589.
[78] Ge L, Zhou X, Ji W-J, et al. Neutrophil extracellular traps in ischemia-reperfusion injury-induced myocardial no-reflow: therapeutic potential of DNase-based reperfusion strategy. *Am J Physiol-Heart Circ Physiol* 2015; 308: H500–H509.
[79] Helseth R, Shetelig C, Andersen GØ, et al. Neutrophil Extracellular Trap Components Associate with Infarct Size, Ventricular Function, and Clinical Outcome in STEMI. *Mediators Inflamm* 2019; 2019: 1–10.
[80] Huang C-C, Chang M-T, Leu H-B, et al. Association of Arachidonic Acid-derived Lipid Mediators with Subsequent Onset of Acute Myocardial Infarction in Patients with Coronary Artery Disease. *Sci Rep* 2020; 10: 8105.
[81] Larose E, Rodés-Cabau J, Pibarot P, et al. Predicting Late Myocardial Recovery and Outcomes in the Early Hours of ST-Segment Elevation Myocardial Infarction. *J Am Coll Cardiol* 2010; 55: 2459–2469.
[82] Wong DTL, Leong DP, Weightman MJ, et al. Magnetic resonance-derived circumferential strain provides a superior and incremental assessment of improvement in contractile function in patients early after ST-segment elevation myocardial infarction. *Eur Radiol* 2014; 24: 1219–1228.
[83] Mangion K, Carrick D, Clerfond G, et al. Predictors of segmental myocardial functional recovery in patients after an acute ST-Elevation myocardial infarction. *Eur J Radiol* 2019; 112: 121–129.
[84] Reindl M, Stiermaier T, Lechner I, et al. Cardiac magnetic resonance imaging improves prognostic stratification of patients with ST-elevation myocardial infarction and preserved ejection fraction. *Eur Heart J Open* 2021; 1: oeab033.
[85] Fertin M, Dubois E, Belliard A, et al. Usefulness of circulating biomarkers for the prediction of left ventricular remodeling after myocardial infarction. *Am J Cardiol* 2012; 110: 277–283.
[86] Di Tano G, Caretta G, De Maria R, et al. Galectin-3 predicts left ventricular remodelling after anterior-wall myocardial infarction treated by primary percutaneous coronary intervention. *Heart* 2017; 103: 71–77.
[87] Weir RAP, Miller AM, Murphy GEJ, et al. Serum Soluble ST2. *J Am Coll Cardiol* 2010; 55: 243–250.

[88] Park Y, Tantry U, Koh J-S, et al. Novel role of platelet reactivity in adverse left ventricular remodelling after ST-segment elevation myocardial infarction: The REMODELING Trial. *Thromb Haemost* 2017; 117: 911–922.
[89] Ibanez B, James S, Agewall S, et al. 2017 ESC Guidelines for the management of acute myocardial infarction in patients presenting with ST-segment elevation. Eur Heart J 2018; 39: 119–177.
[90] Mikami Y, Kolman L, Joncas SX, et al. Accuracy and reproducibility of semi-automated late gadolinium enhancement quantification techniques in patients with hypertrophic cardiomyopathy. *J Cardiovasc Magn Reson Off J Soc Cardiovasc Magn Reson* 2014; 16: 85.
[91] Flett AS, Hasleton J, Cook C, et al. Evaluation of techniques for the quantification of myocardial scar of differing etiology using cardiac magnetic resonance. *JACC Cardiovasc Imaging* 2011; 4: 150–156.
[92] Cerqueira MD, Weissman NJ, Dilsizian V, et al. Standardized myocardial segmentation and nomenclature for tomographic imaging of the heart. A statement for healthcare professionals from the Cardiac Imaging Committee of the Council on Clinical Cardiology of the American Heart Association. *Circulation* 2002; 105: 539–542.
[93] Schober P, Boer C, Schwarte LA. Correlation Coefficients: Appropriate Use and Interpretation. *Anesth Analg* 2018; 126: 1763–1768.
[94] Bujak M, Desperak A, Gierlotka M, et al. Impact of smoking on outcomes in patients with ST-segment elevation myocardial infarction treated with primary percutaneous coronary intervention. *Pol Arch Intern Med* 2023; 133: 16459.
[95] Redfors B, Furer A, Selker HP, et al. Effect of Smoking on Outcomes of Primary PCI in Patients With STEMI. *J Am Coll Cardiol* 2020; 75: 1743–1754.
[96] Hadamitzky M, Langhans B, Hausleiter J, et al. The Assessment of Area at Risk and Myocardial Salvage After Coronary Revascularization in Acute Myocardial Infarction: Comparison Between CMR and SPECT. *JACC Cardiovasc Imaging* 2013; 6: 358–369.
[97] Khan JN, Nazir SA, Horsfield MA, et al. Comparison of semi-automated methods to quantify infarct size and area at risk by cardiovascular magnetic resonance imaging at 1.5T and 3.0T field strengths. *BMC Res Notes* 2015; 8: 52.
[98] Joost A, Stiermaier T, Eitel C, et al. Impact of Initial Culprit Vessel Flow on Infarct Size, Microvascular Obstruction, and Myocardial Salvage in Acute Reperfused ST-Elevation Myocardial Infarction. *Am J Cardiol* 2016; 118: 1316–1322.
[99] Schaaf MJ, Mewton N, Rioufol G, et al. Pre-PCI angiographic TIMI flow in the culprit coronary artery influences infarct size and microvascular obstruction in STEMI patients. *J Cardiol* 2016; 67: 248–253.
[100] Klug G, Mayr A, Mair J, et al. Role of biomarkers in assessment of early infarct size after successful p-PCI for STEMI. *Clin Res Cardiol* 2011; 100: 501–510.
[101] Stevic N, Pinède A, Mewton N, et al. Effect of ventricular fibrillation on infarct size after myocardial infarction: a translational study. *Basic Res Cardiol* 2024; 119: 911–921.
[102] Hallén J, Jensen JK, Buser P, et al. Relation of cardiac troponin I and microvascular obstruction following ST-elevation myocardial infarction. *Acute Card Care* 2011; 13: 48–51.
[103] Li Z, Yin H, Wang D, et al. Prediction of microvascular obstruction by coronary artery angiography score after acute ST-segment elevation myocardial infarction: a single-center retrospective observational study. *BMC Cardiovasc Disord* 2022; 22: 410.
[104] Sadre-Bafghi S-A, Mohebi M, Hadi F, et al. Impact of Baseline Estimated Glomerular Filtration Rate Using CKD-EPI Equation on Long-term Prognosis of STEMI Patients:

A Matter of Small Increments! *Crit Pathw Cardiol J Evid-Based Med* 2022; 21: 153–159.
[105] Savic L, Mrdovic I, Asanin M, et al. The Impact of Kidney Function on the Slow-Flow/No-Reflow Phenomenon in Patients Treated with Primary Percutaneous Coronary Intervention: Registry Analysis. *J Intervent Cardiol* 2022; 2022: 5815274.
[106] Podlesnikar T, Pizarro G, Fernández-Jiménez R, et al. Effect of Early Metoprolol During ST-Segment Elevation Myocardial Infarction on Left Ventricular Strain. *JACC Cardiovasc Imaging* 2019; 12: 1188–1198.
[107] Cui J, Zhao Y, Qian G, et al. Cardiac magnetic resonance for the early prediction of reverse left ventricular remodeling in patients with ST-segment elevation myocardial infarction. *Eur Radiol* 2023; 33: 8501–8512.
[108] Bonfig NL, Soukup CR, Shah AA, et al. Increasing myocardial edema is associated with greater microvascular obstruction in ST-segment elevation myocardial infarction. *Am J Physiol-Heart Circ Physiol* 2022; 323: H818–H824.
[109] Dharmakumar R, Kloner RA, Fishbein M, et al. Reperfused Myocardial Infarction. *JACC Adv* 2025; 4: 101528.
[110] Haaf P, Garg P, Messroghli DR, et al. Cardiac T1 Mapping and Extracellular Volume (ECV) in clinical practice: a comprehensive review. *J Cardiovasc Magn Reson* 2016; 18: 89.
[111] Chen B-H, An D-A, Wu C-W, et al. Prognostic significance of non-infarcted myocardium correlated with microvascular impairment evaluated dynamically by native T1 mapping. *Insights Imaging* 2023; 14: 50.
[112] Bergamaschi L, Landi A, Maurizi N, et al. Acute Response of the Noninfarcted Myocardium and Surrounding Tissue Assessed by T2 Mapping After STEMI. *JACC Cardiovasc Imaging* 2024; 17: 610–621.
[113] Tahir E, Sinn M, Bohnen S, et al. Acute versus Chronic Myocardial Infarction: Diagnostic Accuracy of Quantitative Native T1 and T2 Mapping versus Assessment of Edema on Standard T2-weighted Cardiovascular MR Images for Differentiation. *Radiology* 2017; 285: 83–91.
[114] Frangogiannis NG, Kovacic JC. Extracellular Matrix in Ischemic Heart Disease, Part 4/4. *J Am Coll Cardiol* 2020; 75: 2219–2235.
[115] Kidambi A, Motwani M, Uddin A, et al. Myocardial Extracellular Volume Estimation by CMR Predicts Functional Recovery Following Acute MI. *JACC Cardiovasc Imaging* 2017; 10: 989–999.
[116] Pica S, Crimi G, Castelvecchio S, et al. Cardiac magnetic resonance predictors of left ventricular remodelling following acute ST elevation myocardial infarction: The VavirimS study. *Int J Cardiol* 2023; 370: 8–17.
[117] Guo Q, Wang X, Guo R, et al. Incremental value of high-risk CMR attributes to predict adverse remodeling after ST-segment elevation myocardial infarction across LVEF categories. *Hell J Cardiol HJC Hell Kardiologike Epitheorese* 2025; 86: 100–110.
[118] Dutsch A, Graesser C, Novacek S, et al. Baseline Platelet Count Predicts Infarct Size and Mortality after Acute Myocardial Infarction. *Hämostaseologie* 2024; a-2299-0130.
[119] Liu Y, Gao X-M, Fang L, et al. Novel Role of Platelets in Mediating Inflammatory Responses and Ventricular Rupture or Remodeling Following Myocardial Infarction. *Arterioscler Thromb Vasc Biol* 2011; 31: 834–841.
[120] Čiapienė I, Ivanauskienė A, Kupstytė-Krištaponė N, et al. Reduced circulating 20-hydroxyeicosatetraenoic acid and ACE2 in acute coronary syndrome with exploratory cell-based observations. *Sci Rep*. Epub ahead of print 10 June 2026. DOI: 10.1038/s41598-026-56316-9.
[121] Roman RJ. 20-HETE and Hypertension. *Hypertension* 2024; 81: 2012–2015.

[122] Su M-Y, Huang Y-S, Niisato E, et al. Is a timely assessment of the hematocrit necessary for cardiovascular magnetic resonance–derived extracellular volume measurements? *J Cardiovasc Magn Reson* 2020; 22: 77.
[123] Kramer CM, Barkhausen J, Bucciarelli-Ducci C, et al. Standardized cardiovascular magnetic resonance imaging (CMR) protocols: 2020 update. *J Cardiovasc Magn Reson* 2020; 22: 17.
[124] A X, Dan Q, Li M, et al. Significance of QRS scoring system in left ventricular function recovery after acute myocardial infarction. *ESC Heart Fail* 2024; 11: 2778–2788.

LIST OF PUBLICATIONS

Research articles directly related to the topic of the doctoral dissertation, published in journals with a citation index (Impact Factor) in the Clarivate Analytics Web of Science platform:

1. **Virbickienė A**, Dobilienė O, Leleika A, Jurevičiūtė J, Bučius P, Jonaitienė N, Kazakauskaitė E, Bardauskienė L, Tatarūnas V, Lapinskas T. Infarct Zone Circumferential Strain Independently Predicts Left Ventricular Functional Recovery After ST-Segment Elevation Myocardial Infarction: A Multiparametric CMR Study. Diagnostics. 2026;16(13):1–28. doi:10.3390/diagnostics16131992. IF: 3.8; Q1.
2. **Virbickienė A**, Tatarūnas V, Čiapienė I, Jonaitienė N, Jurevičiūtė J, Bučius P, Leleika A, Jonauskienė I, Kleizaitė L, Lapinskas T, Dobilienė O. Clinical and Biomarker Predictors of Adverse Left Ventricular Remodeling After First STEMI: Insights into Phenotype Variability Using CMR. Pharmaceuticals. 2026;19(5):1–16. doi:10.3390/ph19050794. IF: 5.7; Q1.
3. **Virbickienė A**, Lapinskas T, Garlichs CD, Mattecka S, Tanacli R, Ries W, Torzewski J, Heigl F, Pfluecke C, Darius H, Ince H, Nordbeck P, Butter C, Schuster A, Mitzner S, Dobilienė O, Sheriff A, Kelle S. Imaging Predictors of Left Ventricular Functional Recovery after Reperfusion Therapy of ST-Elevation Myocardial Infarction Assessed by Cardiac Magnetic Resonance. Journal of Cardiovascular Development and Disease. 2023;10(7):1–15. doi:10.3390/jcdd10070294. IF: 2.4; Q2.

LIST OF PRESENTATIONS AT SCIENTIFIC CONFERENCES

Presentations directly related to the topic of doctoral dissertation:

1. **Virbickienė Agneta**, Lapinskas Tomas, Jonaitienė Neda, Jurevičiūtė Justina, Jonauskienė Ieva, Tatarūnas Vacis, Dobilienė Olivija. Unveiling Hidden Inflammatory Biomarkers: Predicting Left Ventricular Remodeling After STEMI with Cardiac Magnetic Resonance. International scientific conference, Riga, Latvia. TOP 3 abstract.
2. **Virbickienė Agneta**, Lapinskas Tomas, Jonaitienė Neda, Jurevičiūtė Justina, Jonauskienė Ieva, Tatarūnas Vacis, Dobilienė Olivija. Integrating novel inflammatory pathways and CMR in STEMI: the role of NETosis and eicosanoids in myocardial infarction. Nordic-Baltic Congress of Cardiology, May 2025, Copenhagen, Denmark.
3. Cieškaitė Sofija Goda, Leleika Arnoldas, **Virbickienė Agneta**, Jonaitienė Neda, Jurevičiūtė Justina, Bučius Paulius, Padervinskienė Lina, Dobilienė Olivija, Lapinskas Tomas. Hemodynamic forces – a potential diagnostic tool to assess left ventricular dysfunction using cardiac magnetic resonance imaging. SCMR 28th Annual Scientific Sessions, 29 January – 1 February 2025, Washington, DC, USA.
4. **Virbickienė Agneta**, Padervinskienė Lina, Krečkauskienė Rita, Bučius Paulius, Jurevičiūtė Justina, Jankauskas Antanas, Dobilienė Olivija, Lapinskas Tomas. Association of myocardial injury biomarkers and cardiovascular magnetic resonance parameters in STEMI patients treated with primary PCI. 90th European Atherosclerosis Society Congress, 22–25 May 2022, Milan, Italy.
5. Ivanova Olesia, Dužinaitė Simona, Jonauskienė Ieva, Lapinskas Tomas, Dobilienė Olivija, **Virbickienė Agneta**. Association of myocardial injury biomarkers and left ventricular functional parameters in STEMI patients treated with PPCI. 6th International Health Sciences Conference, 14–15 April 2022, Kaunas, Lithuania.
6. Leleika Arnoldas, **Virbickienė Agneta**, Jurevičiūtė Justina, Jonaitienė Neda, Dobilienė Olivija, Lapinskas Tomas. Relation of myocardial strain and structural parameters in STEMI patients after Primary Percutaneous Coronary Intervention. Cardiac MRI study. 6th International Health Sciences Conference, 14–15 April 2022, Kaunas, Lithuania.

CURRICULUM VITAE

Name, Surname:	**Agneta Virbickienė**
Address:	Lithuanian University of Health Sciences, A. Mickevičiaus 9, LT-44307, Kaunas, Lithuania
E-mail:	agneta.virbickiene@lsmu.lt
Mobile phone:	+370 672 46050

Education:

2013–2017	Resident of Cardiology at Lithuanian University of Health Sciences, Kaunas, Lithuania
2012–2013	Medical internship (doctor trainee) at Kaunas County Hospital and Klaipėda Seamen's Hospital, Lithuania
2007–2013	Studies at Lithuanian University of Health Sciences Medical doctor diploma at Lithuanian University of Health Sciences, Kaunas, Lithuania

Postgraduate education:

01/09/2019 – until now	PhD student at Lithuanian University of Health Sciences, Kaunas, Lithuania

Professional experience:

01/05/2017 – until now	Cardiologist at Hospital of Lithuanian University of Health Sciences Kauno klinikos, Department of Cardiology, Kaunas, Lithuania
09/2020 – 09/2022	Assistant lecturer at Lithuanian University of Health Sciences, Department of Cardiology, Kaunas, Lithuania
02/2020 – 07/2020	Clinical research fellow at MRI-Core-Lab of German Heart Center Berlin, Department of Internal Medicine / Cardiology, Berlin, Germany
2013–2017	Research assistant at Lithuanian University of Health Sciences, Department of Cardiology, Kaunas, Lithuania

Membership of professional societies:

Member of European Society of Cardiology (ESC)
Member of European Association of Cardiovascular Imaging (EACVI)
Member of the Society for Cardiovascular Magnetic Resonance (SCMR)
Member of Lithuanian Society of Cardiology (LCS)

ACKNOWLEDGEMENTS

I would like to express my deepest gratitude to my scientific supervisor, Prof. Dr. Olivija Dobilienė, for her unwavering trust in me, her thoughtful guidance, and the wisdom she so generously shared at every stage of this work. Her insight, patience, and constant encouragement have been a true source of strength, and I am profoundly thankful for her support throughout the preparation of this dissertation. I am equally and sincerely grateful to my scientific consultant, Prof. Dr. Vacis Tatarūnas, whose expertise, thoughtful advice, and steady support have been invaluable to me. Thank you for so generously sharing your knowledge, for your constructive guidance, and for your belief in this research throughout the entire process.

My special thanks go to the entire Ischaemic Heart Disease team for their understanding, encouragement, and collegiality, and particularly for taking on additional clinical responsibilities while I devoted time to my research. Your support made it possible for me to combine clinical work with my scientific journey.

I sincerely thank the team of the Department of Radiology for their professional collaboration, assistance with cardiovascular magnetic resonance examinations, and important contribution to this research.

I am deeply grateful to Prof. Dr. Sebastian Kelle for the opportunity to train for six months at the German Heart Center of the Charité (Deutsches Herzzentrum der Charité) in Berlin – an experience that gave me invaluable clinical and scientific knowledge and set me on my scientific path.

I would also like to thank Justina Jurevičiūtė, Arnoldas Leleika, Neda Jonauskienė, Ieva Jonauskienė, Dovydas Verikas, Eglė Kazakauskaitė and Ieva Čiapienė – dear colleagues who became true friends along the way. Thank you for your dedication and for all the work, big and small, that we shared side by side throughout this journey. Your warmth, companionship, and willingness to help whenever needed meant more to me than words can express.

A very special acknowledgement is dedicated to Prof. Dr. Tomas Lapinskas, who has guided me from the very beginning, from our first days in the choir Neris to my first steps at the Department of Cardiology. Thank you for believing in me, encouraging me through every challenge, and never allowing me to give up. Your trust and unwavering support have had a profound influence on my professional and scientific journey.

My deepest and most heartfelt gratitude goes to my beloved parents, my husband, my son, my relatives, my dear friends, and all the companions on this journey. Thank you for your endless love, your patience, and your belief

in me. Your warmth, understanding, and constant support have carried me through every challenge, and I could not have reached this point without you by my side. From the bottom of my heart, thank you for standing beside me and supporting me at every single step.

Finally, I sincerely thank all the patients who participated in this study. Their trust and willingness to contribute made this research possible.